

Development and Significance of Paediatric Mesh-type Reference Computational Phantoms

Chansoo Choi, Ph.D.

**Postdoc, University of Florida
Member, ICRP Task Group 103**

ICRP Webinar – 6 August 2025

Contents

- I . Conversion of Paediatric VRCPs to Mesh Format**
- II . Inclusion of Blood in Organs and Tissues**
- III. Inclusion of Thin Target and Source Regions**
- IV. Paediatric MRCPs**
- V. Computational Performance in Monte Carlo Codes**
- VI. Dosimetric Impact**
- VII. Summary**

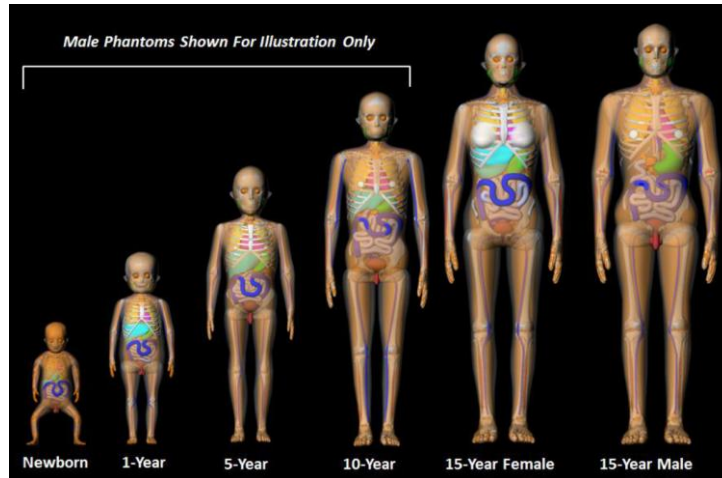
I . Conversion of Paediatric VRCPs to Mesh Format

I . Conversion of Paediatric VRCPs to Mesh Format

- 1. Production of mesh replica of paediatric VRCPs**
- 2. Remodeling or modification of organs and tissues with anatomical or dosimetric issues (e.g., eyes, teeth, colon, thyroid, ...)**

Approach to Produce Mesh Replica of Paediatric VRCPs

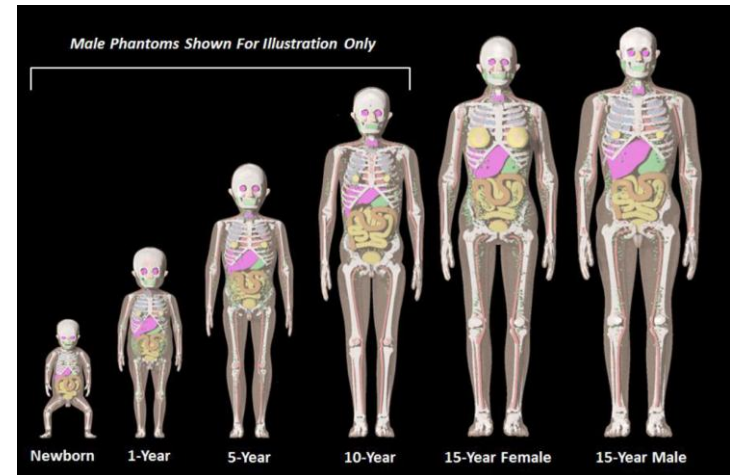
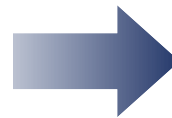
- Paediatric VRCPs were produced from the UF/NCI paediatric phantoms^[1] through voxelization process.
- After the voxelization, some organs or tissues (e.g., muscle, breasts, colon, lymph nodes, ...) were modified or added in the paediatric VRCPs.



UF/NCI paediatric phantoms*

* NURBS: most organs/tissues

PM: skeleton, brain, extrathoracic (ET) region



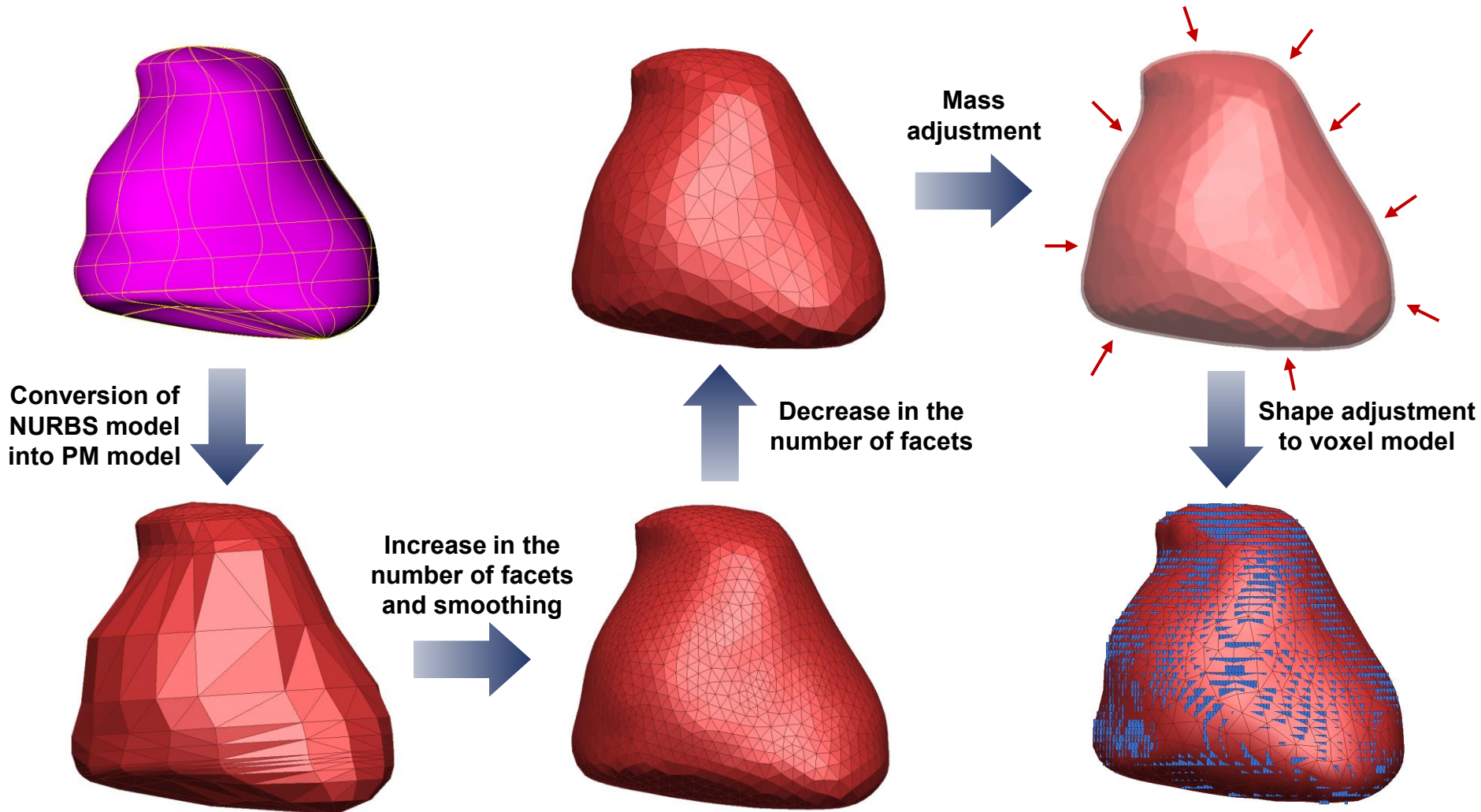
Paediatric VRCPs

➤ Use as a **“starting point”** of conversion project

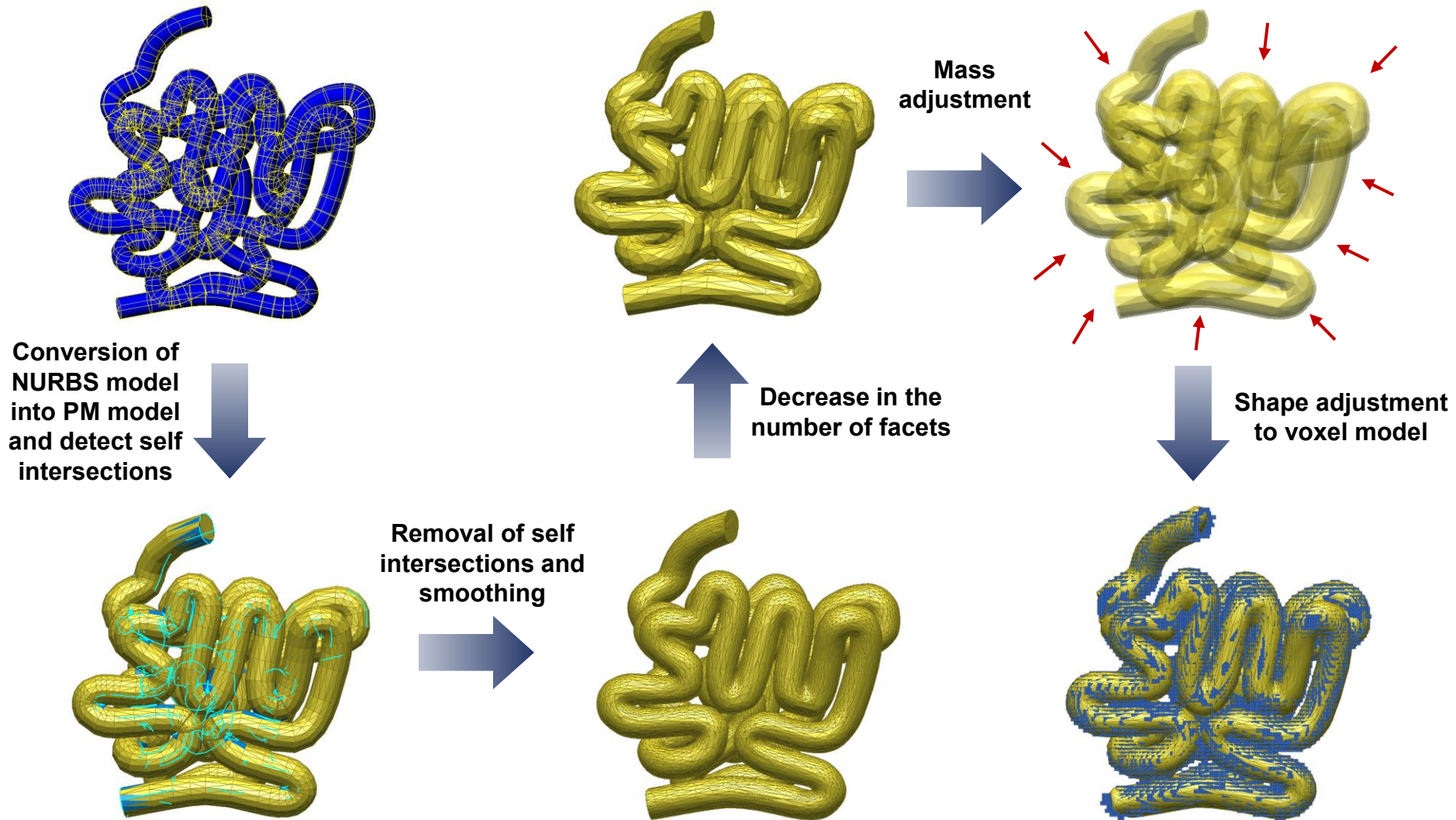
➤ Use as a **“target geometry”**

Example of Conversion

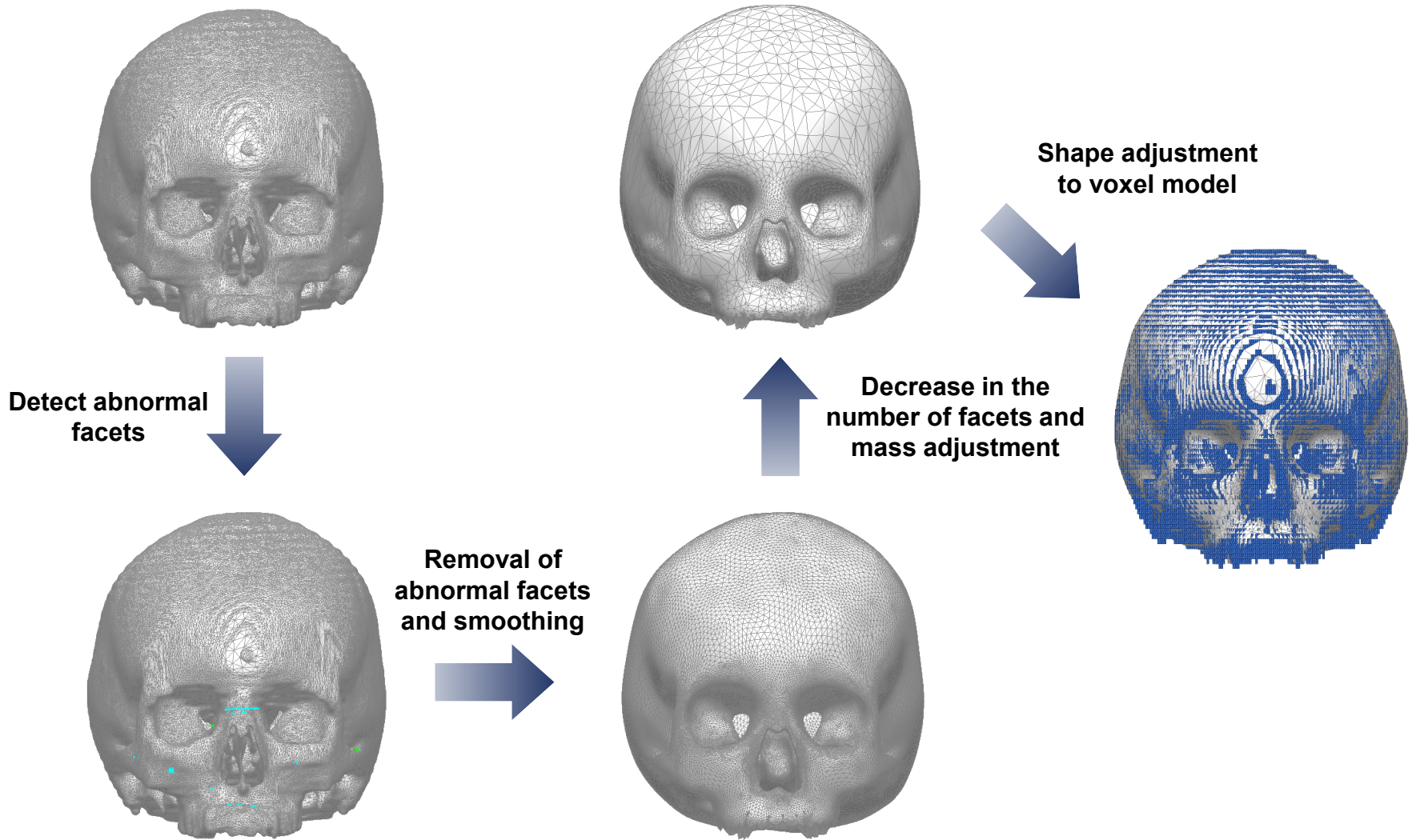
- NURBS format – example 1 (heart)



- **NURBS format – example 2 (small intestine)**

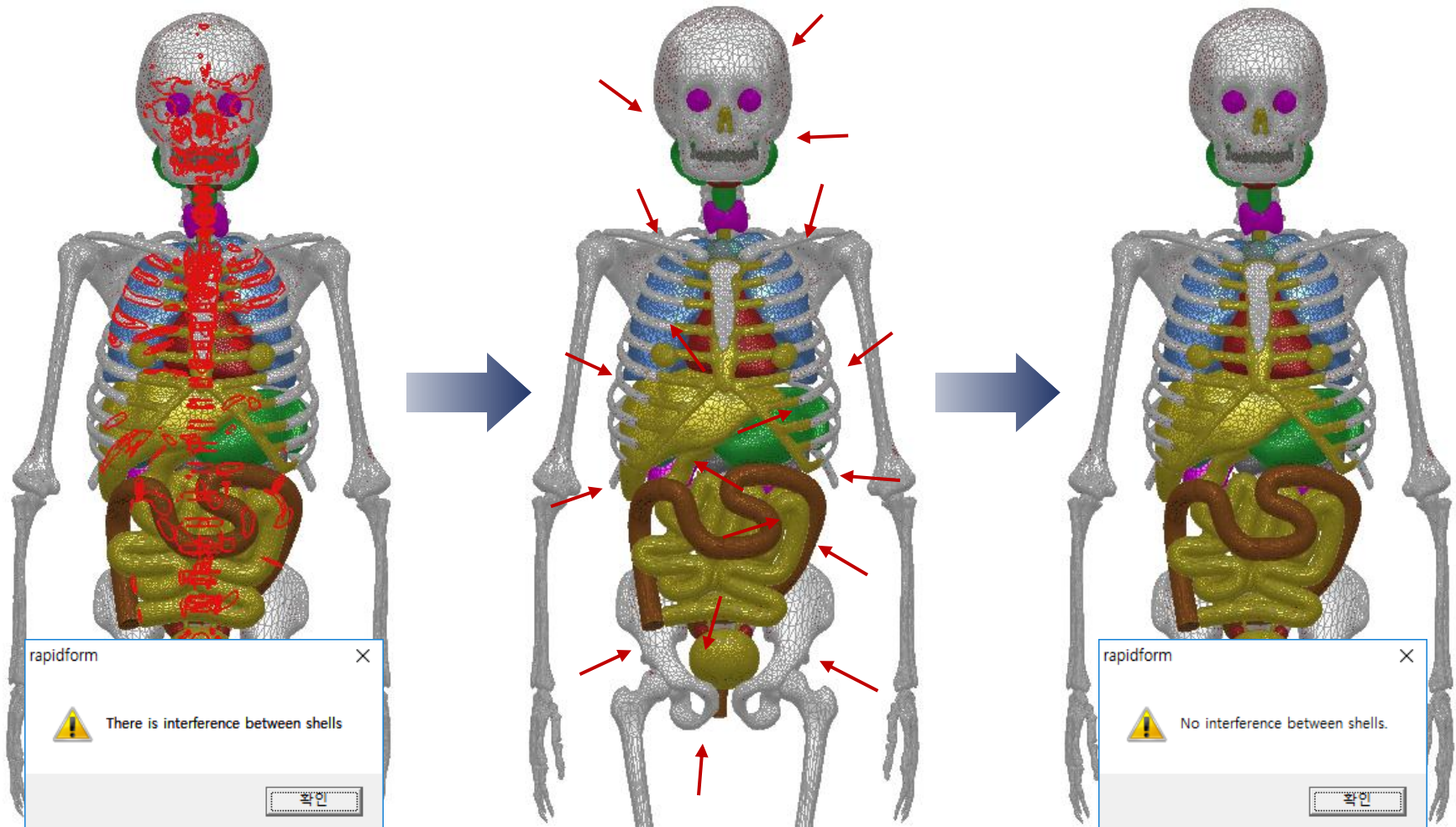


- **PM format – example (cranium)**



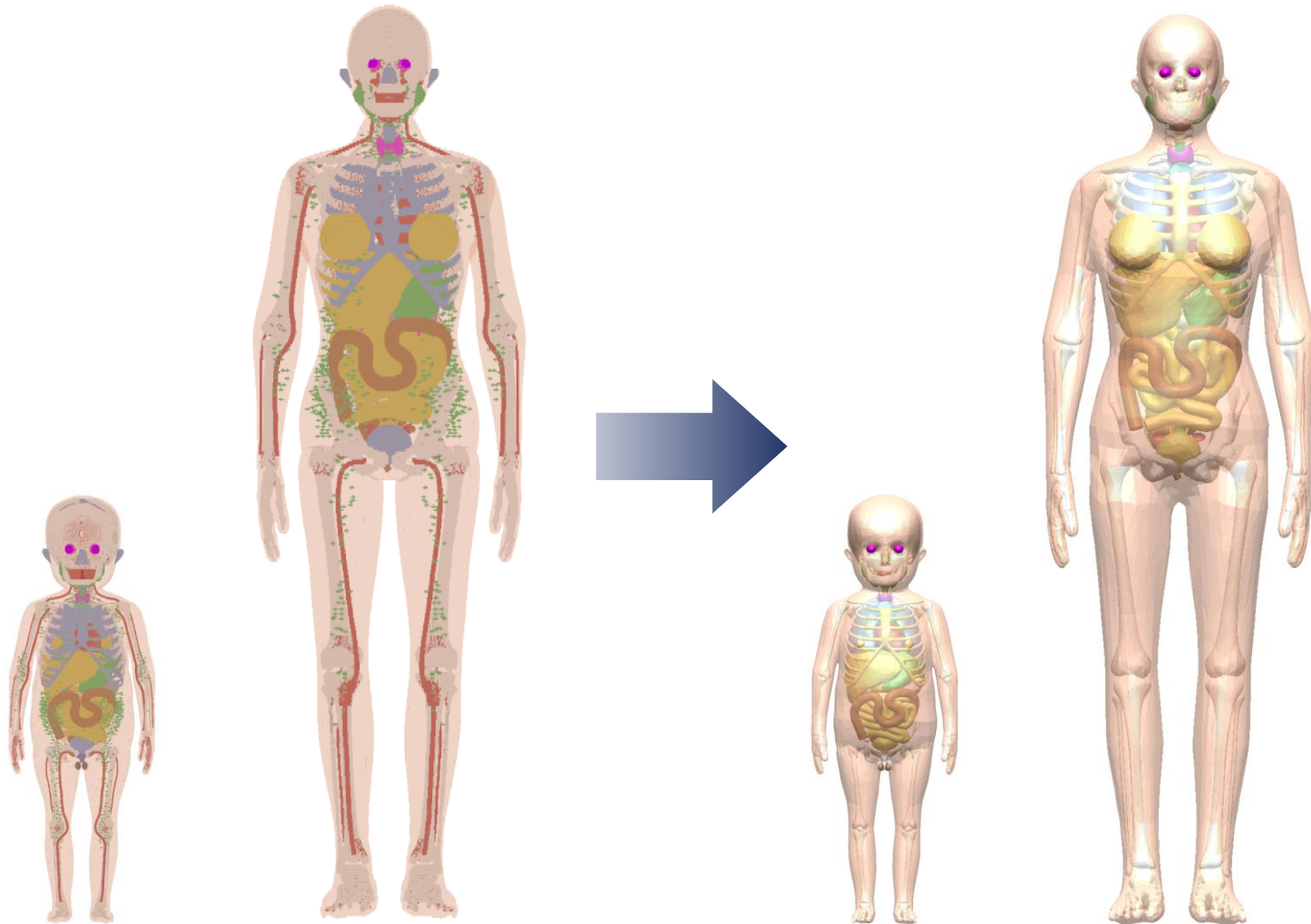
Topological Adjustment of Organs and Tissues

- Constructed PM models were slightly adjusted to avoid the interferences between organs and tissues.



Mesh Replica of Paediatric VRCPs

Example: 1-year male and 15-year female phantoms



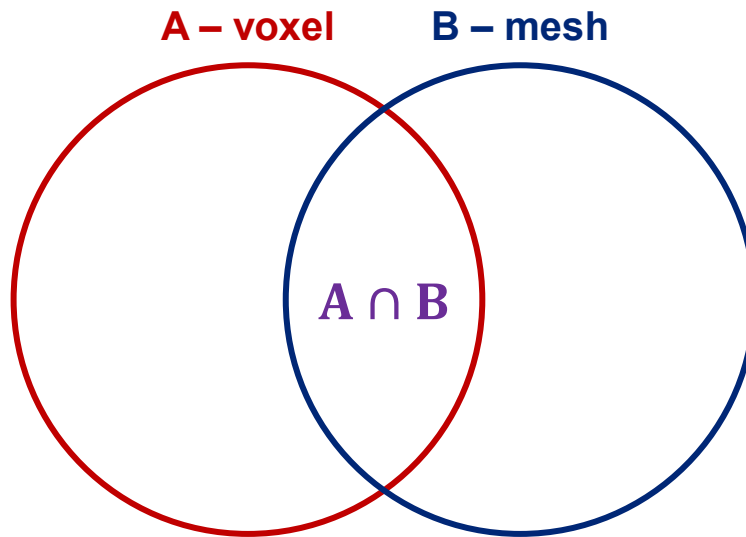
Paediatric VRCPs

Mesh replica of paediatric VRCPs

Conversion Criteria

▪ Dice index (DI)^[2]

- Overlapping volume fraction of two objects (mesh vs. voxel)
- $DI > 0.9$ of the maximum achievable Dice index (MADI)



$$DI = \frac{A \cap B}{(A + B)/2}$$

▪ Centroid distance (CD)

- Distance between the centroids of two objects (mesh vs. voxel)
- $CD \leq 2 \text{ mm}$

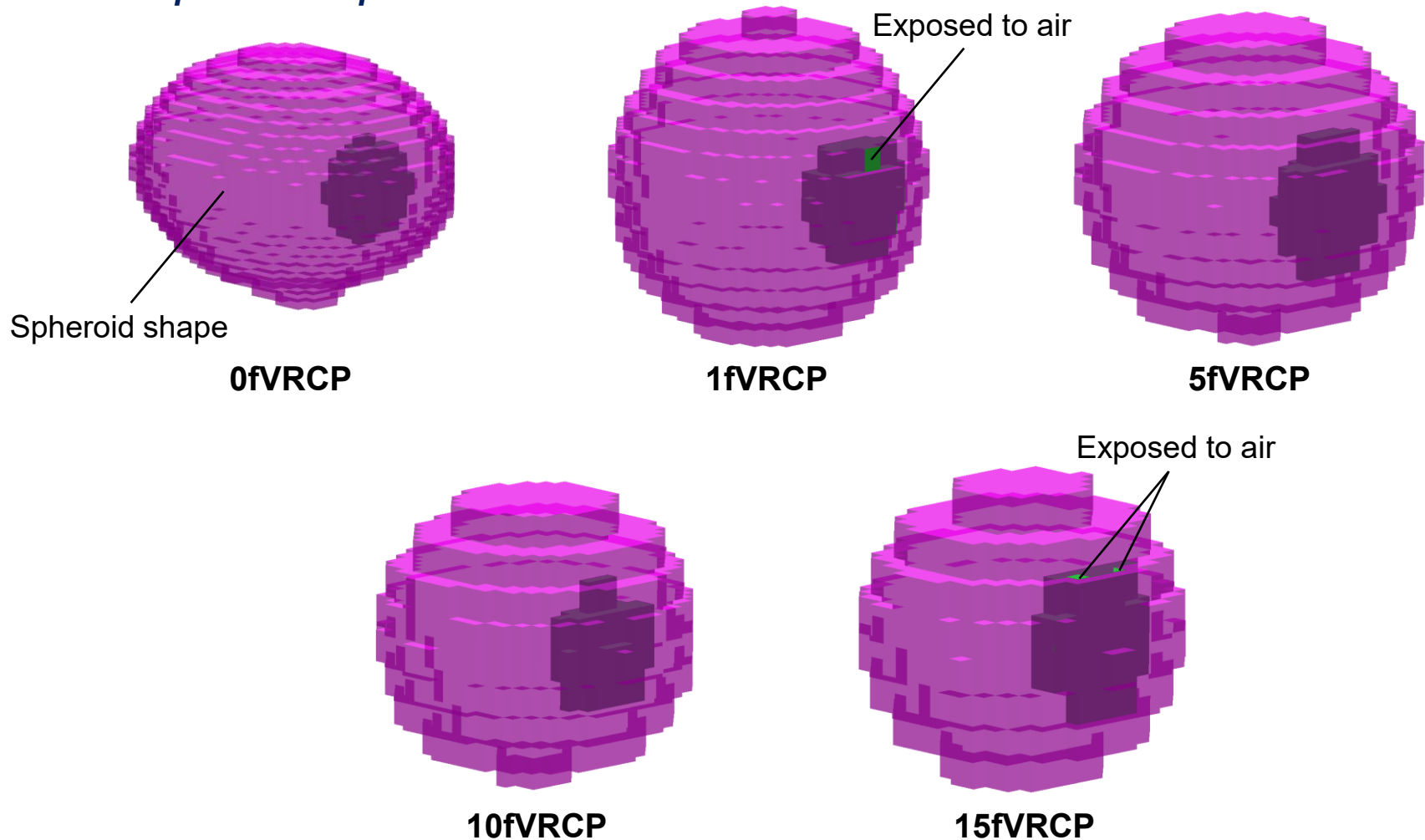
I . Conversion of Paediatric VRCPs to Mesh Format

1. **Production of mesh replica of paediatric VRCPs**
2. **Remodeling or modification of organs and tissues with anatomical or dosimetric issues (e.g., eyes, teeth, colon, thyroid, ...)**

1) Eyes

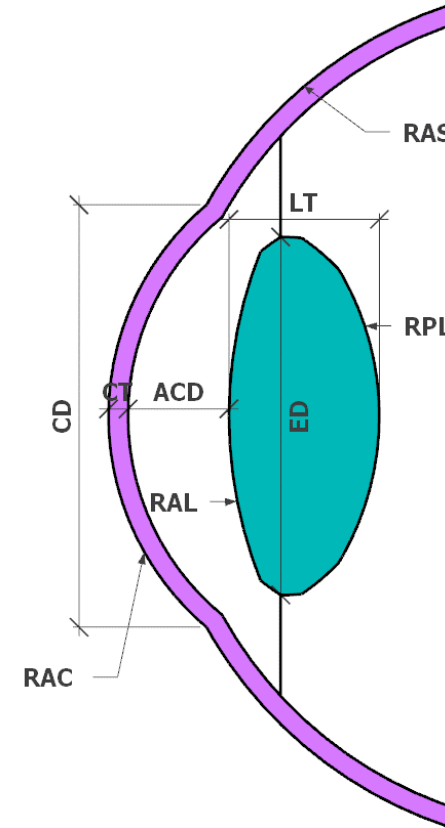
- Due to finite voxel resolutions, the detailed structures of the eyes were not fully modeled in the paediatric VRCPs.

Example: female phantoms



■ Selection of nine anatomical parameters^[3]

| | Parameters | Description |
|--------|------------|-----------------------------------------------------------|
| Lens | ACD | anterior chamber depth along the optical axis |
| | LT | lens thickness along the optical axis |
| | ED | equatorial diameter of the lens |
| | RAL | radius of curvature of the anterior surface of the lens |
| | RPL | radius of curvature of the posterior surface of the lens |
| Cornea | RAC | radius of curvature of the anterior surface of the cornea |
| | CT | corneal thickness along the optical axis |
| | CD | corneal diameter |
| | RAS | radius of curvature of the anterior surface of the sclera |



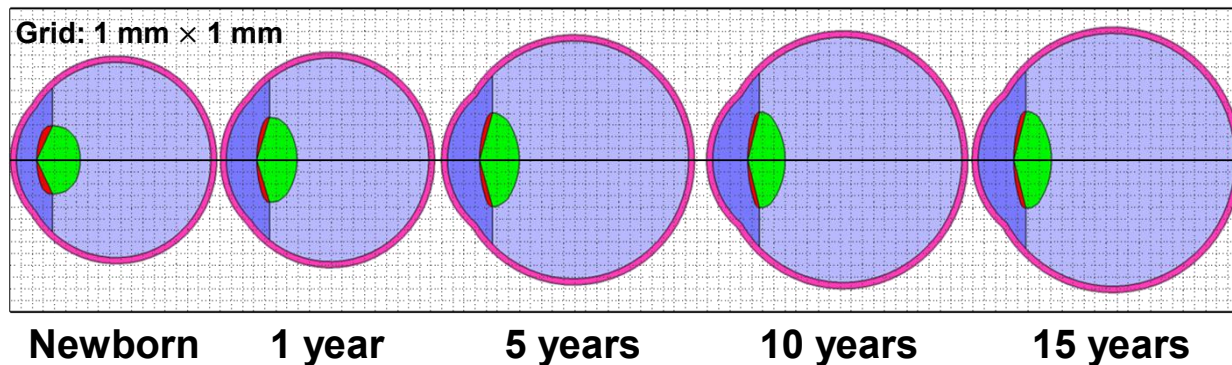
• Data selection criteria

- The large number of samples
- Data measured in vivo
- Unaccommodated eyes
- Normal eyes without any eye disease
- Caucasian paediatric eyes
- Full-term newborns

■ Determination of anatomical parameters

(Unit: mm)

| Parameters | Newborn | 1 year | 5 years | 10 years | 15 years | References |
|------------|---------|--------|---------|----------|----------|--------------------|
| ACD | 1.83 | 2.75 | 2.90 | 3.16 | 3.21 | [4–6] |
| LT | 3.96 | 3.66 | 3.61 | 3.41 | 3.44 | |
| RAL | 6.33 | 9.23 | 10.51 | 11.45 | 11.72 | [7, 8] |
| RPL | 4.48 | 5.27 | 6.05 | 6.24 | 6.55 | |
| RAC | 7.11 | 7.82 | 7.72 | 7.72 | 7.72 | [8–10] |
| CT | 0.55 | 0.55 | 0.56 | 0.57 | 0.57 | [11] |
| CD | 9.66 | 11.15 | 11.80 | 11.80 | 11.80 | [12, 13] |
| ED | 5.95 | 7.40 | 8.20 | 8.37 | 8.43 | [14–19] |
| RAS | 9.10 | 9.45 | 10.96 | 11.30 | 11.63 | Reference eye mass |



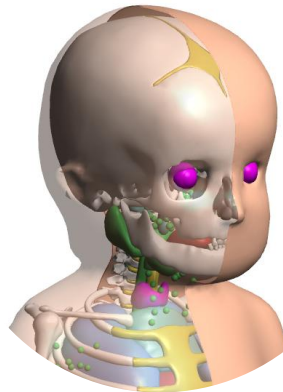
- [4] Larsen, J., 1971. The sagittal growth of the eye: 1. ultrasonic measurement of the depth of the anterior chamber from birth to puberty. *Acta Ophthalmol.* 49, 239–262.
- [5] Larsen, J., 1971. The sagittal growth of the eye: 2. ultrasonic measurement of the axial diameter of the lens and the anterior segment from birth to puberty. *Acta Ophthalmol.* 49, 427–440.
- [6] Zadnik, K., Mutti, D.O., Mitchell, G.L., et al., 2004. Normal eye growth in emmetropic schoolchildren. *Optom. Vis. Sci.* 81, 819–828.
- [7] Mutti, D.O., Zadnik, K., Fusaro, R.E., et al., 1998. Optical and structural development of the crystalline lens in childhood. *Invest. Ophthalmol. Vis. Sci.* 39, 120–133.
- [8] Frane, S.L., Sholtz, R.I., Lin, W.K., et al., 2000. Ocular components before and after acquired, nonaccommodative esotropia. *Optom. Vis. Sci.* 77, 633–636.
- [9] Ehlers, N., Sorensen, T., Bramsen, T., et al., 1976. Central corneal thickness in newborns and children. *Acta Ophthalmol.* 54, 285–290.
- [10] Friedman, N.E., Mutti, D.O., Zadnik, K., 1996. Corneal changes in schoolchildren. *Optom. Vis. Sci.* 73, 552–557.
- [11] PEDIG, 2011. Central corneal thickness in children. *Arch. Ophthalmol.* 129, 1132–1138.
- [12] Müller, A., Doughty, M.J., 2002. Assessments of corneal endothelial cell density in growing children and its relationship to horizontal corneal diameter. *Optom. Vis. Sci.* 79, 762–770.
- [13] Charles, M.W., Brown, N., 1975. Dimensions of the human eye relevant to radiation protection (dosimetry). *Phys. Med. Biol.* 20, 202–218.
- [14] Atchison, D.A., Markwell, E.L., Kasthurirangan, S., et al., 2008. Age-related changes in optical and biometric characteristics of emmetropic eyes. *J. Vis.* 8, 1–20.
- [15] Dilmen, G., Oktener, A., Turhan, T.O., et al., 2002. Growth of the fetal lens and orbit. *Int. J. Gynecol. Obstet.* 76, 267–271.
- [16] Goldstein, I., Tamir, A., Zimmer, E.Z., et al., 1998. Growth of the fetal orbit and lens in normal pregnancies. *Ultrasound Obstet. Gynecol.* 12, 175–179.
- [17] Ishii, K., Yamanari, M., Iwata, H., et al., 2013. Relationship between changes in crystalline lens shape and axial elongation in young children. *Invest. Ophthalmol. Vis. Sci.* 54, 771–777.
- [18] Paquette, L.B., Jackson, H.A., Tavaré, C.J., et al., 2009. In utero eye development documented by fetal MR imaging. *Am. J. Neuroradiol.* 30, 1787–1791.
- [19] Sukonpan, K., Phupong, V., 2009. A biometric study of the fetal orbit and lens in normal pregnancies. *J. Clin. Ultrasound* 37, 69–74.

- **Conversion to mesh format and installation in paediatric MRCPs**

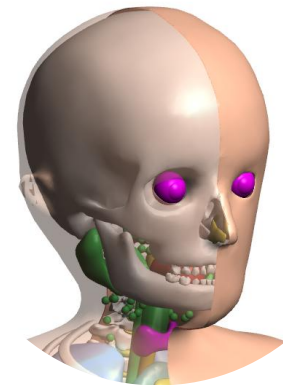
Example: female phantoms



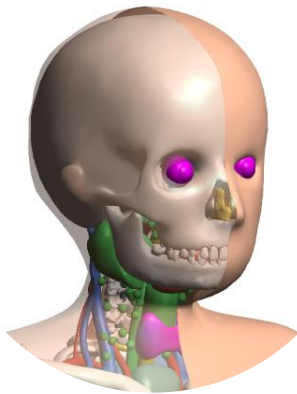
0fMRCP



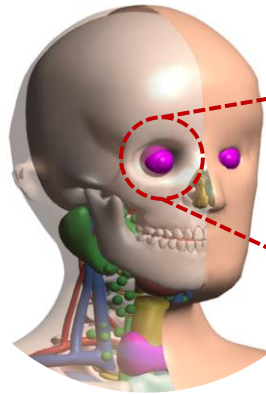
1fMRCP



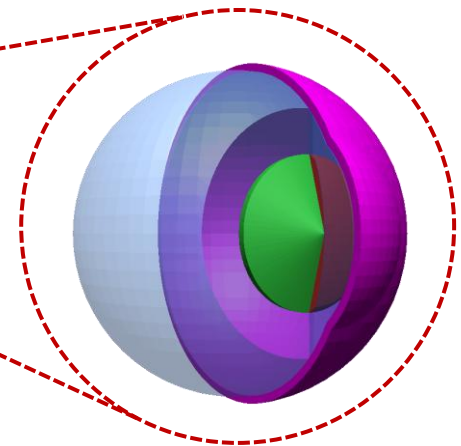
5fMRCP



10fMRCP



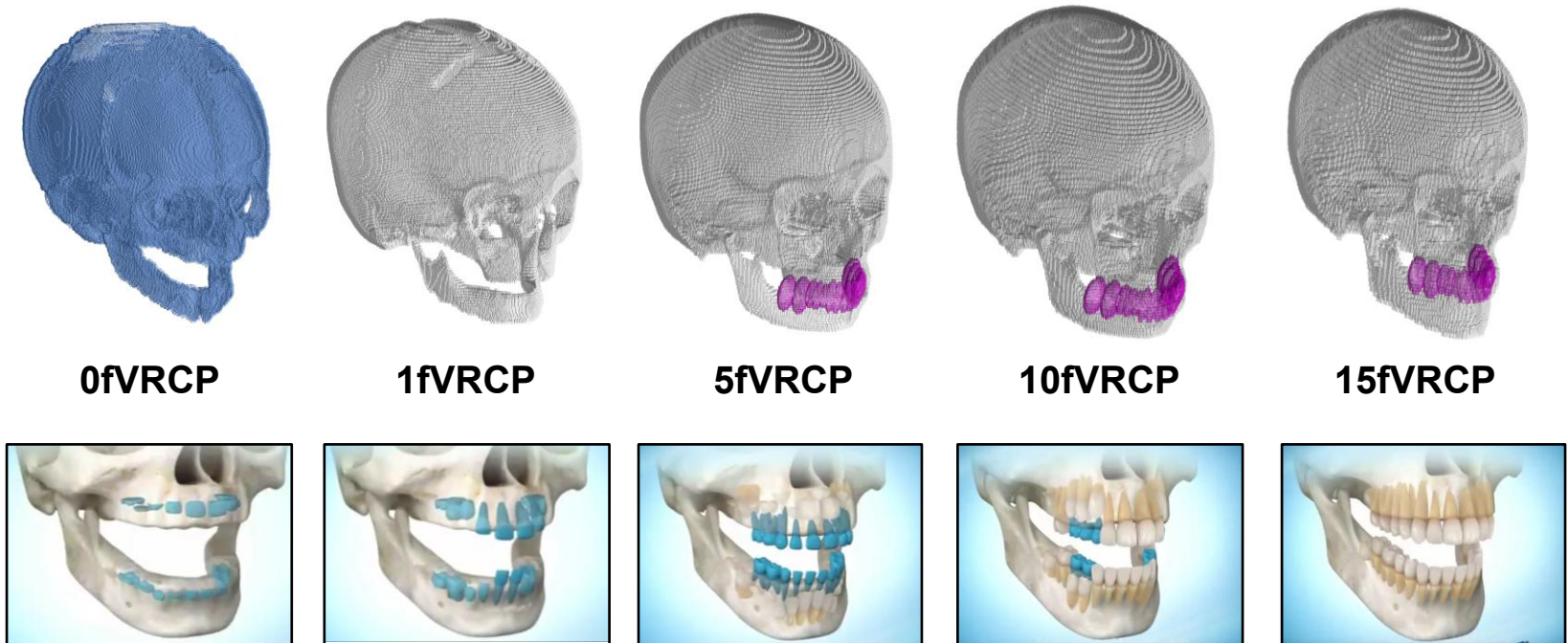
15fMRCP



2) Teeth

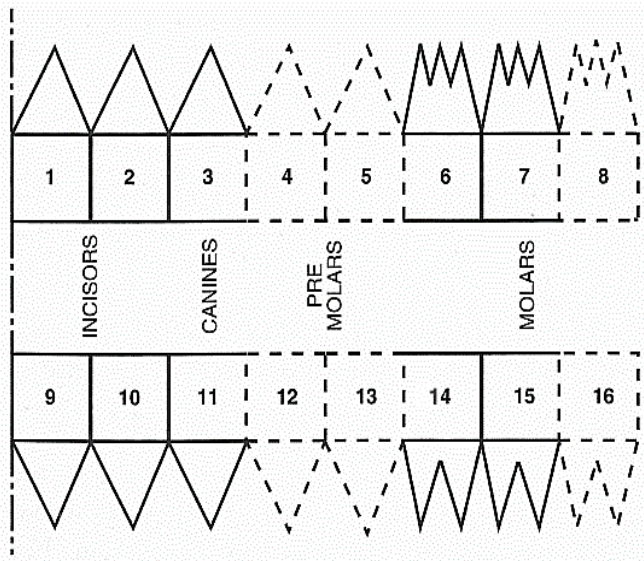
- Teeth of the paediatric VRCPs were defined as a single homogeneous region with a simplified geometry, and anatomical changes with ages were not reflected.

Example: female phantoms



- In the paediatric MRCPs, detailed tooth tissues (i.e., enamel, dentin, cementum, and pulp) were defined, which can be used for separately EPR/ESR dosimetry.

■ Determination of eruption period of teeth^[20, 21]



| Tooth eruption time | | | |
|---------------------|------------------------|-----------------|-----------------------|
| Deciduous teeth | | Permanent teeth | |
| Tooth (i) | Eruption time (months) | Tooth (i) | Eruption time (years) |
| Upper teeth | | Upper teeth | |
| 1 | 8-11 | 1 | 7-8 |
| 2 | 8-11 | 2 | 8-10 |
| 3 | 16-24 | 3 | 11-12 |
| 4 | | 4 | 10-11 |
| 5 | | 5 | 10-12 |
| 6 | 9-21 | 6 | 6-7 |
| 7 | 20-36 | 7 | 12-13 |
| 8 | | 8 | 17-30 |
| Lower teeth | | Lower teeth | |
| 9 | 4-8 | 9 | 6-7 |
| 10 | 7-12 | 10 | 7-10 |
| 11 | 16-25 | 11 | 9-10 |
| 12 | | 12 | 10-12 |
| 13 | | 13 | 11-12 |
| 14 | 9-21 | 14 | 6-7 |
| 15 | 20-36 | 15 | 11-13 |
| 16 | | 16 | 16-30 |

■ Calculation of mass of growing teeth^[21]

$$m_i = m_{0i} \left[1 - \exp\left(-\frac{t - T_{0i}}{\tau_i}\right) \right]$$

m_i : the mass of tooth (i is defined as the relaxational time of the respective tooth(i))

m_0 : the average mass of fully developed permanent and deciduous teeth

T_{0i} : the time when the mineralization of the formation of the tooth mass is observed

τ_i : the relaxational time when m_i is 63.2% of the final mass m_0

t : the time at the moments

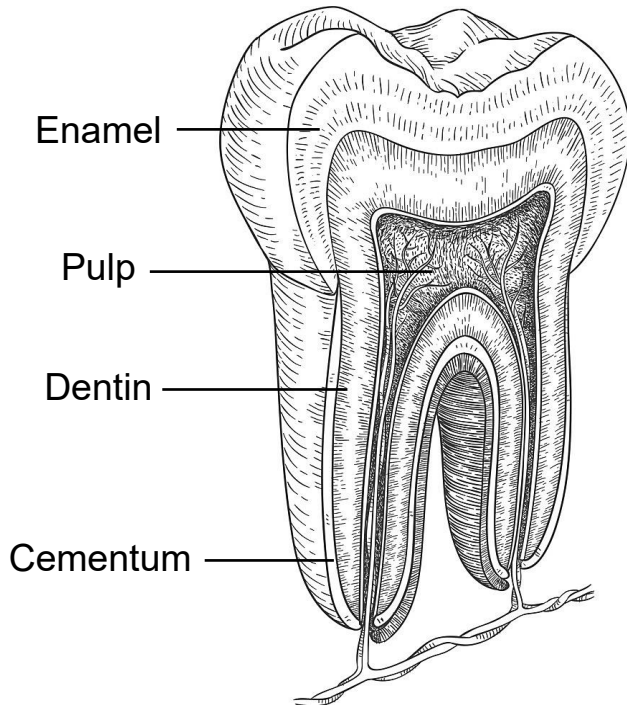
[20] Schwartz, J.H., 1995. *Skeleton keys: an introduction to human skeletal morphology, development, and analysis*. Oxford University Press, Oxford.

[21] Ogorelec, Z., 1997. *The growth of human teeth: a simple description of its kinetics*. *Acta Stomatol. Croat.* 31, 389–395.

■ Calculated individual tooth mass

| Mass of teeth (left + right, g) | | | | | | | | | | | | |
|---------------------------------|---------|-----------|--------------------|-----------|--------------------|-----------|---------------------|-----------|--------------|-----------|----------------|-----------|
| Teeth | Newborn | | 1-year male/female | | 5-year male/female | | 10-year male/female | | 15-year male | | 15-year female | |
| Upper teeth | Erupted | Unerupted | Erupted | Unerupted | Erupted | Unerupted | Erupted | Unerupted | Erupted | Unerupted | Erupted | Unerupted |
| 1 | - | 0.0347 | 0.2838 | 0.2864 | 0.4400 | 0.5292 | 1.9800 | - | 2.2296 | - | 1.7304 | - |
| 2 | - | 0.0310 | 0.2044 | 0.0253 | 0.3200 | 0.3416 | 1.2694 | - | 1.5990 | - | 1.2410 | - |
| 3 | - | 0.0447 | - | 0.2416 | 0.5800 | 0.5848 | 0.5800 | 1.2862 | 2.9504 | - | 2.2896 | - |
| 4 | - | - | - | - | - | 0.4106 | 1.7840 | - | 2.4098 | - | 1.8702 | - |
| 5 | - | - | - | - | - | 0.3680 | - | 1.0750 | 2.5674 | - | 1.9926 | - |
| 6 | - | 0.1111 | - | 0.8044 | 1.1400 | 1.1842 | 4.1198 | - | 5.1124 | - | 3.9676 | - |
| 7 | - | 0.1092 | - | 0.5135 | 1.1600 | 0.4617 | 1.1600 | 1.7649 | 4.1562 | - | 3.2256 | - |
| 8 | - | - | - | - | - | - | - | 0.5336 | - | 2.7232 | - | 2.1135 |
| Lower teeth | Erupted | Unerupted | Erupted | Unerupted | Erupted | Unerupted | Erupted | Unerupted | Erupted | Unerupted | Erupted | Unerupted |
| 9 | - | 0.0398 | 0.1420 | 0.1684 | 0.2200 | 0.2953 | 1.0400 | - | 1.1712 | - | 0.9088 | - |
| 10 | - | 0.0355 | 0.1864 | 0.1903 | 0.2800 | 0.3497 | 1.3000 | - | 1.4638 | - | 1.1362 | - |
| 11 | - | 0.0512 | - | 0.2240 | 0.5200 | 0.5352 | 2.0026 | - | 2.6350 | - | 2.0450 | - |
| 12 | - | - | - | - | - | 0.3402 | - | 0.8562 | 1.9818 | - | 1.5382 | - |
| 13 | - | - | - | - | - | 0.3298 | - | 0.9671 | 2.3198 | - | 1.8002 | - |
| 14 | - | 0.1271 | - | 0.8607 | 1.1400 | 1.2109 | 4.4000 | - | 4.9548 | - | 3.8452 | - |
| 15 | - | 0.1251 | - | 0.9125 | 1.9200 | 0.5368 | 1.9200 | 1.9697 | 4.5278 | - | 3.5140 | - |
| 16 | - | - | - | - | - | - | - | 0.4062 | - | 2.8802 | - | 2.2354 |
| Total teeth | 0.7094 | | 5.0437 | | 15.1980 | | 30.4147 | | 45.6824 | | 35.4535 | |
| Reference teeth mass | 0.7094 | | 5.0437 | | 15.1980 | | 30.4147 | | 45.6824 | | 35.4535 | |

■ Determination of tooth tissue parameters



Tooth anatomy

• Density of tooth tissues^[22–25]

| Tooth type | Density of tooth tissue (g/cm ³) | | | |
|------------|----------------------------------------------|--------|----------|-------|
| | Enamel | Dentin | Cementum | Pulp |
| Deciduous | 2.840 | 2.185 | 2.030 | 1.021 |
| Permanent | 3.000 | 2.140 | 2.030 | 1.021 |

• Volume ratio of tooth tissues^[26, 27]

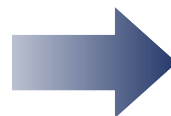
| Tooth type | Tooth tissue | | |
|------------|--------------|---------|-------|
| | Enamel | Dentin* | Pulp |
| Deciduous | 0.199 | 0.625 | 0.177 |
| Permanent | 0.161 | 0.791 | 0.047 |

* According to consultation with our dental anatomist, it was considered as the ratio inclusive of cementum.

• Cementum thickness^[28]

$$y = 0.0325 + 0.00307x$$

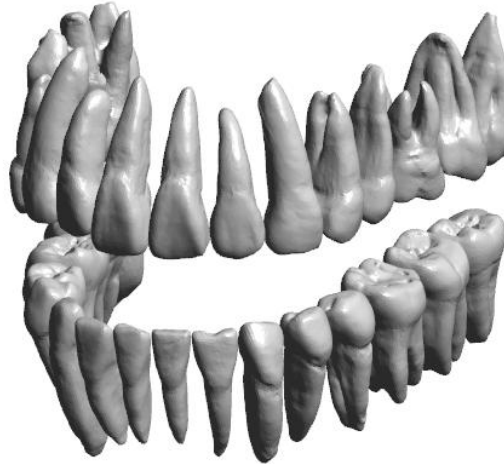
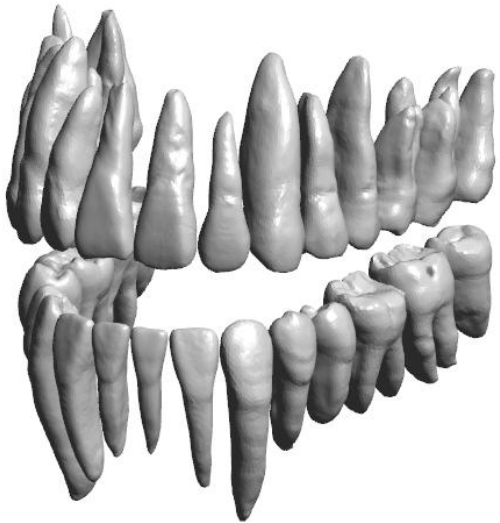
y: thickness of cementum (mm), x: age (year)



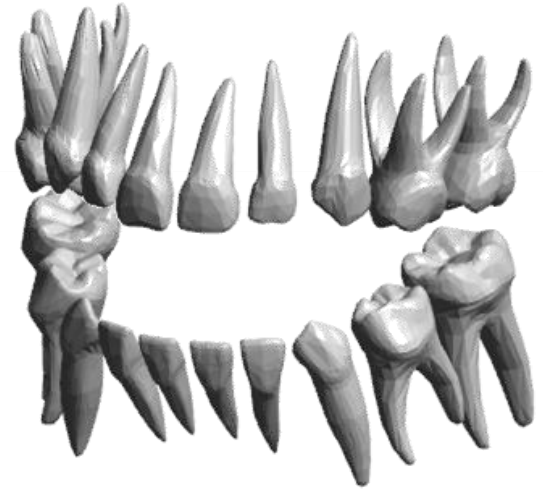
Determine target mass (or volumes) of tooth tissues for each individual tooth

- [22] ICRP, 2002. *Basic anatomical and physiological data for use in radiological protection reference values*. ICRP Publication 89. Ann. ICRP 32.
- [23] Bhussry, B.R., 1958. Chemical and physical studies of enamel from human teeth: 1. Specific gravity and nitrogen content of netael from different surfaces. *J. Dental Research* 37, 832–836.
- [24] Berghash, S.R. and Hodge, H.C., 1940. Density and refractive index studies of dental hard tissues: III. Density distribution of deciduous enamel and dentin. *J. Dental Research* 19, 487–495.
- [25] Trudnowski, R.J. and Rico, R.C., 1974. Specific gravity of blood and plasma at 4 and 37 °C. *Clin. Chem.* 20, 615–616.
- [26] Bayle, P., Braga, J., Mazurier, A., et al., 2009. Brief communication: high-resolution assessment of the dental developmental pattern and characterization of tooth tissue proportions in the late Upper Paleolithic child from La Madeleine, France. *Am. J. Phys. Anthropol.* 138, 493–498.
- [27] ICRP, 1975. *Report on the task group on reference man*. ICRP Publication 23. Pergamon Press, Oxford.
- [28] Zander, H.A., Hürzeler, B., 1958. Continuous cementum apposition. *J. Dent. Research.* 37, 1035–1044.

- **High-quality PM tooth models used to develop the teeth of paediatric MRCPs**



Permanent teeth model: male (left) and female (right)^[29]



Deciduous teeth model^[30]

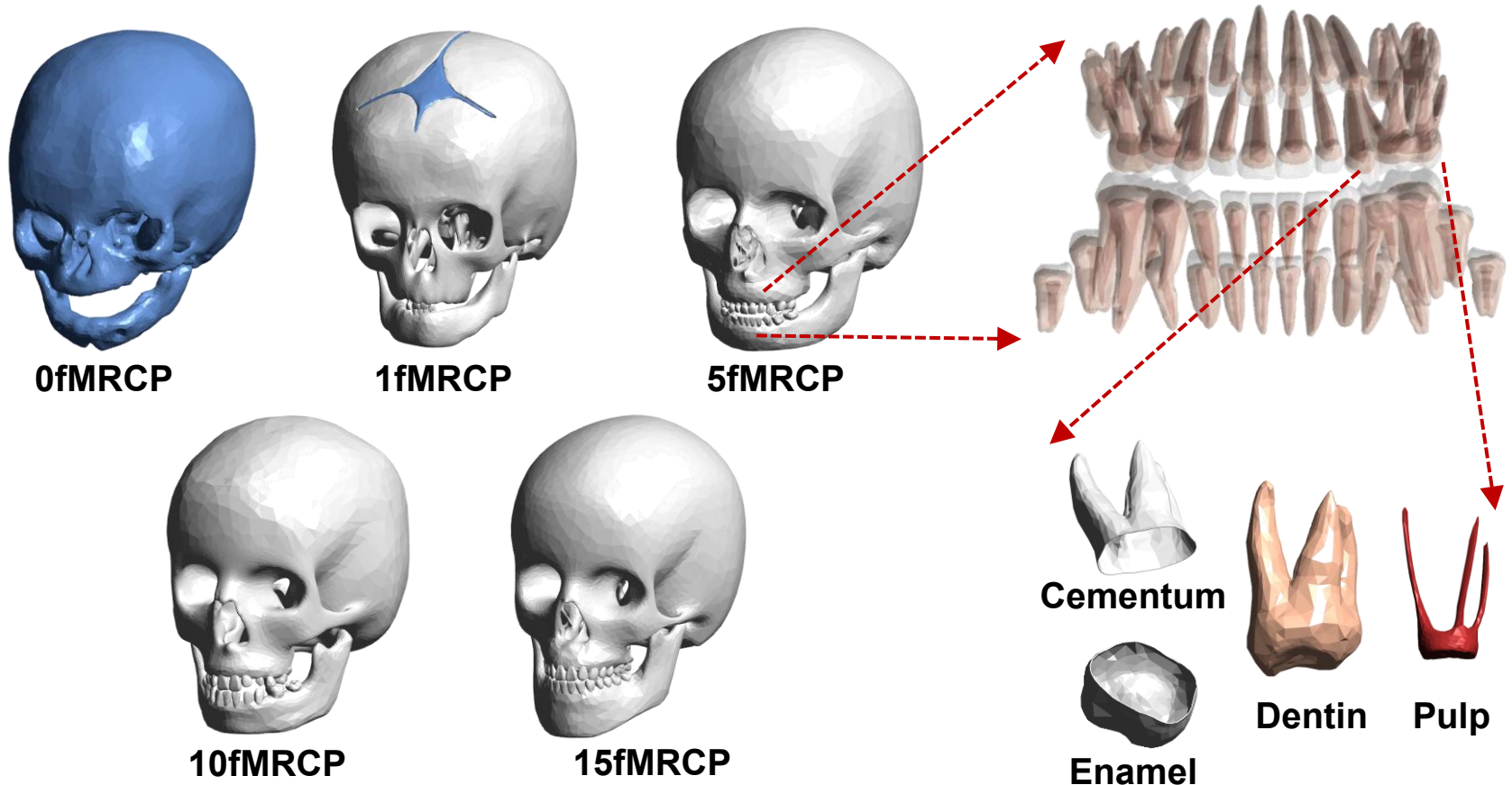
[29] Digital Korean Project. <http://dk.kisti.re.kr>

[30] TurboSquid. Primary Teeth 3D Model. <https://www.turbosquid.com/3d-models/primary-teeth-dentition-max/953912>

■ Construction and installation in paediatric MRCPs

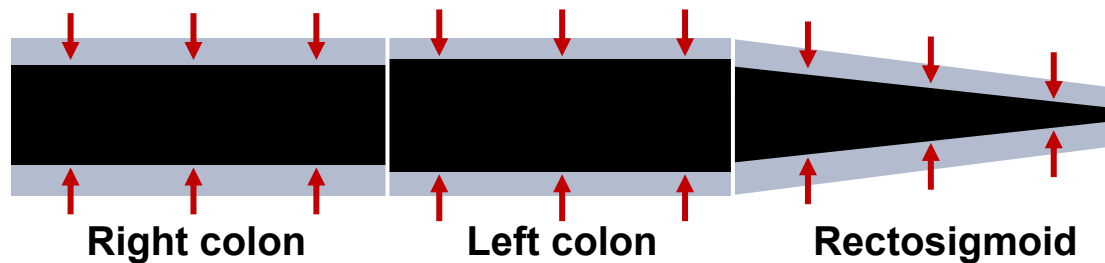
- A total of 332 detailed tooth models (i.e., newborn: 20, 1-year: 28, 5-year: 48, 10-year: 38, 15-year: 32 for male and female, respectively) were constructed individually and then installed into the paediatric MRCPs.

Example: female phantoms



3) Colon

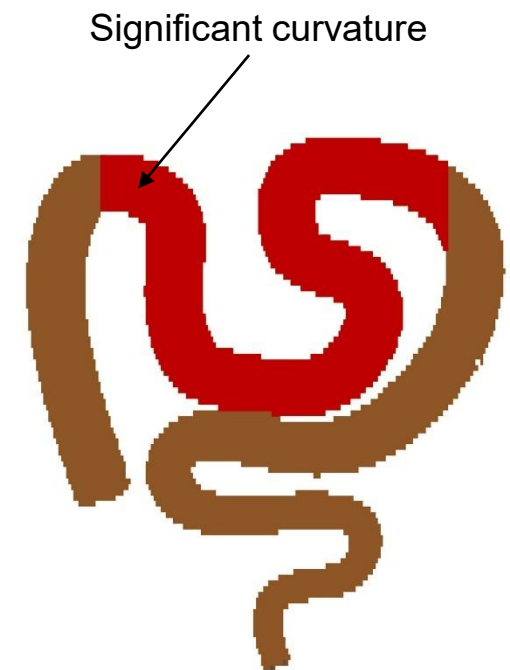
- In the paediatric VRCPs, either the mass or the density of the colon contents was significantly different from the reference values, due to the limitation of the modeling approach using a simple cylinder^[1].
- In addition, the middle part of the transverse colon showed significantly downward curvature.



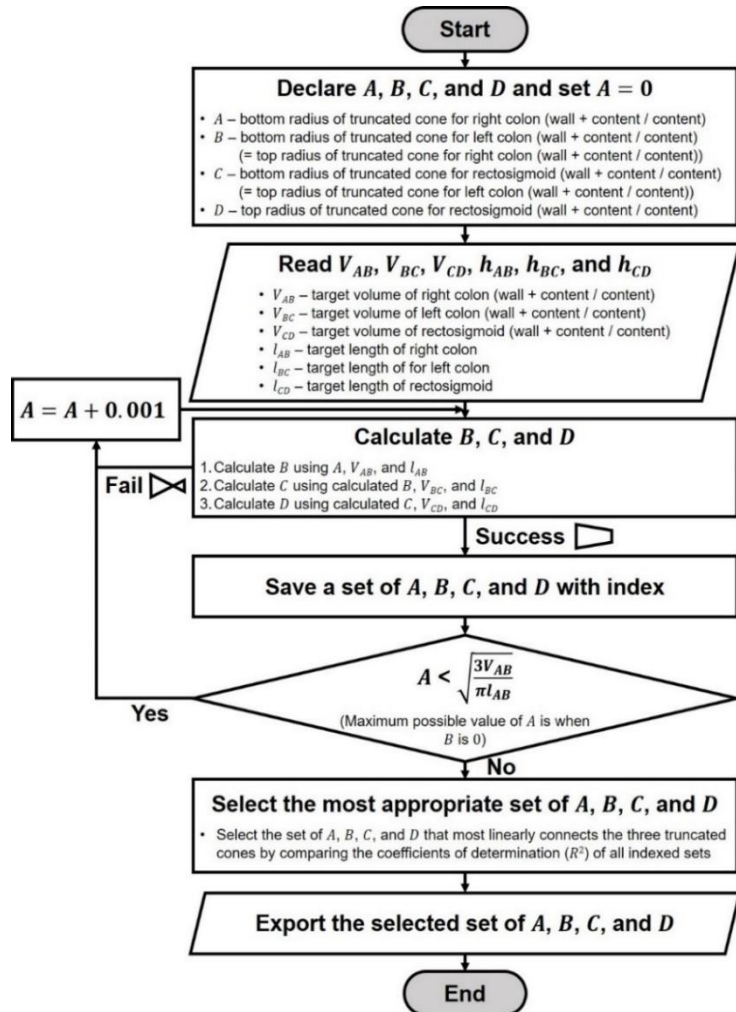
→ Only matched to reference length and wall mass

Example: 1-year male

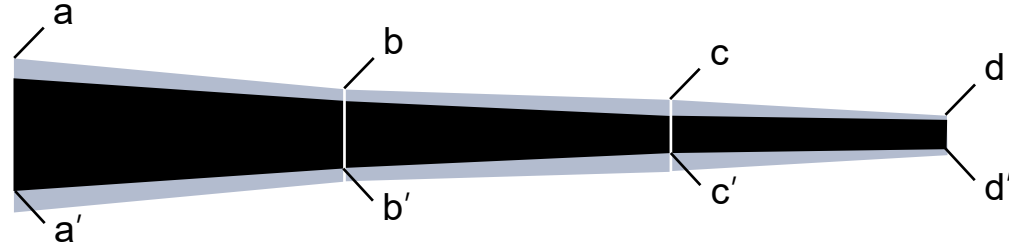
| Content | Volume (cm ³) | Density (g/cm ³) | Mass (g) | Reference mass (g) | Mass ratio |
|--------------|---------------------------|------------------------------|----------|--------------------|------------|
| Right colon | 15 | 1.03 | 15.4 | 40 | 2.6 |
| Left colon | 21 | 0.95 | 19.9 | 20 | 1.0 |
| Rectosigmoid | 14 | 1.03 | 14.6 | 20 | 1.4 |



■ Development of truncated cone model for each colon region



Program flowchart



• Radii of colon wall

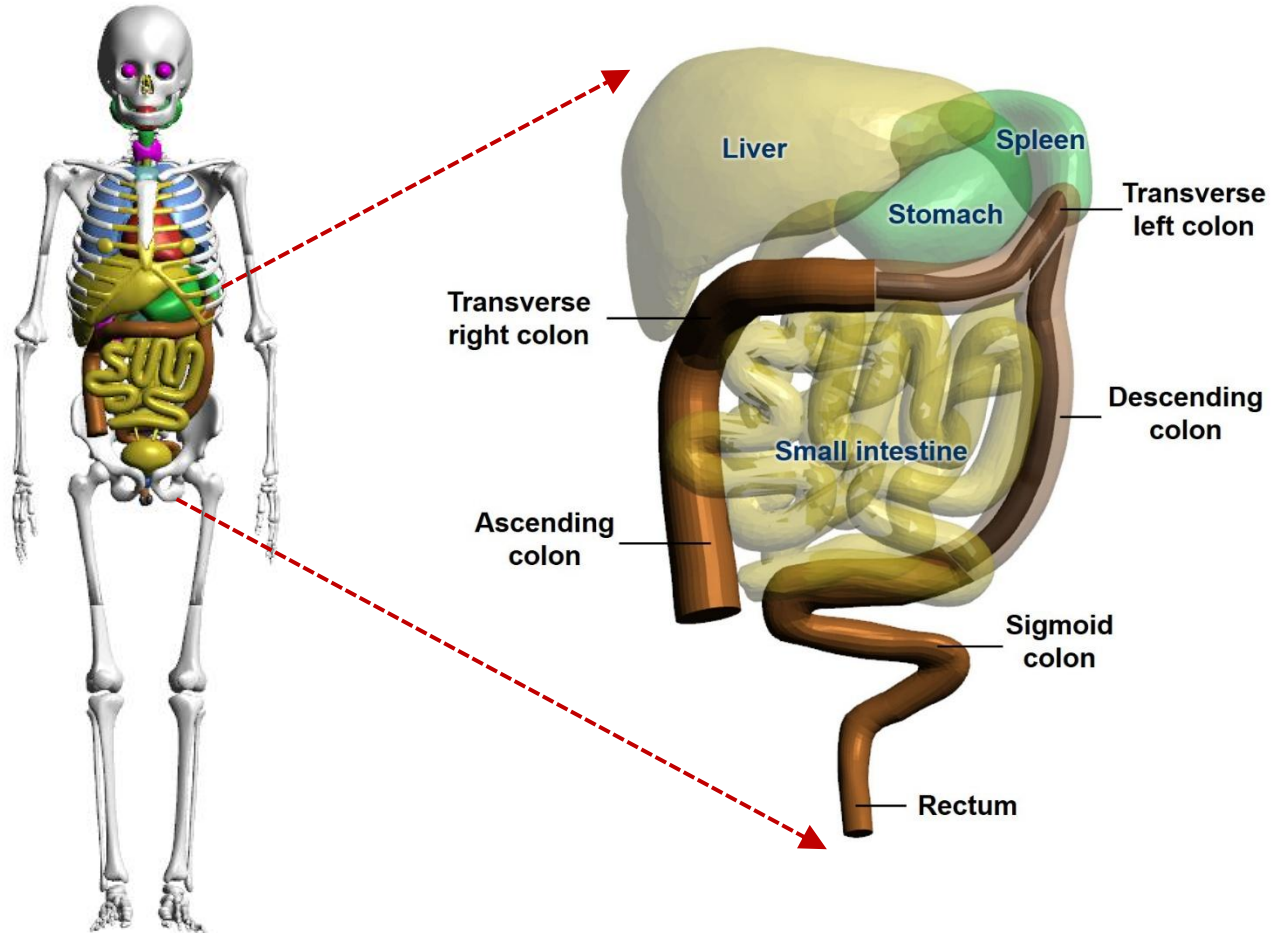
| Age/sex | Determined radius (cm) | | | |
|---------------------|------------------------|-------|-------|-------|
| | a | b | c | d |
| Newborn male/female | 1.011 | 0.681 | 0.587 | 0.554 |
| 1-year male/female | 1.214 | 0.861 | 0.734 | 0.630 |
| 5-year male/female | 1.368 | 1.074 | 0.953 | 0.617 |
| 10-year male/female | 1.555 | 1.231 | 1.145 | 0.678 |
| 15-year male | 1.901 | 1.499 | 1.298 | 0.865 |
| 15-year female | 1.856 | 1.452 | 1.249 | 0.861 |

• Radii of colon content

| Age/sex | Determined radius (cm) | | | |
|---------------------|------------------------|-------|-------|-------|
| | a' | b' | c' | d' |
| Newborn male/female | 0.938 | 0.495 | 0.468 | 0.526 |
| 1-year male/female | 1.069 | 0.562 | 0.522 | 0.562 |
| 5-year male/female | 1.054 | 0.560 | 0.530 | 0.560 |
| 10-year male/female | 1.128 | 0.604 | 0.578 | 0.604 |
| 15-year male | 1.430 | 0.760 | 0.696 | 0.760 |
| 15-year female | 1.430 | 0.760 | 0.696 | 0.760 |

- Construction and installation in paediatric MRCPs

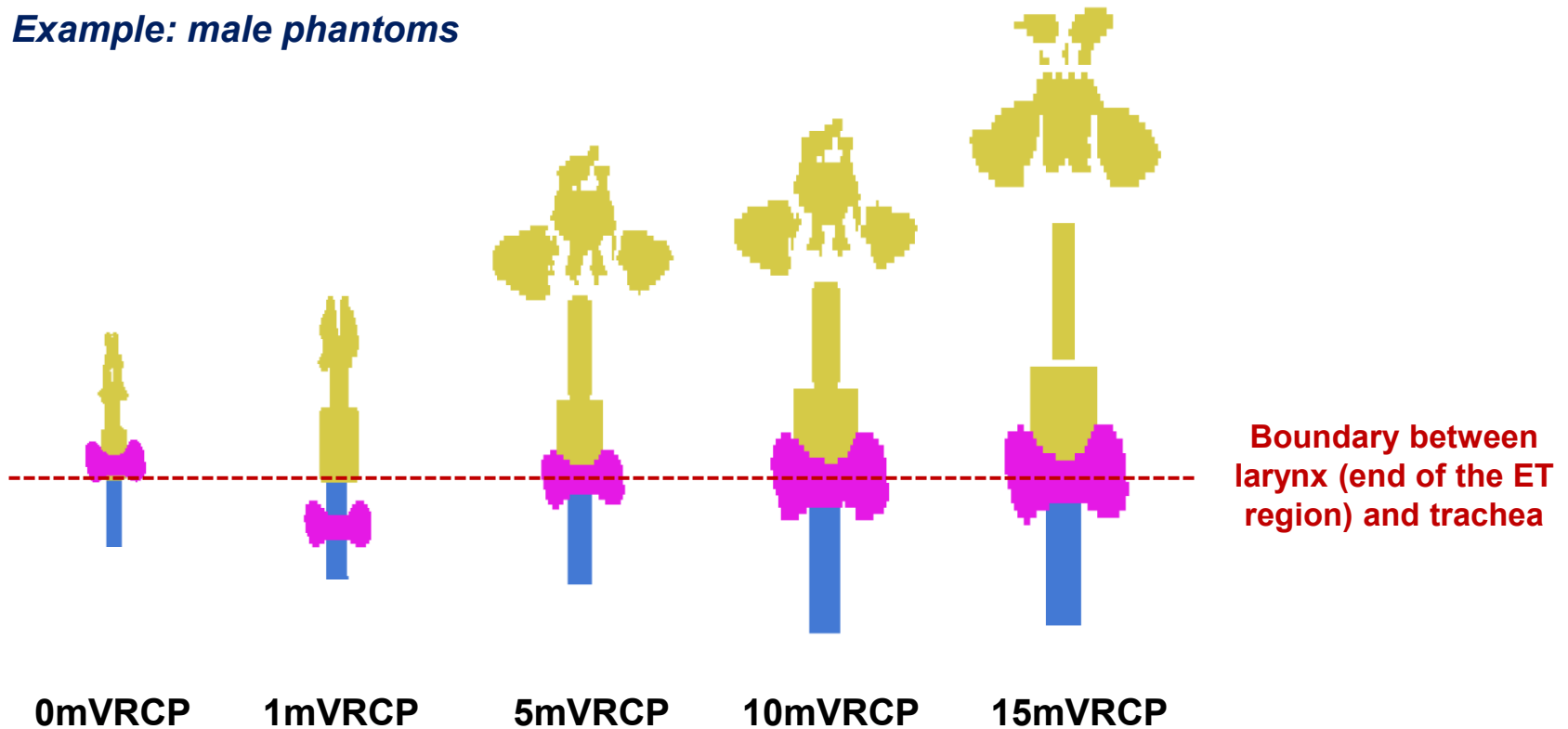
Example: 10mMRCP



4) Thyroid

- For some ages, the thyroid of the paediatric VRCPs is located in an untypical position.

Example: male phantoms

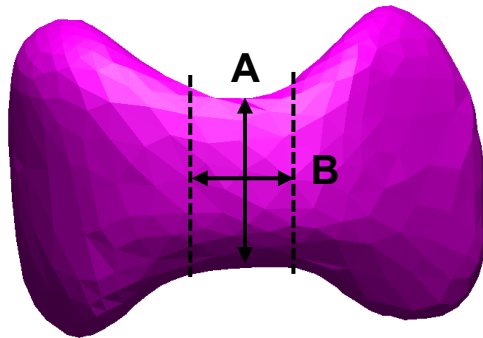


- In addition, the isthmus region of the thyroid of the paediatric VRCPs is thicker than the typical shape.

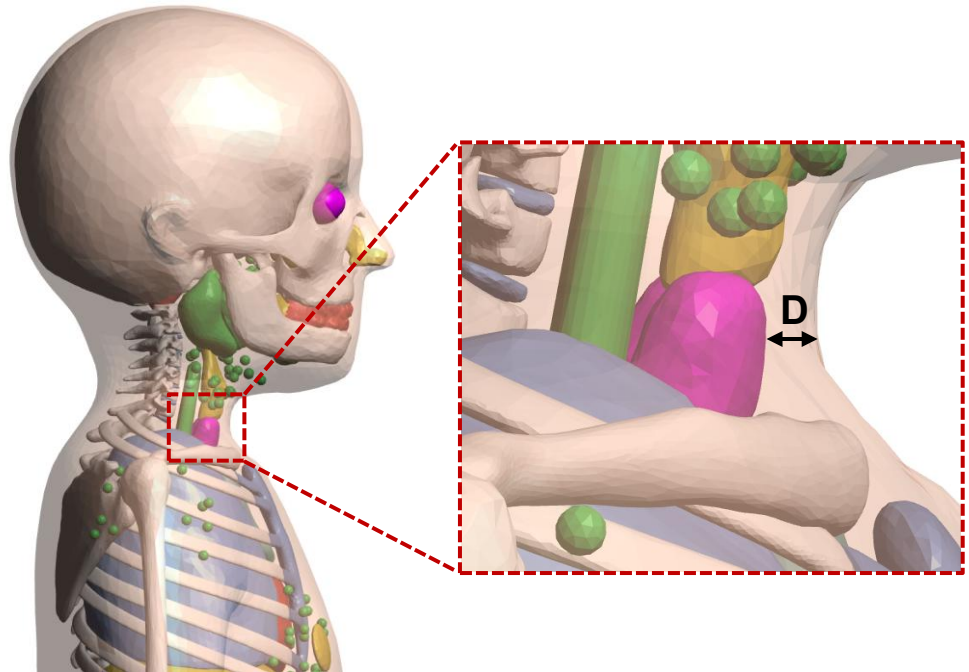
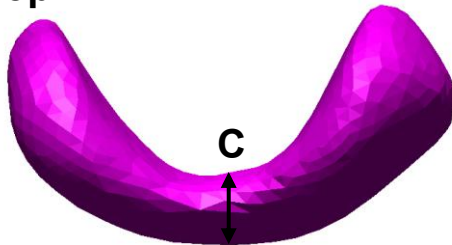
■ Selection of five anatomical parameters

- Isthmus height (A)
- Isthmus width (B)
- Isthmus thickness (C)
- Overlying tissue thickness (D)
- Anatomical location

Front



Top



■ Determination of anatomical parameters

• Isthmus dimensions

| Dimensions | Newborn | 1 year | 5 years | 10 years | 15 years | Adult* |
|------------|---------|------------------------------------------------------------------|---------|----------|----------|---------|
| Height | [31] | <div><div></div><div>Linear interpolation</div><div></div></div> | | | | [32–36] |
| Width | | | | | | |
| Thickness | [37] | | | | | |

* For the interpolation, the adult values were assumed to be the same for 18 years of age, considering that the shape of the thyroid gland hardly changes after reaching young adulthood^[33, 36, 38].

| Dimensions | Newborn | 1 year | 5 years | 10 years | 15 years |
|------------|---------|--------|---------|----------|----------|
| Height | 8.6 mm | 8.9 mm | 10.2 mm | 11.8 mm | 13.5 mm |
| Width | 9.2 mm | 9.5 mm | 10.4 mm | 11.5 mm | 12.6 mm |
| Thickness | 1.5 mm | 1.5 mm | 2.0 mm | 3.0 mm | 3.0 mm |

• Overlying tissue thickness^[39]

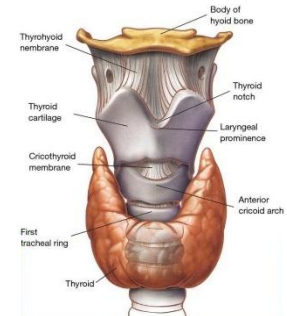
$$d = 0.0007a^2 + 0.025a + 5.2$$

d = overlying tissue thickness (mm)

a = age (y)

• Anatomical location^[40, 41]

- Typically located in front of the second and third tracheal cartilage.

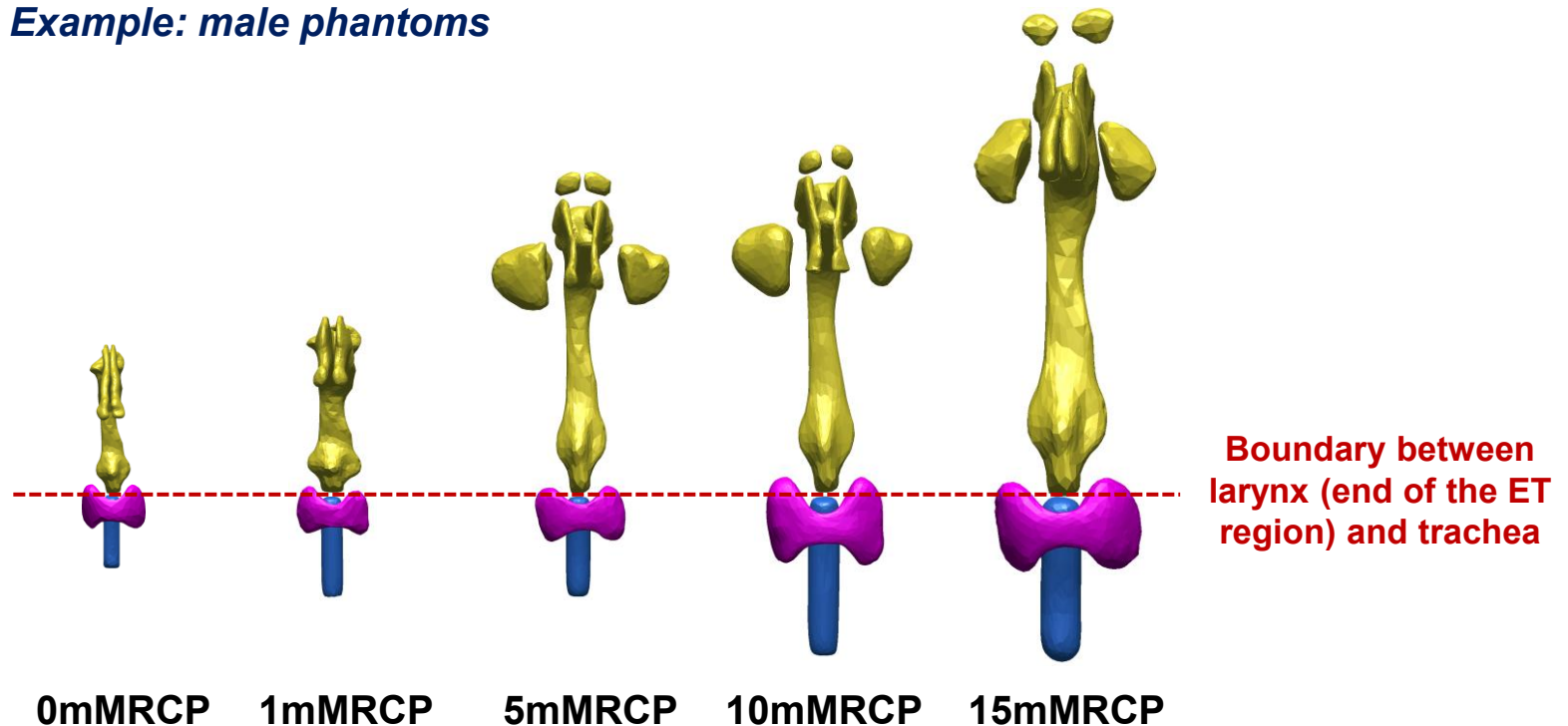


- [31] Ozguner, G., Sulak, O., 2014. Size and location of thyroid gland in the fetal period. *Surg. Radiol. Anat.* 36, 359–367.
- [32] Tong, E.C.K., Rubinfeld, S., 1972. Scan measurements of normal and enlarged thyroid gland. *Am. J. Roentgenol. Radium Ther. Nucl. Med.* 115, 706–708.
- [33] Harjeet, A., Sahni, D., Jit, I., et al., 2004. Shape, measurements and weight of the thyroid gland in northwest Indians. *Surg. Radio. Anat.* 26, 91–95.
- [34] Joshi, S.D., Joshi, S.S., Daimi, S.R., et al., 2010. The thyroid gland and its variations: a cadaveric study. *Folia Morphol.* 69, 47–50.
- [35] Ozgur, Z., Celik, S., Govsa, F., et al., 2011. Anatomical and surgical aspects of the lobes of the thyroid glands. *Eur. Arch. Otorhinolaryngol.* 268, 1357–1363.
- [36] Won, H.S., Han, S.H. Oh, C.S., et al., 2013. The location and morphometry of the thyroid isthmus in adult Korean cadavers. *Anat. Sci. Int.* 88, 212–216.
- [37] Sea, J.H., Ji, H., You, S.K., et al. 2019. Age-dependent reference values of the thyroid gland in paediatric population; from routine computed tomography data. *Clin. Imag.* 56, 88–92.
- [38] Sultana, S.Z., Khalil, M., Khan, M.K., et al., 2011. Morphometry of isthmus of thyroid gland in Bangladeshi cadaver. *Mymensingh Med. J.* 20, 366–370.
- [39] Likhtarev, I.A., Gulko, G.M., Sobolev, B.G., et al., 1995. Evaluation of the ¹³¹I thyroid-monitoring measurements performed in Ukraine during May and June of 1986. *Health Phys.* 69, 6–15.
- [40] Ellis, H, 2007. *Anatomy of the thyroid and parathyroid glands. Surgery, Oxford* 25, 467–468.
- [41] Naqshi, B.F., Seth, S., Shah, A.B., et al., 2016. Thyroid hemiagenesis with agenesis of isthmus a case report. *J. Med. Sci. Clin. Res.* 4, 10799–10801.

■ Modification in paediatric MRCPs

- The height, width, and thickness of the isthmus and the overlying tissue thickness for the thyroid were adjusted to match the target values with the deviations below 3%.
- Thyroids were located in front of the second and third tracheal cartilages.

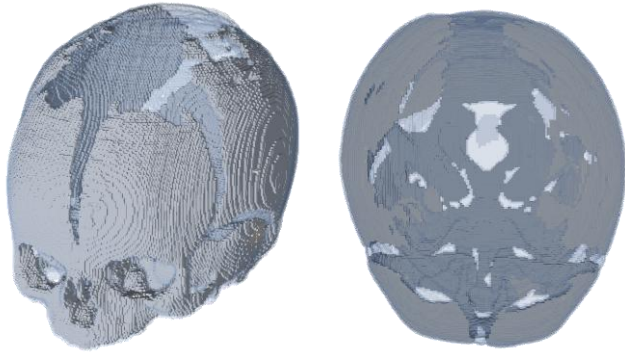
Example: male phantoms



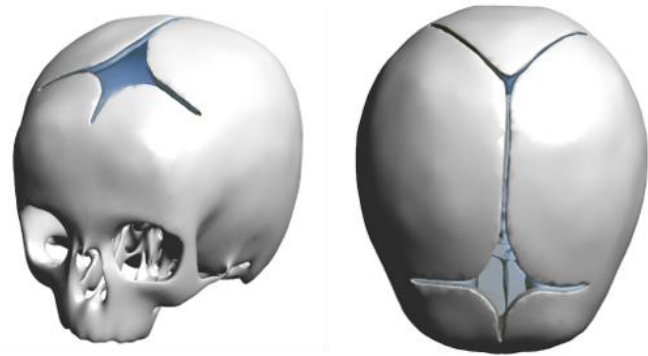
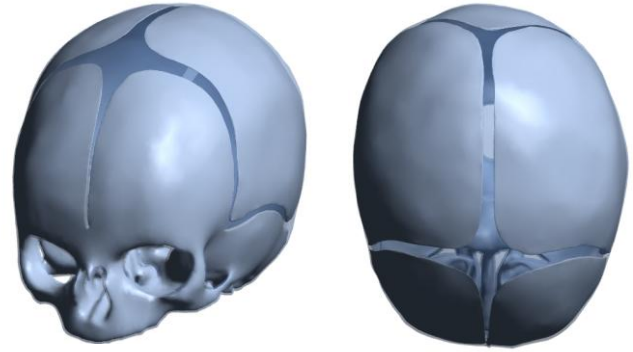
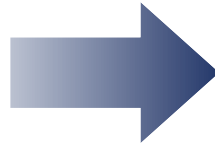
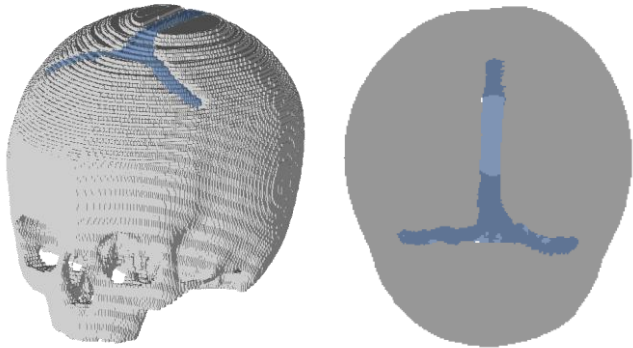
5) Cranium (Newborn and 1 year)

- For the paediatric MRCPs, the cranium was remodeled for newborn and 1 year, referring to anatomical literature^[42–46].

Example: newborn male phantom



Example: 1-year male phantom



Paediatric VRCPs

Paediatric MRCPs

[42] Noorizadeh, N., Kazemi, K., Grebe, R., et al., 2015. Evaluation of anterior fontanel size and area in the newborn using CT images. J. Intell. Fuzzy. Syst. 29, 443–450.

[43] Duc, G., Largo, R.H., 1986. Anterior fontanel: size and closure in term and preterm infants. Pediatrics 78, 904–908

[44] Faix, R.G., 1982. Fontanelle size in black and white term newborn infants. J. Pediatr. 100, 304–306.

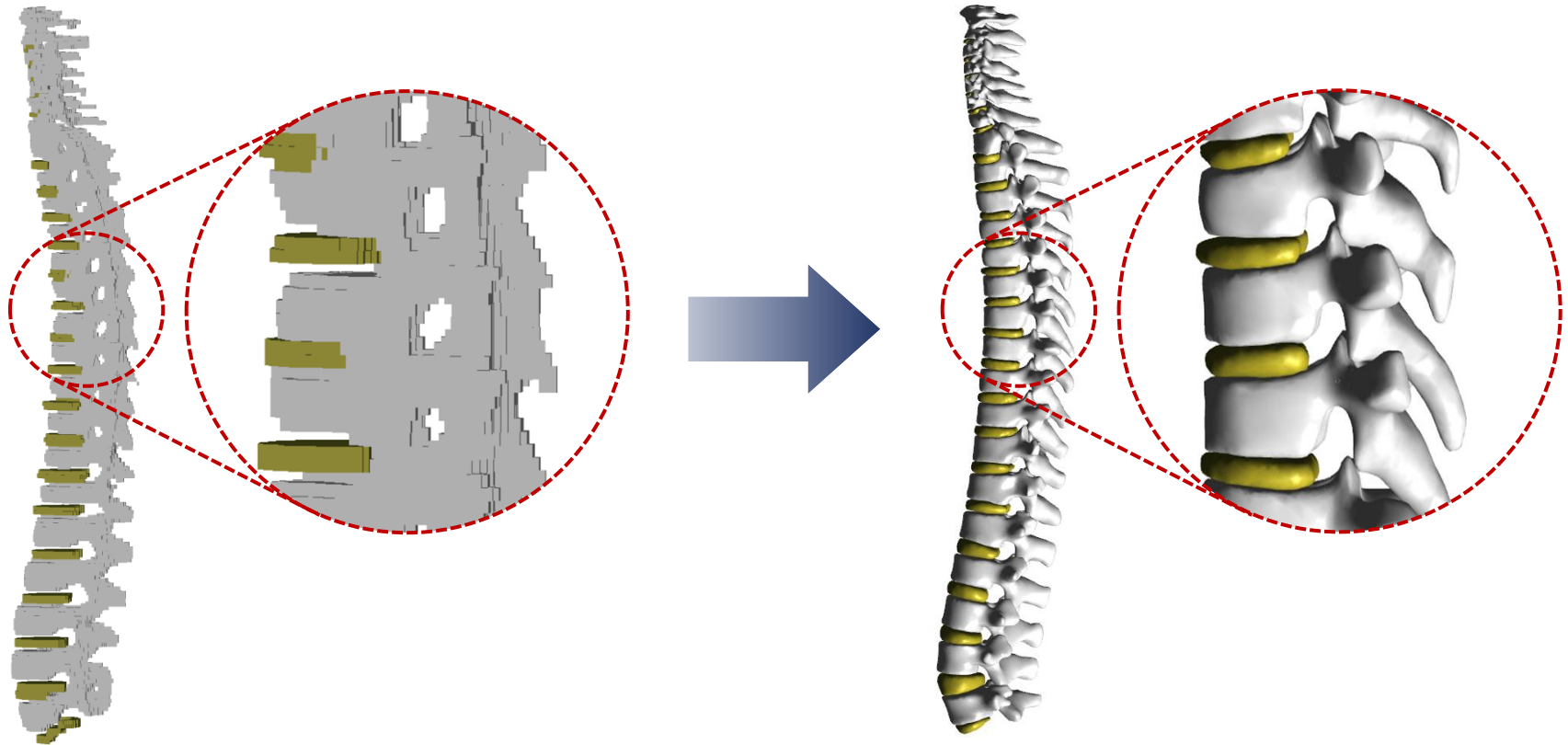
[45] Usman, N., Dilkash, N.A., Khan, S., et al. 2011. Study of relationship between changes in size of posterior fontanelle with gestational age. Natl. J. Integr. Res. Med. 2, 1–3.

[46] Li, Z., Park, B.K., Liu, W., et al., 2015. A statistical skull geometry model for children 0–3 years old. PLoS One 10, 1–13.

6) Spine (1, 5, 10, and 15 years)

- For the paediatric MRCPs, the spine was developed by adjusting the high-quality spine models^[47] to the paediatric VRCPs, piece by piece^[48].

Example: 5-year male phantom



Paediatric VRCPs

Paediatric MRCPs

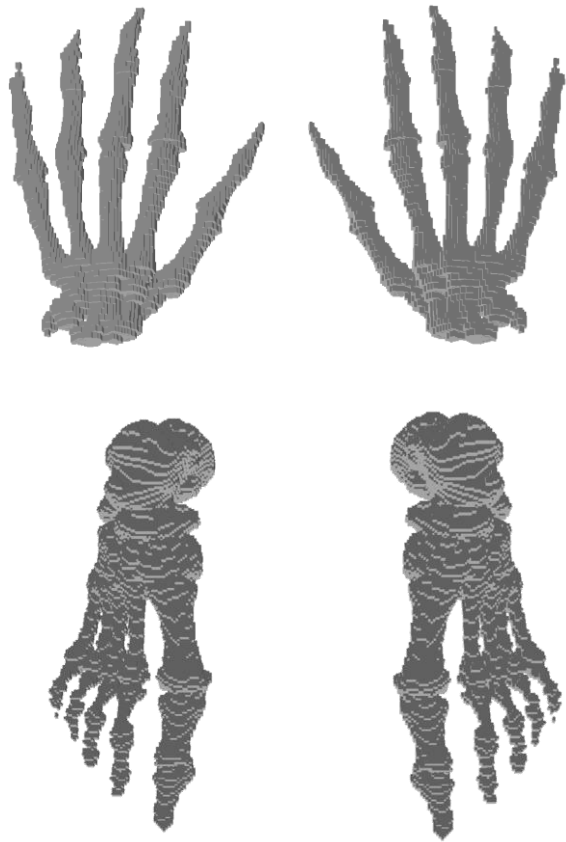
[47] Park, J.S., Chung, M.S., Hwang, S.B., et al., 2005. Visible Korean Human: improved serially sectioned images of the entire body. *IEEE Trans. Med. Imaging* 24, 352–360.

[48] Taylor, J.R., 1975. Growth of human intervertebral discs and vertebral bodies. *J. Anat.* 120, 49–68.

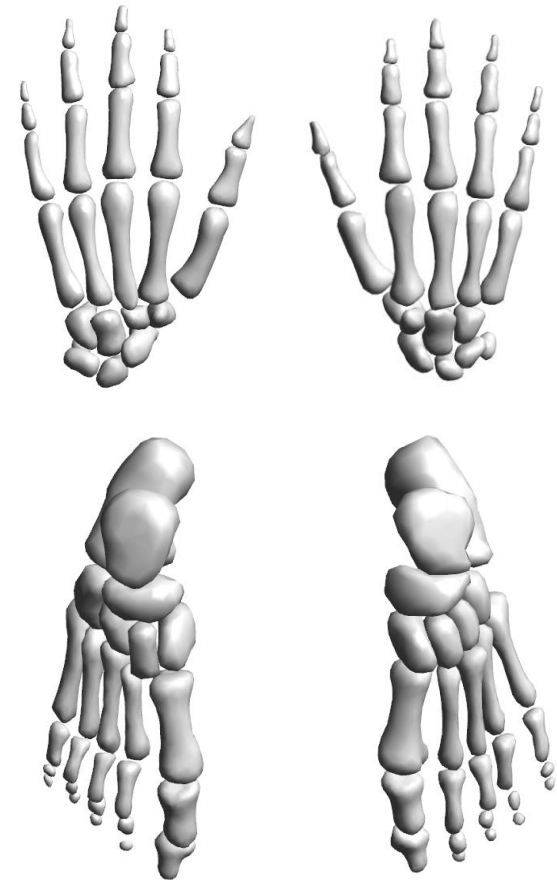
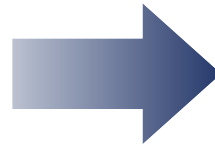
7) Hand/Foot Bones (1, 5, 10, and 15 years)

- For the paediatric MRCPs, the same approach was used for the hand and foot bones^[29].

Example: 10-year male phantom



Paediatric VRCPs

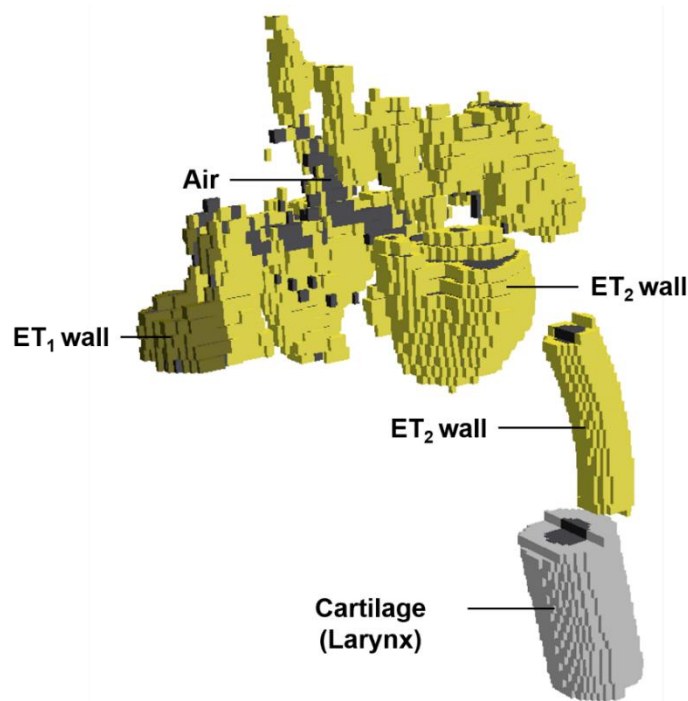


Paediatric MRCPs

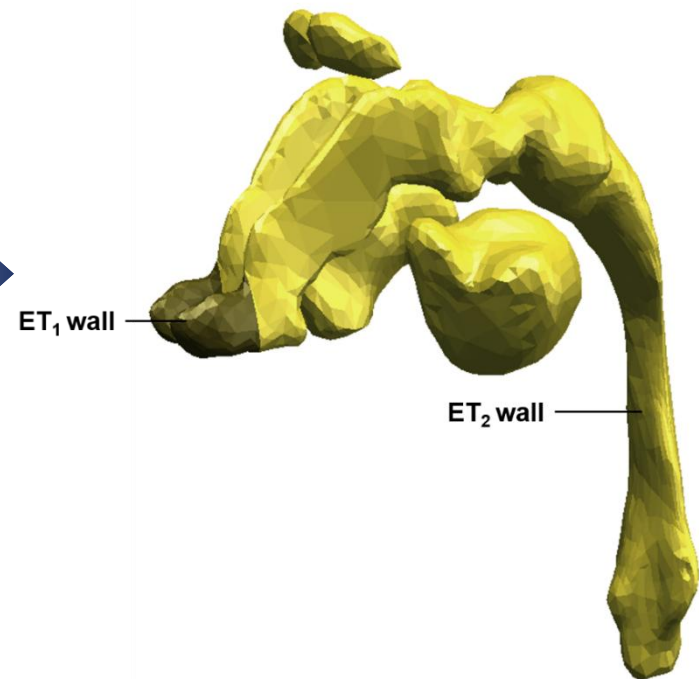
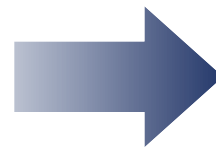
8) Extrathoracic (ET) Region

- For the paediatric MRCPs, the ET region was remodeled; the anterior nose and the posterior nasal passage were modified referring to anatomical literature^[49], and the remaining parts were constructed by scaling down those of the adult MRCPs.

Example: 5-year male phantom



Paediatric VRCPs

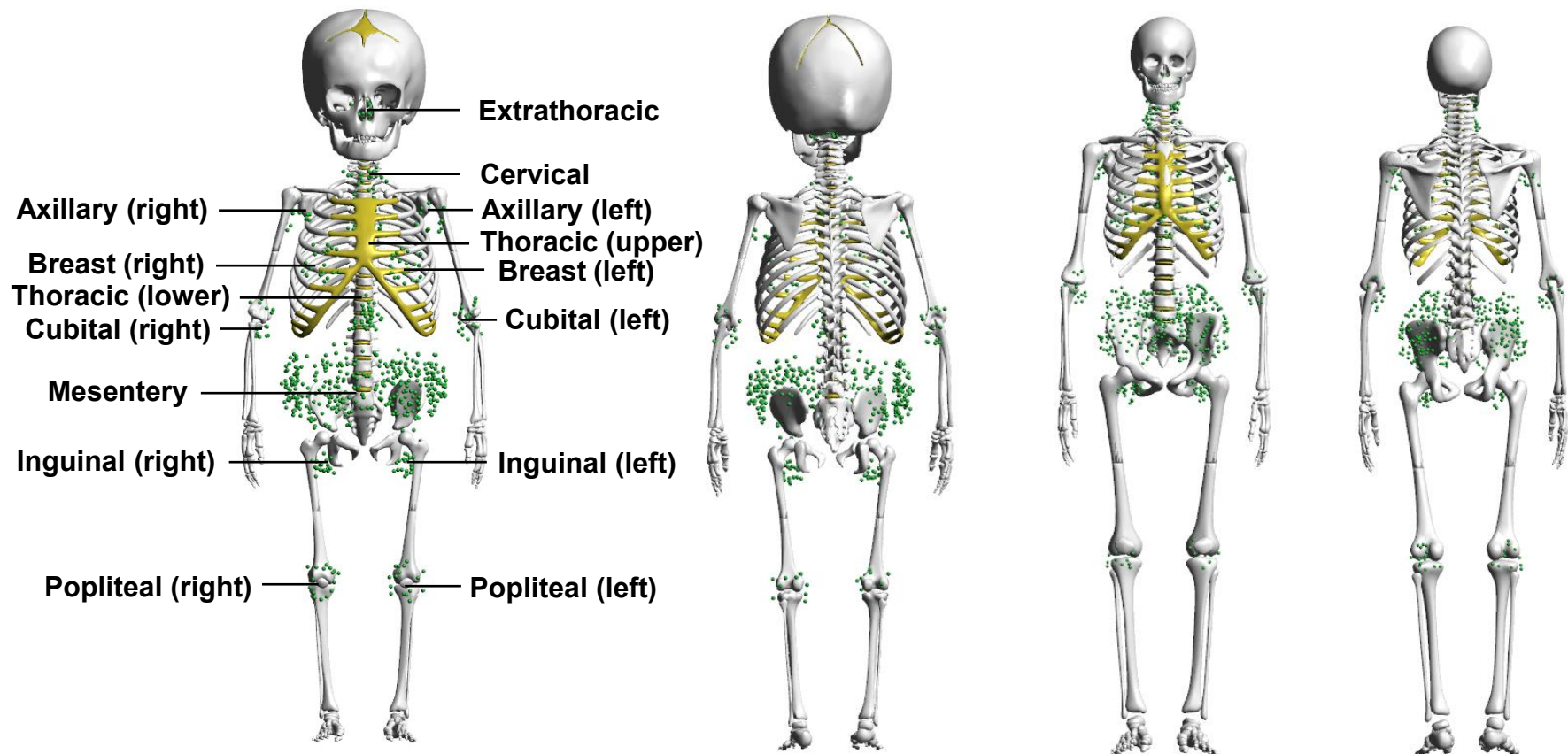


Paediatric MRCPs

9) Lymphatic Nodes

- For the paediatric MRCPs, the lymphatic nodes were generated using the same computer program that was used for the adult MRCPs.

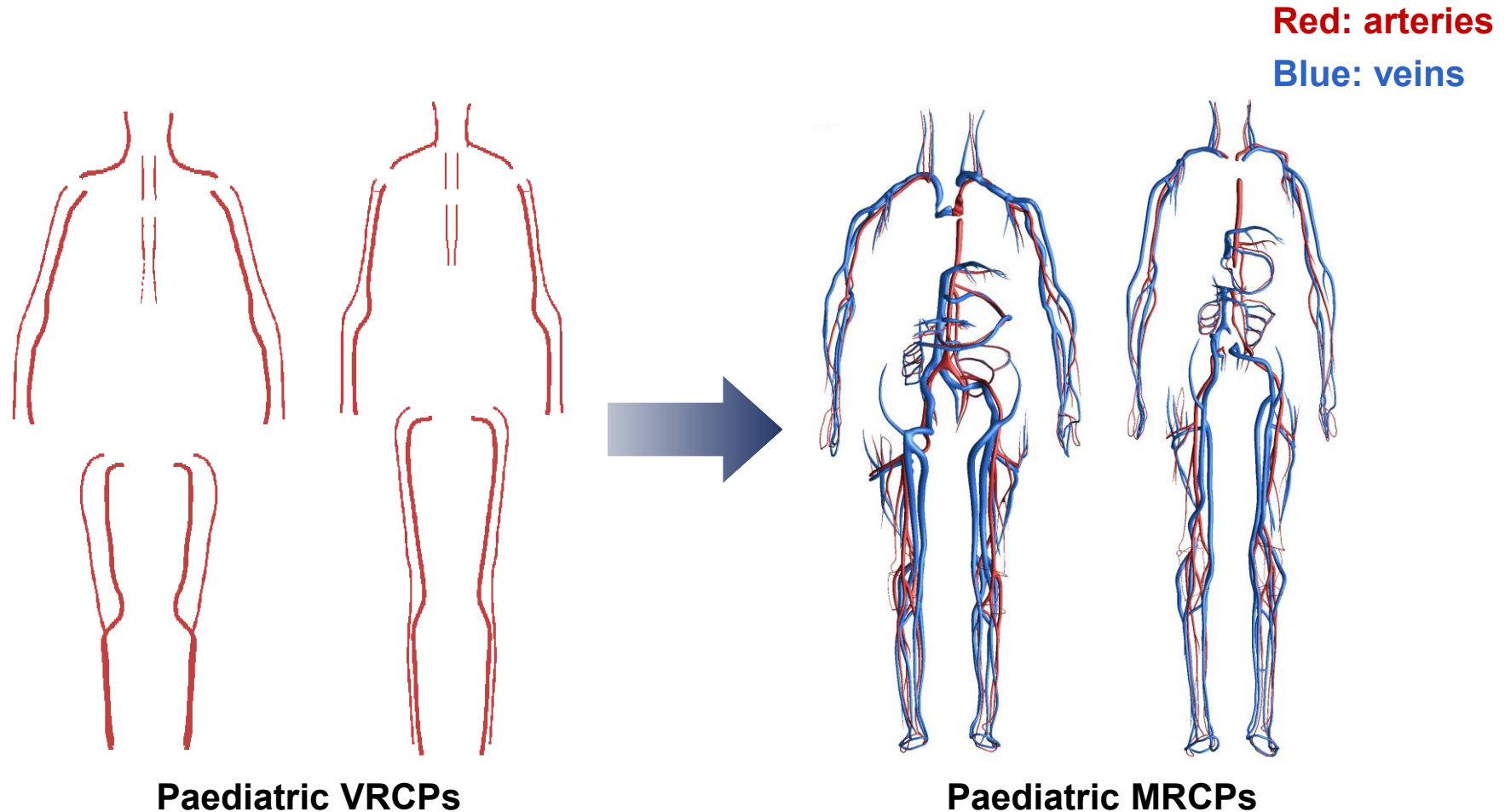
Example: 1mMRCP (left) and 15fMRCP (right)



10) Blood in Large Vessels

- For the paediatric MRCPs, the blood in large vessels was remodeled referring to anatomical literature^[50] and in consultation with the anatomist.

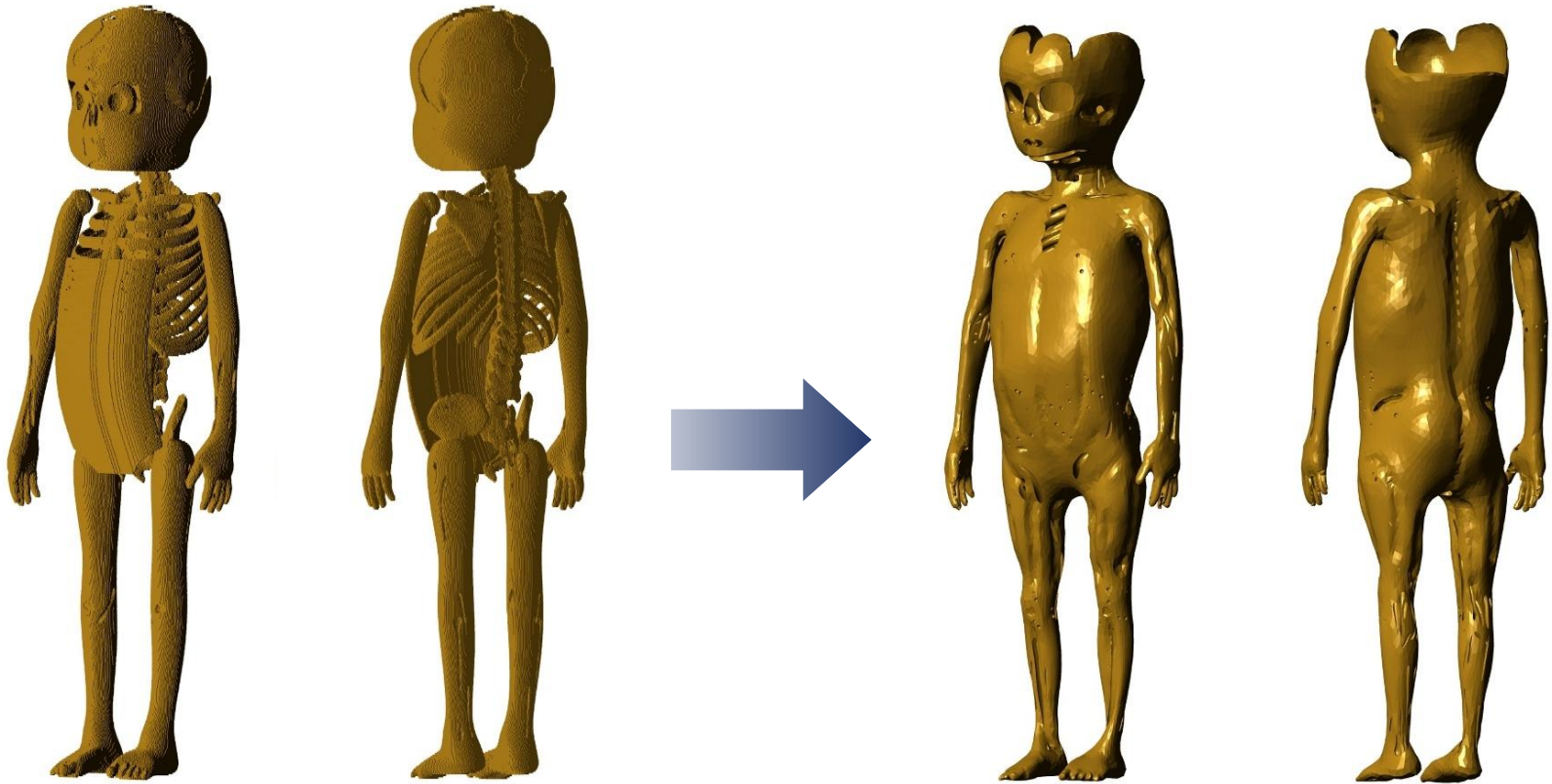
Example: 1-year male (left) and 15-year female (right) phantoms



11) Muscle

- For the paediatric MRCPs, the muscle was constructed in consultation with the anatomist.

Example: 1-year female phantom



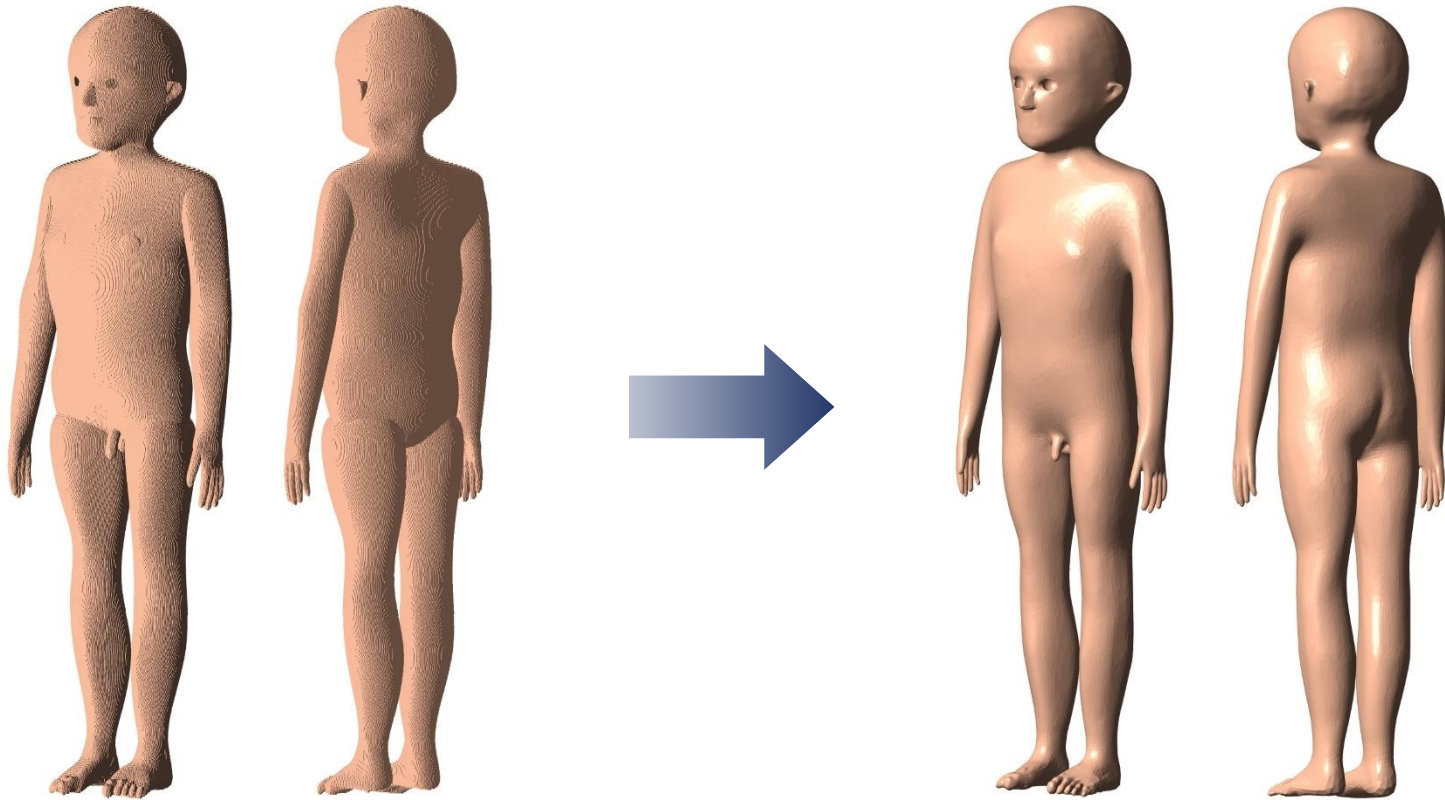
Paediatric VRCPs

Paediatric MRCPs

12) Exterior Body Contour

- For the paediatric MRCPs, the exterior body shape was modified to have more natural shape, matching the reference morphometric values within 5% of difference.

Example: 5-year male phantom



Paediatric VRCPs

Paediatric MRCPs

Other Organs

- **Oesophagus**
- **Tongue**
- **Sacrum (1, 5, 10, and 15 years)**
- **Sternum (1, 5, and 10 years)**
- **Mandible (1 and 10 years)**
- **Liver (newborn)**



II . Inclusion of Blood in Organs and Tissues

Necessity to Consider Intra-organ Blood Content

- Organs of the VRCs are generally based on the ICRP-89 reference masses^[22], which are not inclusive of intra-organ blood content.
- In a living person, a considerable amount of blood is situated in the small vessels and capillaries in the organs.
- Consideration of the blood content is necessary in phantom construction, especially for the purpose of internal dosimetry (e.g., cross-fire of weakly-penetrating radiations and self-irradiation).

ICRP Publication 89

Table 2.8 (continued)

| Organ/tissue | Newborn | 1 year | 5 years | 10 years | 15 years | | Adult | | Sec Section |
|--------------|---------|--------|---------|----------|----------|---|-------|---|-------------|
| | | | | | M | F | M | F | |

ICRP Publication 89

2.3. Postnatal period

2.3.1. Anatomical data

Table 2.8. Reference values for masses of organs and tissues as a function of age (g)

| Organ/tissue | Newborn | 1 year | 5 years | 10 years | 15 years | | Adult | | Sec Section |
|---------------------------------------------------|---------|--------|-----------|-----------|----------|--------|--------|--------|-------------|
| | | | | | M | F | M | F | |
| Adipose tissue* | 930 | 3800 | 5500 | 8600 | 12 000 | 18 700 | 18 200 | 22 500 | 11.1,2 |
| Separable adipose tissue, excluding yellow marrow | 890 | 3600 | 5000 | 7500 | 9500 | 16 000 | 14 500 | 19 000 | 11.1,2 |
| Adrenals (2) | 6 | 4 | 5 | 7 | 10 | 9 | 14 | 13 | 11.2,1 |
| Alimentary system | | | | | | | | | |
| Tongue | 3.5 | 10 | 19 | 32 | 56 | 53 | 73 | 60 | 6.3,4 |
| Salivary glands | 6 | 24 | 34 | 44 | 68 | 65 | 85 | 70 | 6.3,2 |
| Oesophagus | 2 | 5 | 10 | 18 | 30 | 30 | 40 | 35 | 6.3,8 |
| Stomach | 7 | 20 | 50 | 85 | 120 | 120 | 150 | 140 | 6.3,9 |
| Contents | 40 | 67 | 83 | 117 | 200 | 200 | 250 | 230 | 6.4,5 |
| Small intestine | 30 | 85 | 220 | 370 | 520 | 520 | 650 | 600 | 6.3,10 |
| Wall | 56 | 93 | 117 | 163 | 280 | 280 | 350 | 280 | 6.4,5 |
| Contents | | | | | | | | | |
| Large intestine | | | | | | | | | |
| Right colon | 7 | 20 | 49 | 85 | 122 | 122 | 150 | 145 | 6.3,11 |
| Wall | 24 | 40 | 50 | 70 | 120 | 120 | 150 | 160 | 6.4,5 |
| Contents | | | | | | | | | |
| Left colon | 7 | 20 | 49 | 85 | 122 | 122 | 150 | 145 | 6.3,11 |
| Wall | 12 | 20 | 25 | 35 | 60 | 60 | 75 | 80 | 6.4,5 |
| Contents | | | | | | | | | |
| Rectosigmoid | 3 | 10 | 22 | 40 | 56 | 56 | 70 | 70 | 6.3,11 |
| Wall | 12 | 20 | 25 | 35 | 60 | 60 | 75 | 80 | 6.4,5 |
| Contents | 130 | 330 | 570 | 830 | 1300 | 1300 | 1800 | 1400 | 6.3,12 |
| Liver | | | | | | | | | |
| Gallbladder | 0.5 | 1.4 | 2.6 | 4.4 | 7.7 | 7.7 | 10 | 8 | 6.3,13 |
| Wall | 2.8 | 8 | 15 | 26 | 45 | 42 | 58 | 48 | 6.3,13 |
| Pancreas | 6 | 20 | 35 | 60 | 110 | 100 | 140 | 120 | 6.3,14 |
| Brain | 380 | 950 | 1310/1180 | 1400/1220 | 1420 | 1300 | 1450 | 1300 | 11.3,1 |
| Breasts | | | | | 15 | 250 | 25 | 500 | 11.4,1 |
| Circulatory system | | | | | | | | | |
| Heart - with blood* | 46 | 98 | 220 | 370 | 660 | 540 | 840 | 620 | 7.1,1 |
| Heart - tissue only | 20 | 50 | 85 | 140 | 230 | 220 | 330 | 250 | 7.1,1 |
| Blood | 290 | 530 | 1500 | 2500 | 4800 | 3500 | 5600 | 4100 | 7.4 |
| Eyes (2) | 6 | 7 | 11 | 12 | 13 | 13 | 15 | 15 | 11.7,1 |
| Fat (storage fat)* | 370 | 2300 | 3600 | 6000 | 9000 | 14 000 | 14 600 | 18 000 | 4.3,3 |
| Integumentary system | | | | | | | | | |
| Skin | 175 | 350 | 570 | 820 | 2000 | 1700 | 3300 | 2300 | 10.5 |
| Muscle, skeletal | 800 | 1900 | 5600 | 11 000 | 24 000 | 17 000 | 29 000 | 17 500 | 11.8,3 |
| Pituitary gland | 0.1 | 0.15 | 0.25 | 0.35 | 0.5 | 0.5 | 0.6 | 0.6 | 11.9 |

(continued on next page)

18

(continued on next page)

Calculation of Blood Content Mass

- Blood-content masses were calculated based on ICRP-89 reference blood masses and regional blood volume fractions^[51].

ICRP-89 reference blood masses

- Newborn male/female: 290 g
- 1-year male/female: 530 g
- 5-year male/female: 1500 g
- 10-year male/female: 2500 g
- 15-year male: 4800 g
- 15-year female: 3500 g

Table 6. Suggested reference values for regional blood distribution (% total BV) for the ICRP reference persons.

| Organ or tissue | Newborn | 1 year | 5 year | 10 year | 15 year | | Adult | |
|------------------------------|-------------|-------------|-------------|-------------|---------|--------|-------|--------|
| | Male/female | Male/female | Male/female | Male/female | Male | Female | Male | Female |
| Fat | 2.2 | 5.0 | 4.1 | 4.2 | 3.6 | 6.6 | 5.0 | 8.5 |
| Brain | 5.4 | 5.3 | 4.3 | 2.7 | 1.6 | 1.4 | 1.2 | 1.2 |
| Stomach & esophagus wall | 0.8 | 0.7 | 0.9 | 1.0 | 0.9 | 0.9 | 1.0 | 1.0 |
| Small intestine wall | 2.8 | 2.8 | 3.8 | 3.9 | 3.6 | 3.3 | 3.8 | 3.8 |
| Colon wall | 1.6 | 1.6 | 2.1 | 2.2 | 2.1 | 1.8 | 2.2 | 2.2 |
| Right heart contents | 4.5 | 4.5 | 4.5 | 4.5 | 4.5 | 4.5 | 4.5 | 4.5 |
| Left heart contents | 4.5 | 4.5 | 4.5 | 4.5 | 4.5 | 4.5 | 4.5 | 4.5 |
| Coronary tissues | 1.1 | 0.9 | 0.8 | 0.9 | 0.8 | 0.9 | 1.0 | 1.0 |
| Kidneys | 0.7 | 1.8 | 2.2 | 2.2 | 1.9 | 1.8 | 2.0 | 2.0 |
| Liver | 12.9 | 11.4 | 10.3 | 9.2 | 8.5 | 9.4 | 10.0 | 10.0 |
| Lungs | | | | | | | | |
| Pulmonary gas exchange blood | 10.5 | 10.5 | 10.5 | 10.5 | 10.5 | 10.5 | 10.5 | 10.5 |
| Pulmonary nutrient blood | 2.0 | 2.0 | 2.0 | 2.0 | 2.0 | 2.0 | 2.0 | 2.0 |
| Skeletal muscle | 6.8 | 5.5 | 8.5 | 10.3 | 13.7 | 10.3 | 14.0 | 10.5 |
| Pancreas | 0.4 | 0.5 | 0.5 | 0.5 | 0.6 | 0.5 | 0.6 | 0.6 |
| Skeletal tissues | | | | | | | | |
| Active marrow | 5.2 | 5.0 | 4.9 | 4.9 | 4.8 | 5.0 | 4.0 | 4.0 |
| Trabecular bone | 3.6 | 4.4 | 4.4 | 4.4 | 4.0 | 4.4 | 1.2 | 1.2 |
| Cortical bone | 1.3 | 1.6 | 1.6 | 1.6 | 1.4 | 1.5 | 0.8 | 0.8 |
| Other skeletal tissues | 0.7 | 0.7 | 0.7 | 0.8 | 0.9 | 0.9 | 1.0 | 1.0 |
| Skin | 3.0 | 2.0 | 1.8 | 1.6 | 2.2 | 2.2 | 3.0 | 3.0 |
| Spleen | 1.5 | 1.6 | 1.4 | 1.4 | 1.4 | 1.4 | 1.4 | 1.4 |
| Thyroid | 0.07 | 0.03 | 0.03 | 0.04 | 0.04 | 0.04 | 0.06 | 0.06 |
| Lymphatic nodes | 0.2 | 0.2 | 0.2 | 0.2 | 0.2 | 0.2 | 0.2 | 0.2 |
| Testes or ovaries | 0.01 | 0.01 | 0.01 | 0.01 | 0.02 | 0.01 | 0.04 | 0.02 |
| Adrenal glands | 0.4 | 0.1 | 0.1 | 0.1 | 0.1 | 0.04 | 0.06 | 0.06 |
| Urinary bladder wall | 0.02 | 0.02 | 0.02 | 0.02 | 0.02 | 0.02 | 0.02 | 0.02 |
| All other tissues | 3.8 | 3.3 | 1.9 | 2.4 | 2.2 | 1.9 | 1.9 | 1.9 |
| Aorta and large arteries | 6.0 | 6.0 | 6.0 | 6.0 | 6.0 | 6.0 | 6.0 | 6.0 |
| Large veins | 18.0 | 18.0 | 18.0 | 18.0 | 18.0 | 18.0 | 18.0 | 18.0 |
| | 100.0 | 100.0 | 100.0 | 100.0 | 100.0 | 100.0 | 100.0 | 100.0 |

Regional blood volume fractions

Example: liver

$$m_{\text{blood-in-liver}} = (m_{\text{total-blood}}^{\text{ICRP89}}) (f_{\text{liver}}^{\text{total-blood}})$$

Calculation of Density and Elemental Composition

- Subsequently, densities and elemental compositions of the organs inclusive of blood content were calculated using data given in the scientific literature^[22, 52, 53], assuming that the blood content is uniformly distributed within the organs.

Example: brain

- Density**

$$\rho_{brain}^{with-blood} = \frac{m_{brain}^{ICRP89} + m_{blood-in-brain}}{\frac{m_{brain}^{ICRP89}}{\rho_{brain}^{ICRU46}} + \frac{m_{blood-in-brain}}{\rho_{blood}^{ICRU46}}}$$

- Mass percentage of hydrogen**

$$(\%H)_{brain}^{with-blood} = \frac{(\%H)_{brain}^{ICRU46} m_{brain}^{ICRP89} + (\%H)_{blood}^{ICRU46} m_{blood-in-brain}}{m_{brain}^{ICRP89} + m_{blood-in-brain}}$$

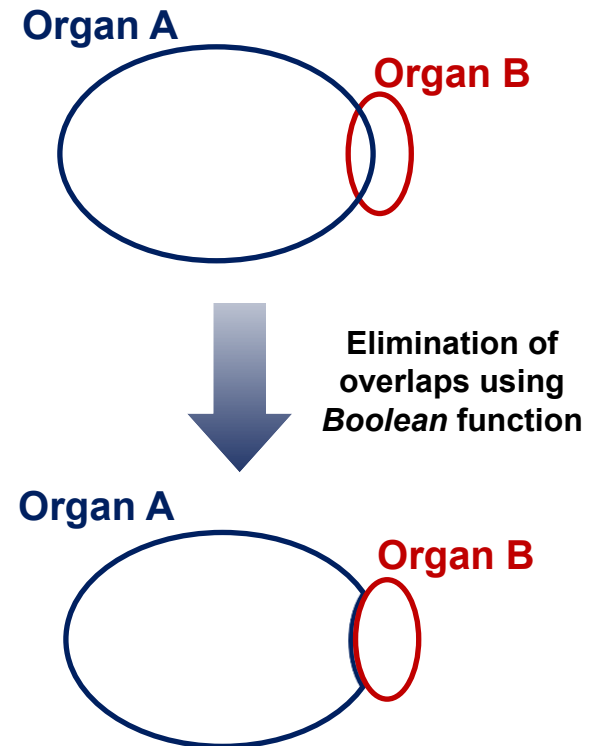
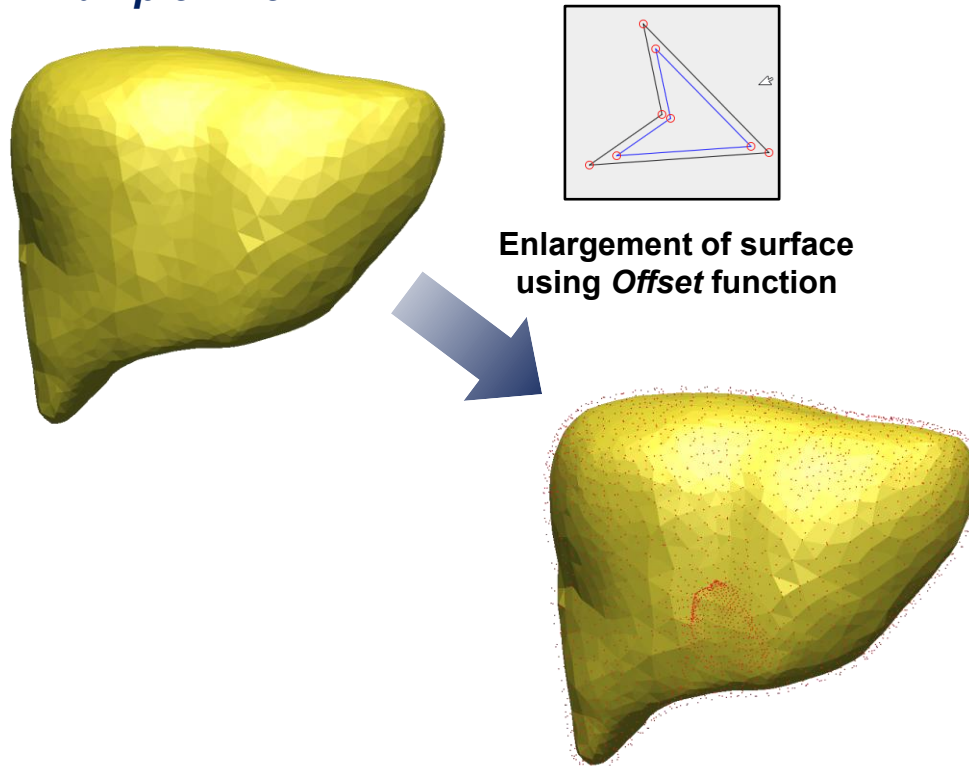
[52] ICRU, 1992. Photon, electron, proton, and neutron interaction data for body tissues. ICRU Report 46. International Commission on Radiation Units and Measurements, Bethesda, MD.

[53] White, D.R., Woodard, H.Q. and Hammond, S.M., 1987. Average soft-tissue and bone models for use in radiation dosimetry. Br. J. Radiol. 60, 907–9013.

Adjustment for Blood Inclusion

- Organs were isotropically increased, preserving the original shape and centroid of the organs.
- After enlargement, resulting overlaps between some of the neighboring organs were eliminated by preferentially modifying the larger organs, rather than the smaller ones.

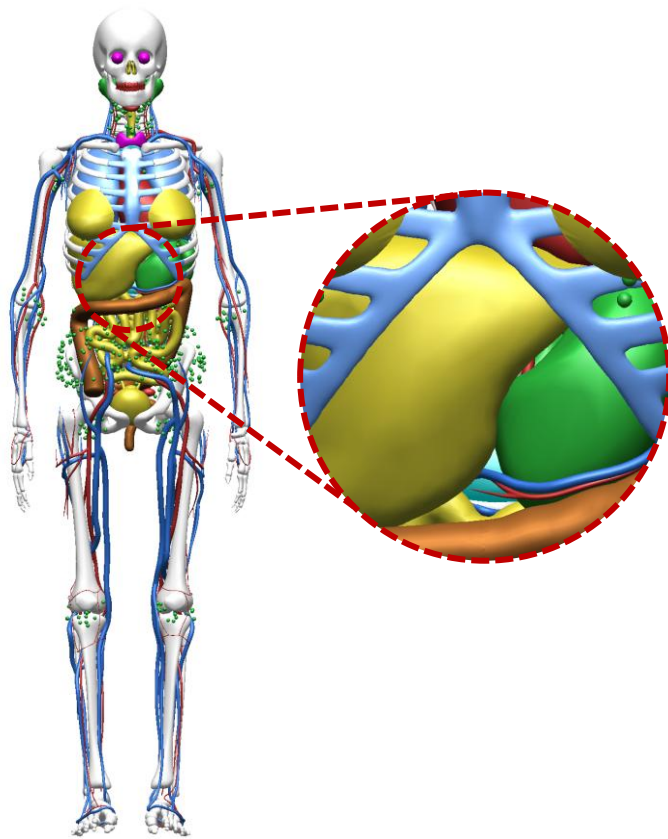
Example: liver



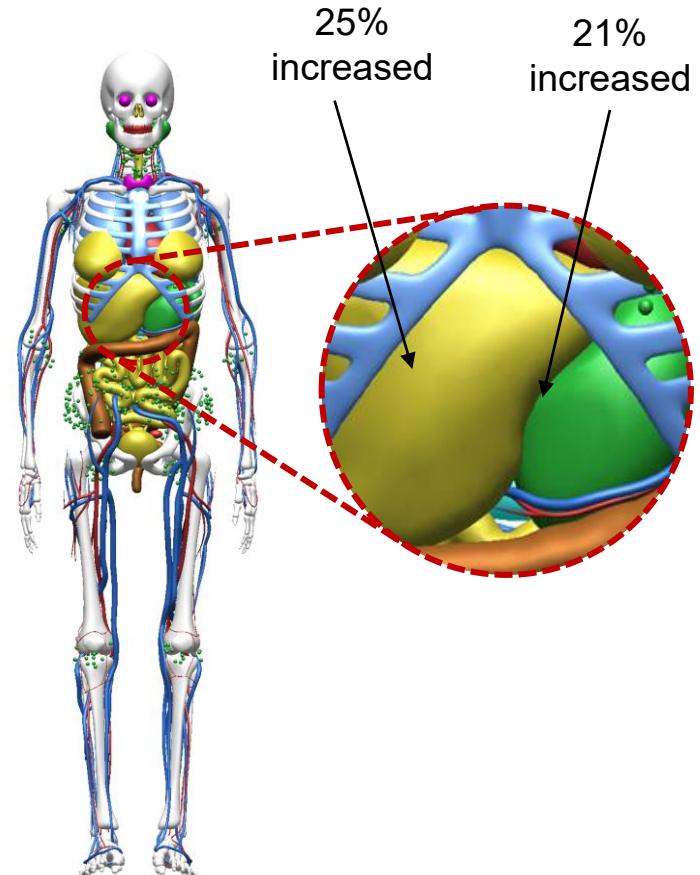
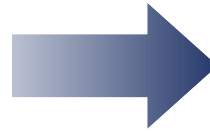
Comparison of Changes Caused by Blood Inclusion

- Most of internal organs were increased by 20–30% in size.

Example: 15fMRCP



Organs exclusive of blood content



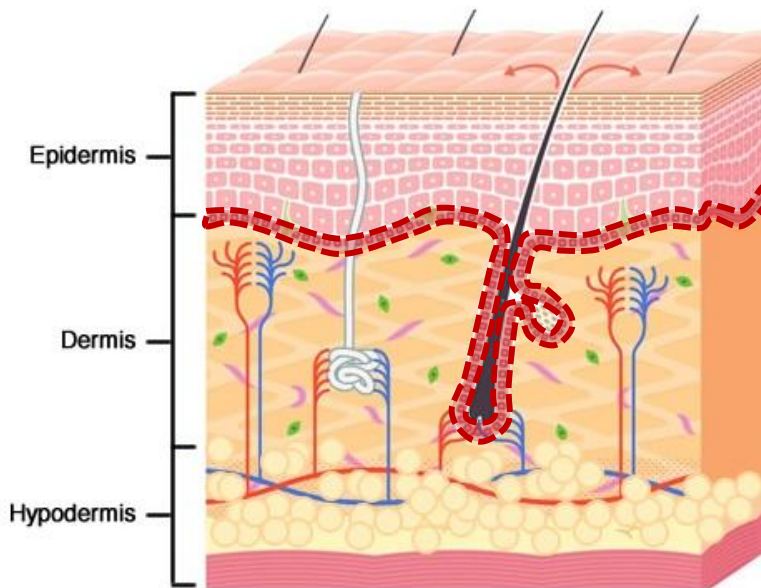
Organs inclusive of blood content



III. Inclusion of Thin Target and Source Regions

■ Target region in skin

- The ICRP assumes that the target region of the skin is at a depth of 50 to 100 μm below the skin surface for the adult^[54, 55].
- Dr. John Harrison and Dr. John Hopewell carefully discussed the skin target layer issue and decided to use the skin target layer of 50–100 μm for the 15 years and 40–100 μm for the 10 years and younger.



Anatomical structure of the skin

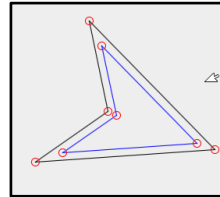
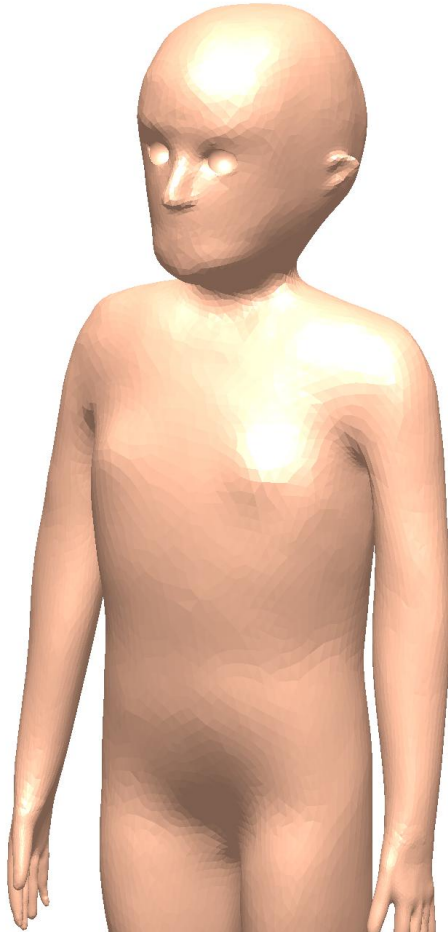
'We came to the conclusion that it would not make sense to use the shallower depths in the way we had tentatively discussed in Beijing. This is because a substantial proportion of the target cells for skin cancer are not in the inter-follicular basal layer between hair follicles but in the hair follicles themselves that penetrate through the dermis. John points out that the hair follicles are closer together in the skin of children and so a greater proportion of target cells will actually be at greater depths. Given that we are committed to previous use of 50–100 μm for adults (nominal 70 μm), we propose that this depth should also be used for the 15 y old, and that a slightly wider band of 40–100 μm should be used for ages 10 y and younger.'

**Mail from Dr. John Harrison
(30 September 2018)**

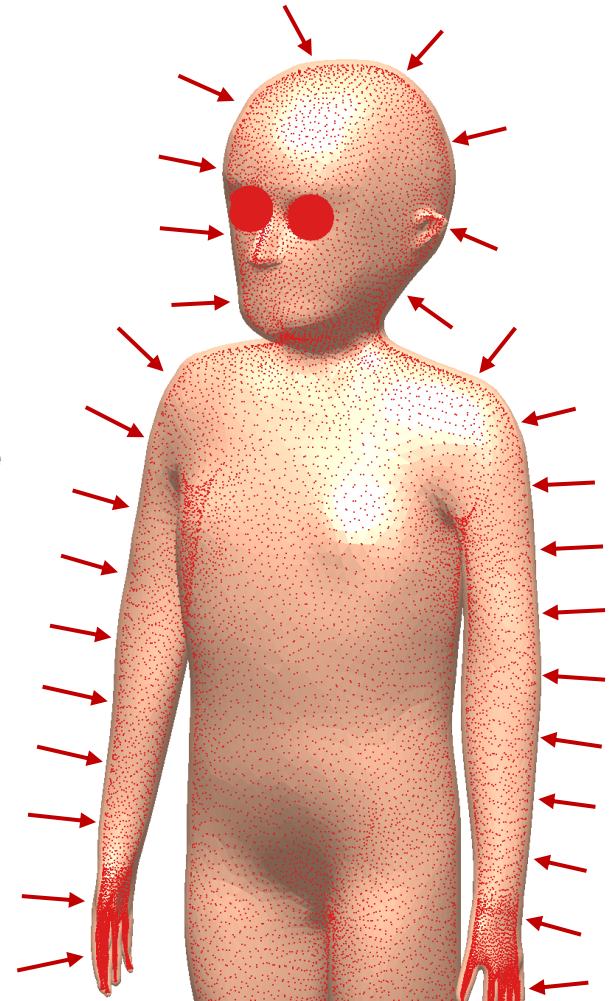
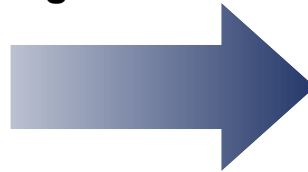
[54] ICRP, 2015. Occupational intakes of radionuclides: part 1. ICRP Publication 130. Ann. ICRP 44.

[55] ICRP, 1977. Recommendations of the International Commission on Radiological Protection. ICRP Publication 26. Ann. ICRP 1.

- Construction of target region in skin

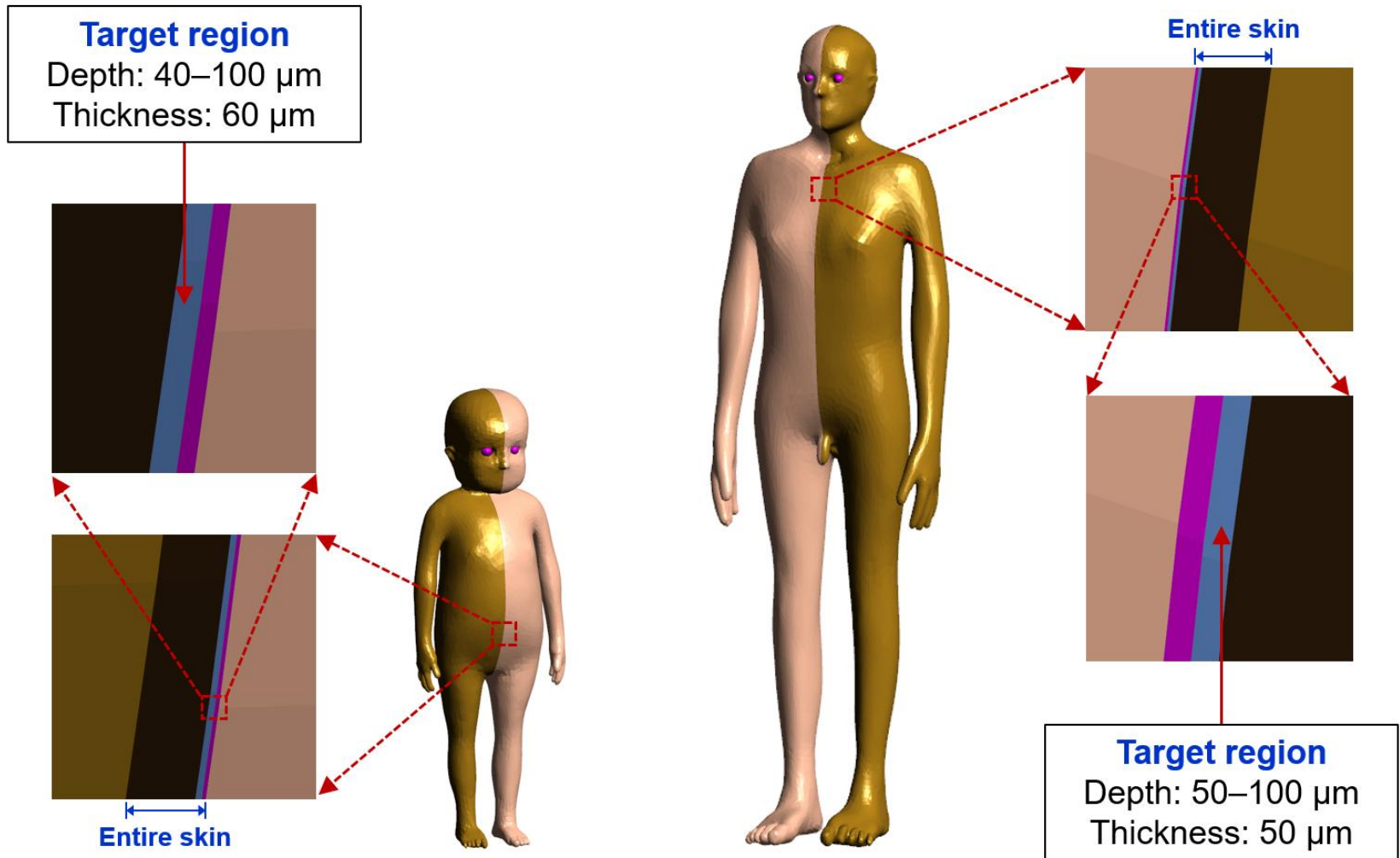


Reduction of skin surface
using *Offset* function



- Target region defined in skin of paediatric MRCPs

Example: 1fMRCP (left) and 15mMRCP (right)



Urinary Bladder

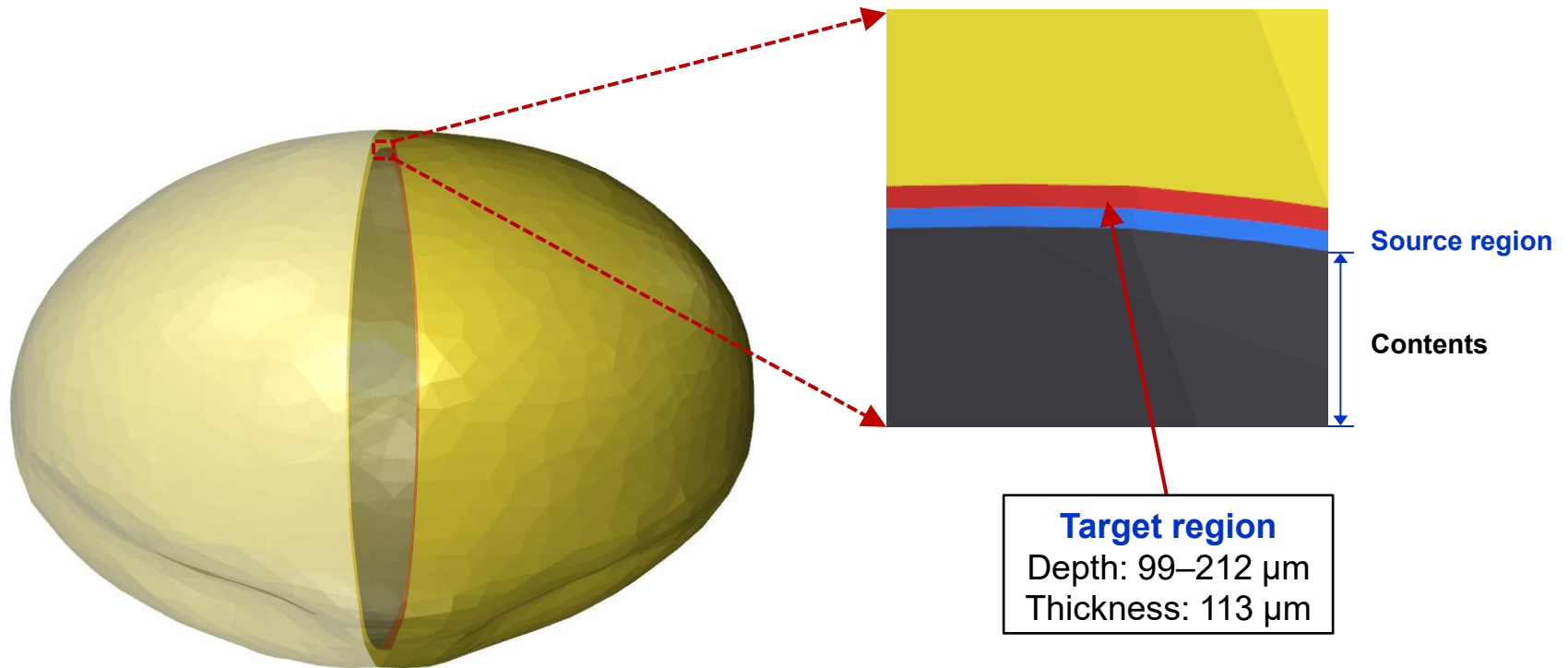
▪ Target region in urinary bladder

- Eckerman and Veinot^[56] derived the depth and thickness of the target region of the urinary bladder for adults.
- In their subsequent study, the depth and thickness of the target region for children and adolescents were also derived.

| Age/sex | Depth (μm) | Thickness (μm) |
|---------------------|------------|----------------|
| Newborn male/female | 54 | 178 |
| 1-year male/female | 71 | 167 |
| 5-year male/female | 86 | 107 |
| 10-year male/female | 99 | 113 |
| 15-year male | 116 | 122 |
| 15-year female | 111 | 116 |

- Target region defined in urinary bladder of paediatric MRCPs

Example: 10mMRCP



Alimentary Tract Organs

■ Source and target regions in alimentary tract organs

- The ICRP provides the information on the source and target regions of the alimentary tract organs through ICRP *Publication 100*.
- ICRP *Publication 100* assumes that the depth of the target and source regions are the same for all ages, except for the villi.

| Alimentary tract organ | Source | Source location [†] |
|------------------------|------------------------|-----------------------------------------------------------|
| Oral Cavity | Food (or liquid) | 5 mm (on top of the tongue, outward) |
| | Retention on teeth | 10 µm (on inner and outer surfaces of the teeth, outward) |
| Oesophagus | Contents (fast) | * |
| | Luminal surface (slow) | ** |
| Stomach | Mucosa | 0–300 µm (outward) |
| | Contents | * |
| Small intestine | Villi | 0–400 [†] /500 ^{††} µm (inward) |
| | Mucosa | 0–200 µm (outward) |
| | Contents | * |
| Right colon | Mucosa | 0–300 µm (outward) |
| | Contents | * |
| Left colon | Mucosa | 0–300 µm (outward) |
| | Contents | * |
| Rectosigmoid | Mucosa | 0–300 µm (outward) |
| | Contents | * |

[†] Default depth is from the luminal surface.

* Volume of the contents is the source region.

** Surface of the contents is the source region.

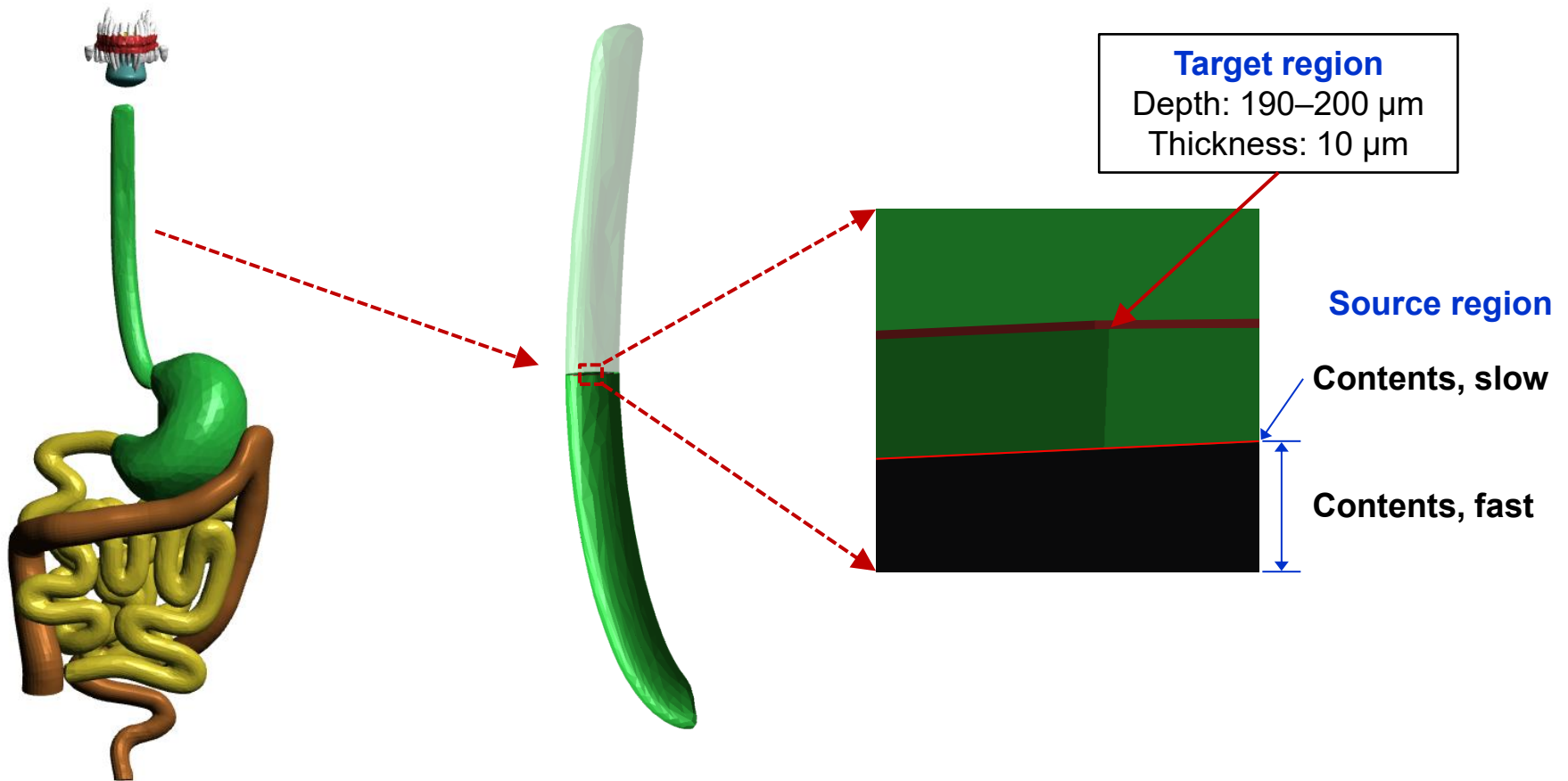
| Alimentary tract organ | Target region | Target location [†] |
|------------------------|----------------|--------------------------------------------------------------------|
| Oral Cavity | Roof of mouth | 190–200 µm (from the top surface of the food, outward) |
| | Tongue | 190–200 µm (from the surface of the tongue, inward) |
| | Lips and cheek | 190–200 µm (from the outer surface of retention on teeth, outward) |
| Oesophagus | Basal cells | 190–200 µm (outward) |
| Stomach | Stem cells | 60–100 µm (outward) |
| Small intestine | Stem cells | 130–150 µm (outward) |
| Right colon | Stem cells | 280–300 µm (outward) |
| Left colon | Stem cells | 280–300 µm (outward) |
| Rectosigmoid | Stem cells | 280–300 µm (outward) |

[†] Depth of the small intestine villi for newborn, 1 year and 5 years.

^{††} Depth of the small intestine villi for 10 years and 15 years.

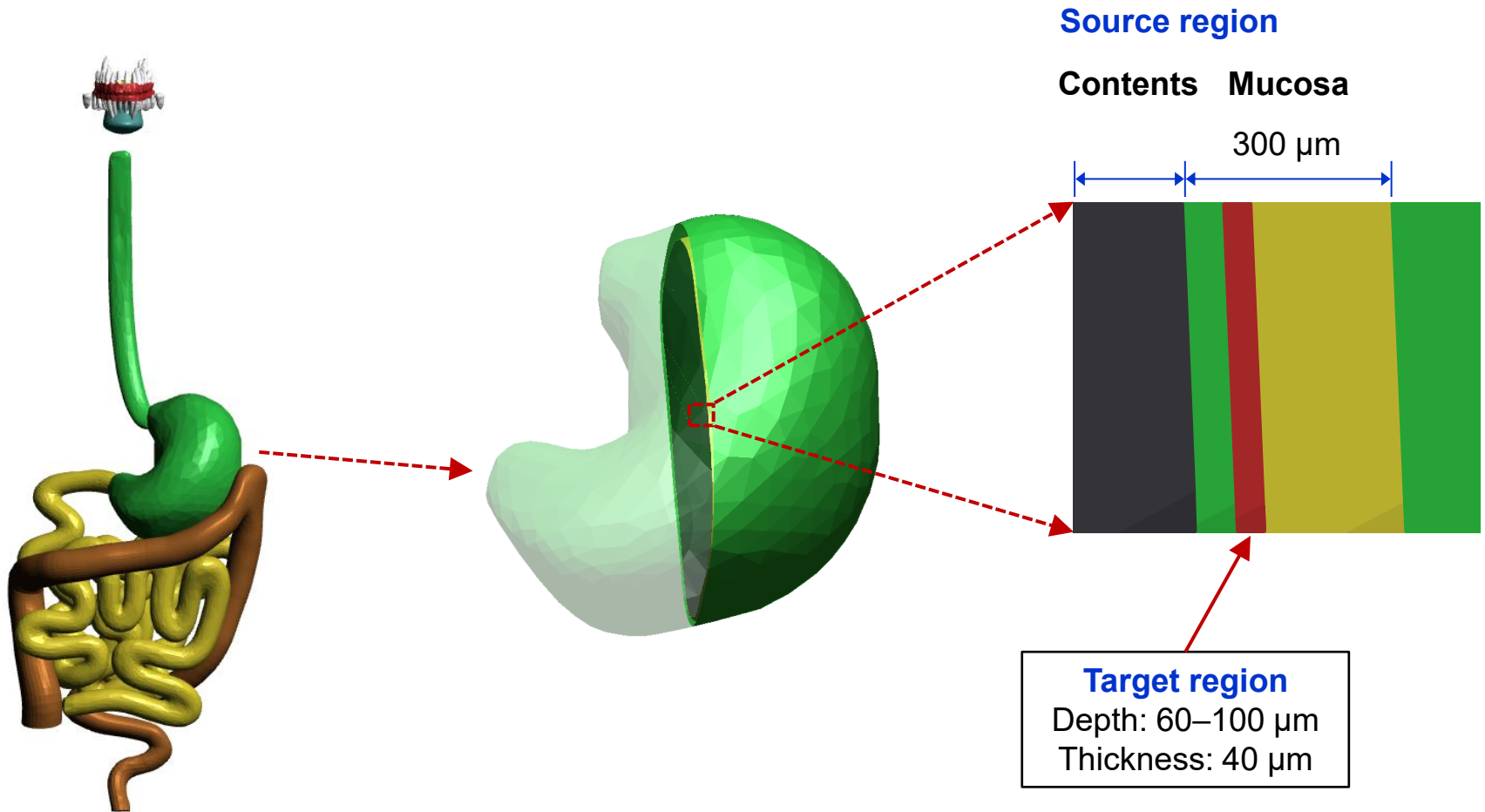
- Source and target regions defined in **oesophagus** of paediatric MRCPs

Example: 15mMRCP



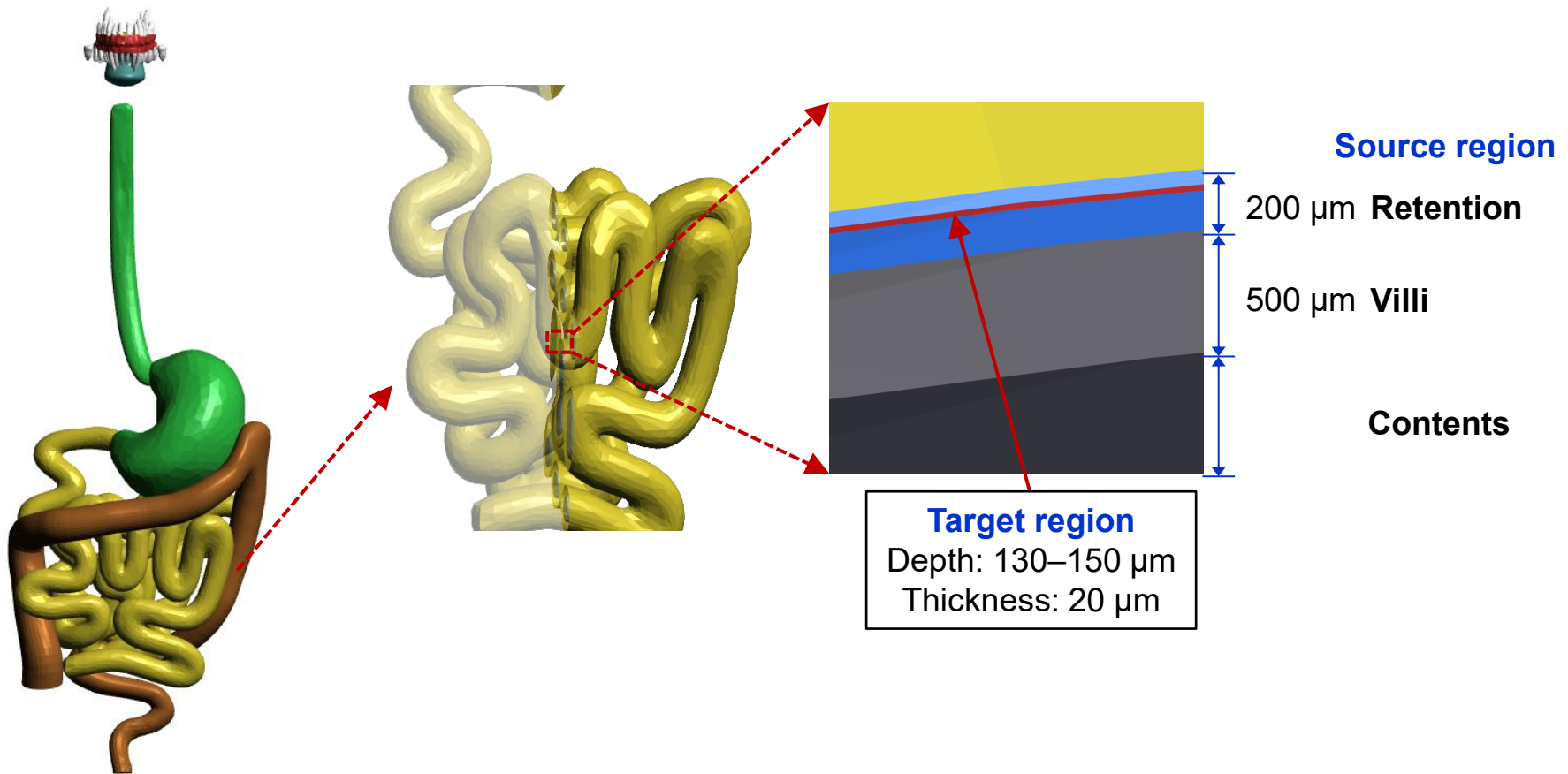
- Source and target regions defined in **stomach** of paediatric MRCPs

Example: 15mMRCP



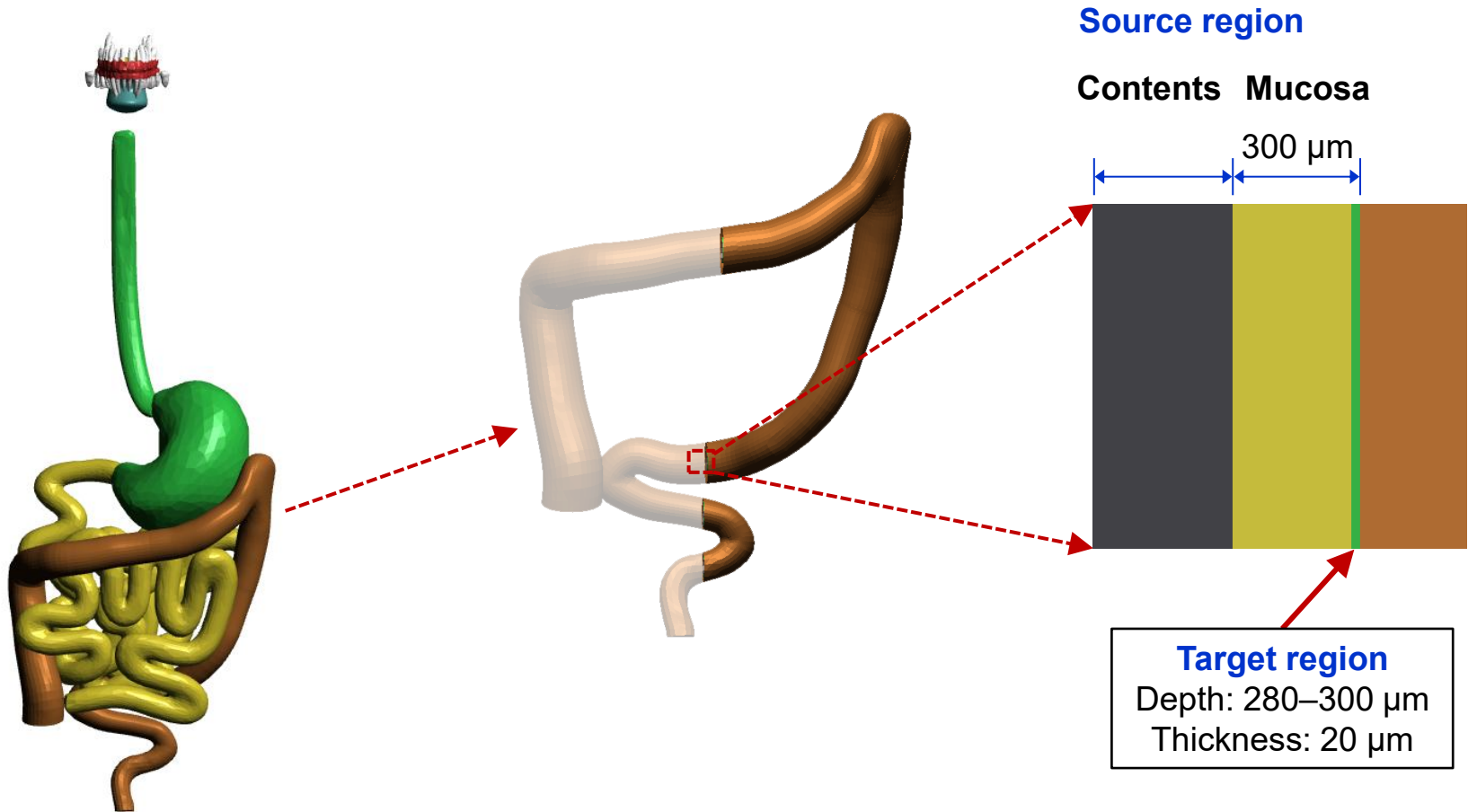
- Source and target regions defined in **small intestine** of paediatric MRCPs

Example: 15mMRCP

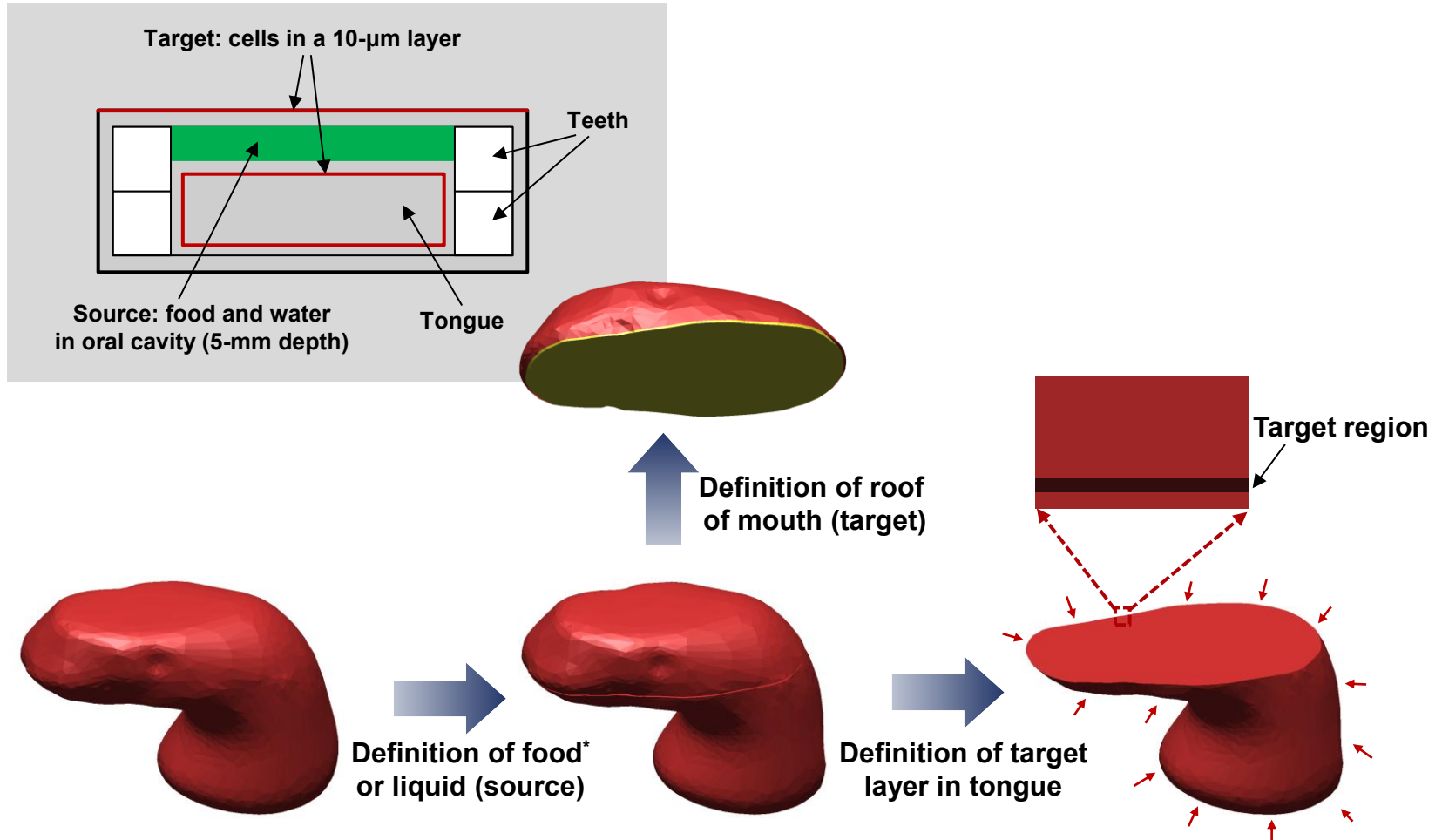


- Source and target regions defined in **colon** of paediatric MRCPs

Example: 15mMRCP

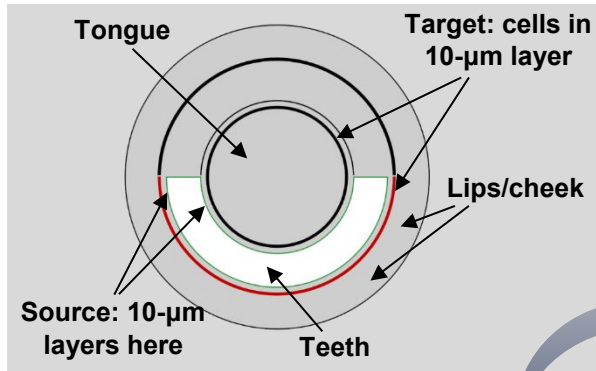


■ Construction of target and source regions in oral cavity (1)

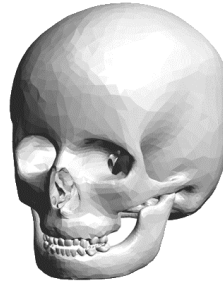


* The food volume has been estimated only for the adults (= 20 cm³); for the paediatric MRCPs, therefore, the food volume was estimated by *scaling in proportion to the area of the tongue*, assuming that the thickness of the food region (= 5 mm) is identical for all ages.

Construction of target and source regions in oral cavity (2)



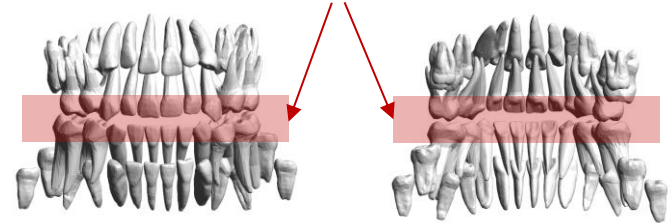
Definition of retention region on teeth (source)



Definition of oral mucosa in lips/cheek (target)

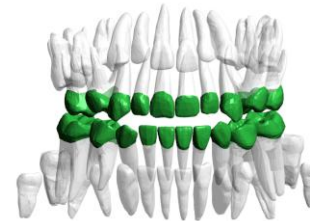


Erupted region (enamel region)

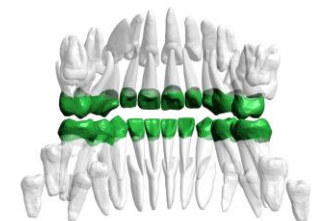


Front

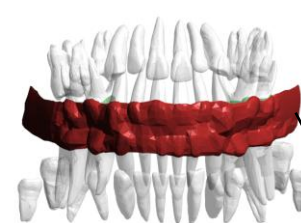
Back



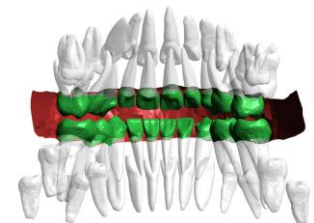
Front



Back



Front

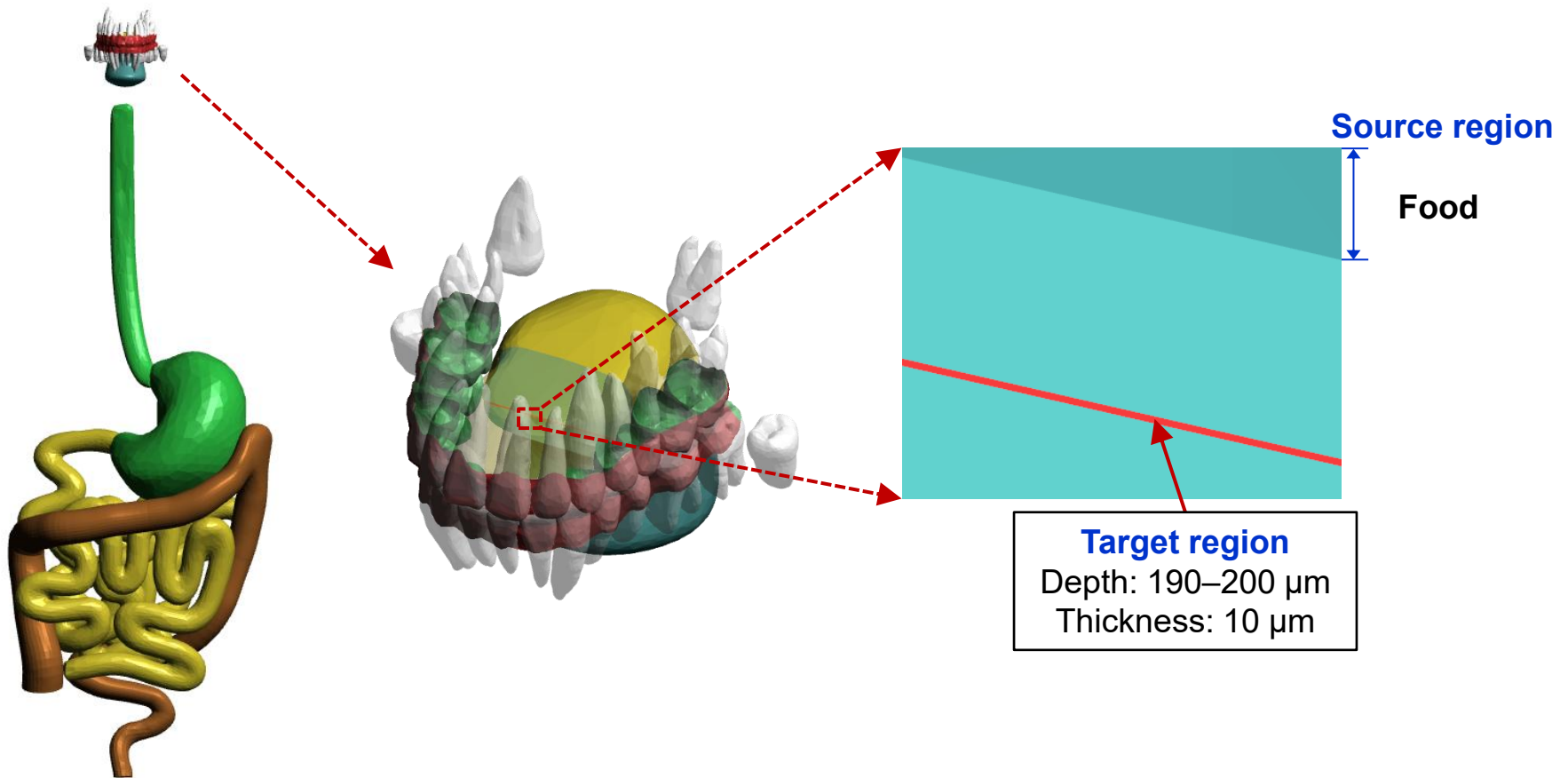


Back

This region was *manually constructed* along cranium and mandible for ages *whose teeth on the side are not erupted*. 60

- Source and target regions defined in **oral cavity** of paediatric MRCPs

Example: 15mMRCP



Respiratory Tract Organs

■ Source and target regions in respiratory tract organs

- The ICRP provides the information on the source and target regions of the respiratory tract organs through ICRP *Publication 66*.
- ICRP *Publication 66* assumes that the depth of the target and source regions are the same for all ages.

| Respiratory tract organ | Source | Source location [†] |
|-------------------------|-------------|------------------------------|
| ET ₁ | Surface | 0–8 µm (outward) |
| ET ₂ | Surface | 0–15 µm (inward) |
| | Bound | 0–55 µm (outward) |
| | Sequestered | 55–65 µm (outward) |
| BB | Fast mucus | 6–11 µm (inward) |
| | Slow mucus | 0–6 µm (inward) |
| | Bound | 0–60 µm (outward) |
| | Sequestered | 60–70 µm (outward) |
| | AI | * |
| bb | Fast mucus | 4–6 µm (inward) |
| | Slow mucus | 0–4 µm (inward) |
| | Bound | 0–20 µm (outward) |
| | Sequestered | 20–25 µm (outward) |
| | AI | * |

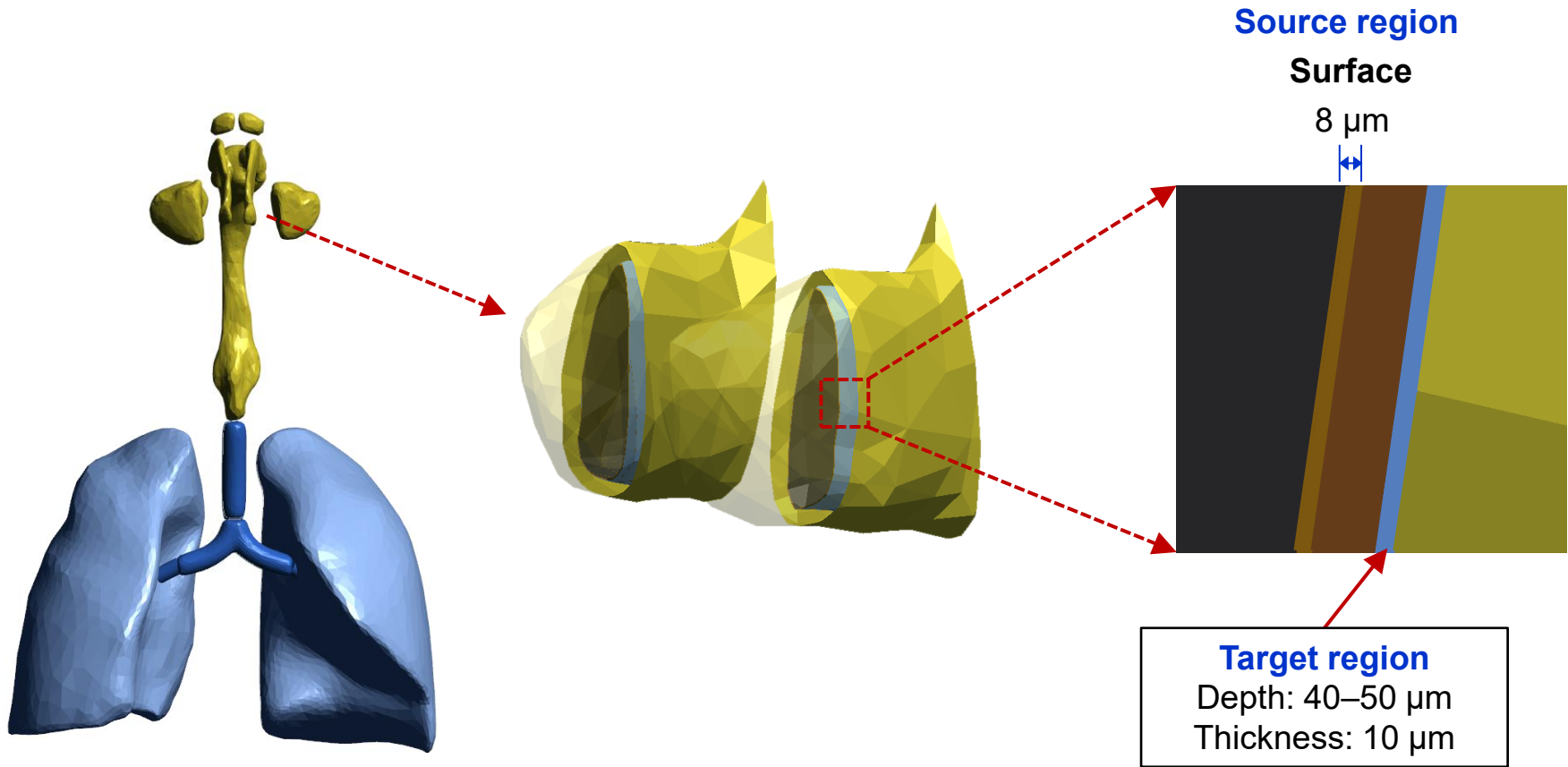
| Respiratory tract organ | Target region | Target location [†] |
|-------------------------|-----------------|------------------------------|
| ET ₁ | Basal cells | 40–50 µm (outward) |
| ET ₂ | Basal cells | 40–50 µm (outward) |
| BB | Basal cells | 35–50 µm (outward) |
| | Secretory cells | 10–40 µm (outward) |
| bb | Secretory cells | 4–12 µm (outward) |

[†] Default depth is from the airway surface.

* AI as a source region is determined by radiation types and energies.

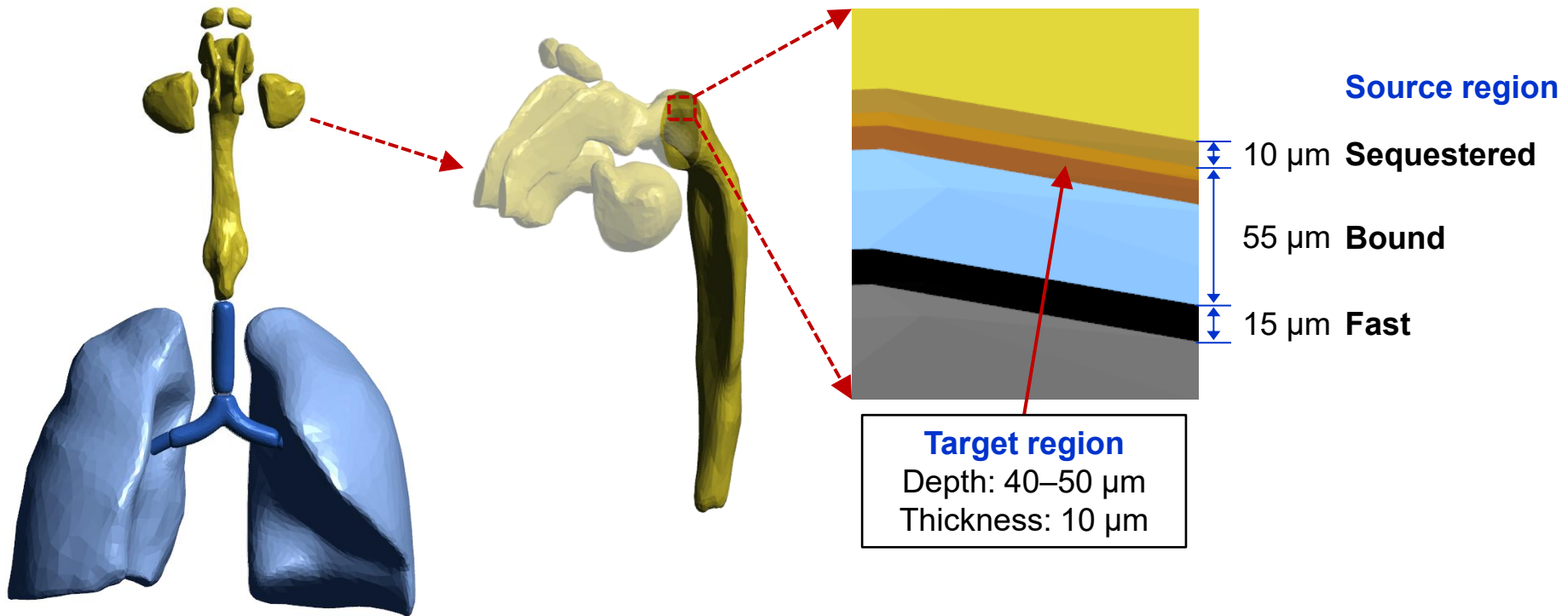
- Source and target regions defined in **ET₁ region** of paediatric MRCPs

Example: 5mMRCP



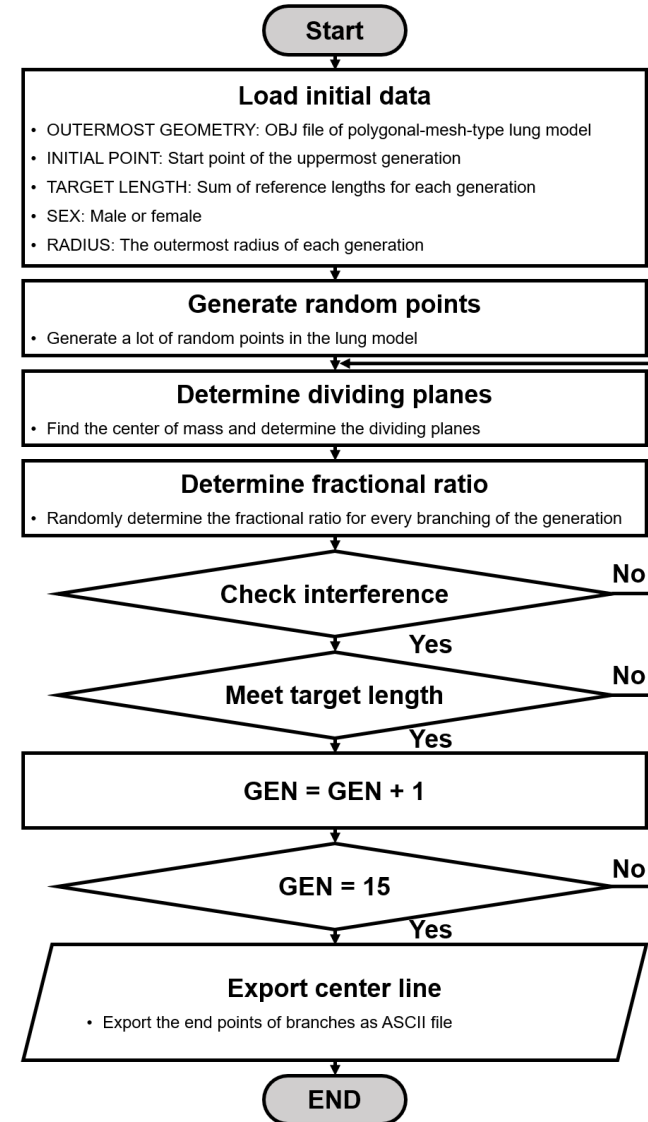
- Source and target regions defined in **ET₂ region** of paediatric MRCPs

Example: 5mMRCP



■ Construction of BB/bb regions in paediatric MRCPs

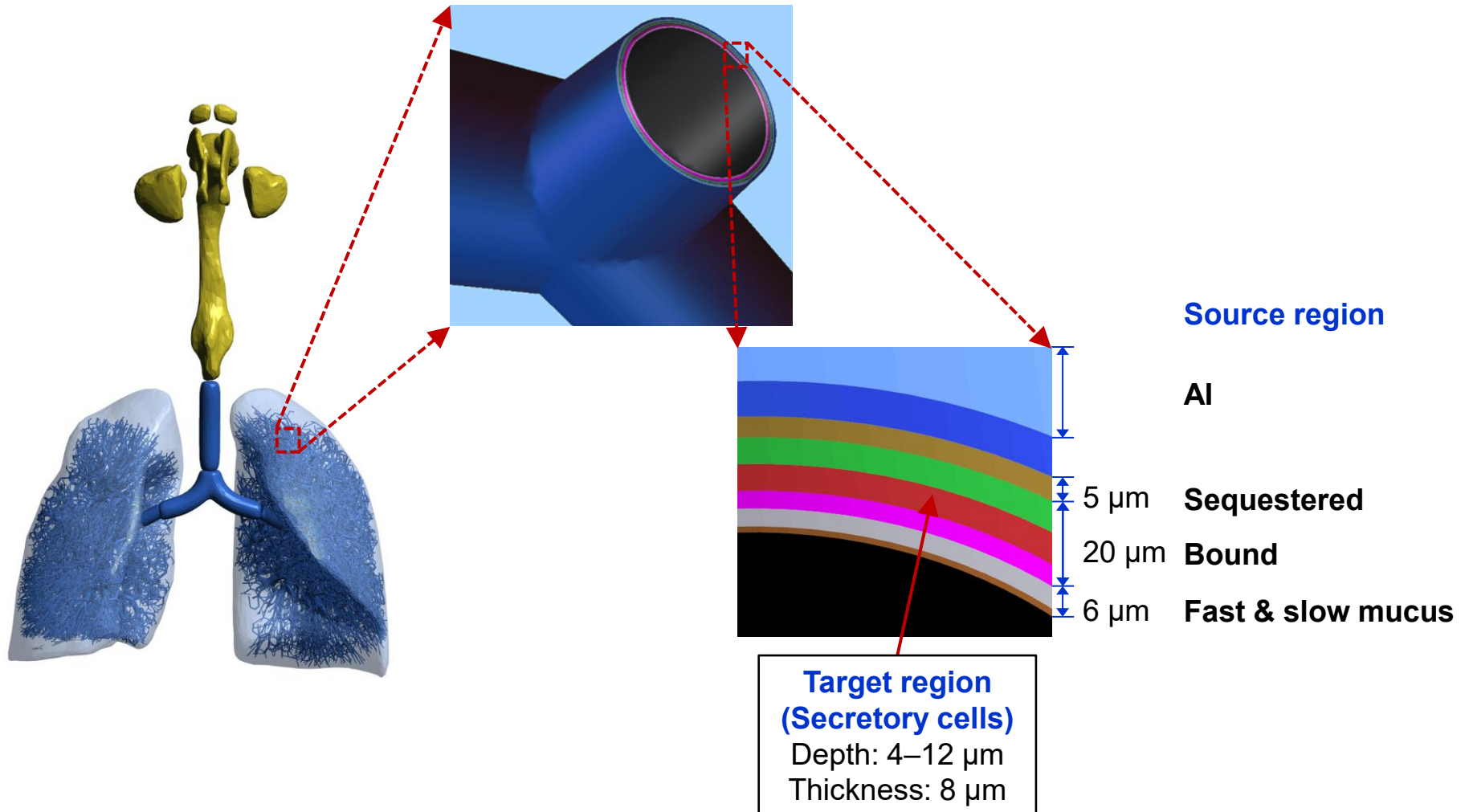
- BB/bb regions were modeled in constructive solid geometry (CSG) format based on airway dimensions (i.e., lengths and diameters) derived using the scaling method of ICRP *Publication 66*, using the computer program applied for adult MRCPs^[57].
- As an exception, newborn airway dimensions were derived by scaling the adult male values in proportion to the cube root of lung volume.



Program flowchart

- Source and target regions defined in **BB/bb regions** of paediatric MRCPs

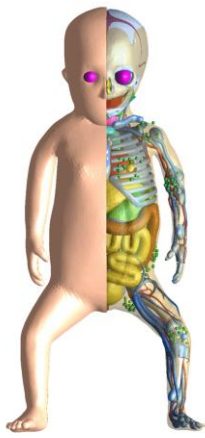
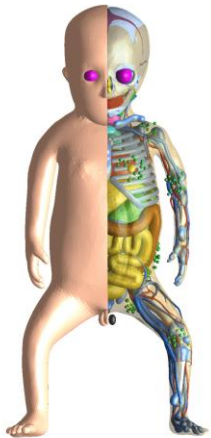
Example: bb region of 5mMRCP



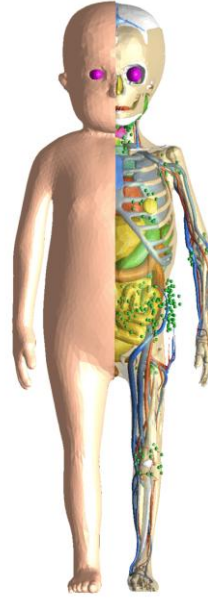
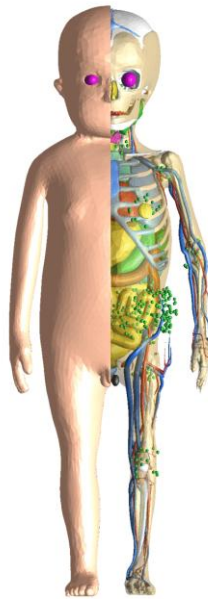


IV. Paediatric MRCP

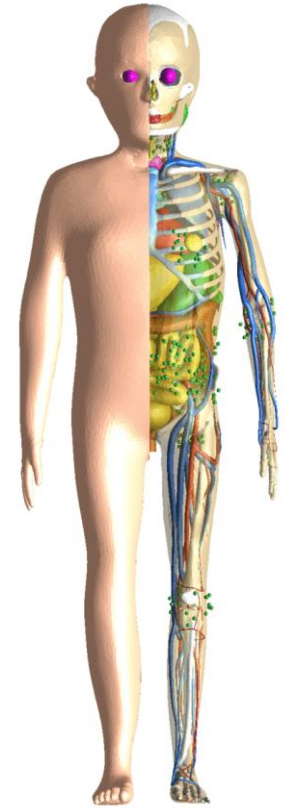
Paediatric MRCPs – Rotational View (1)



Newborn male/female

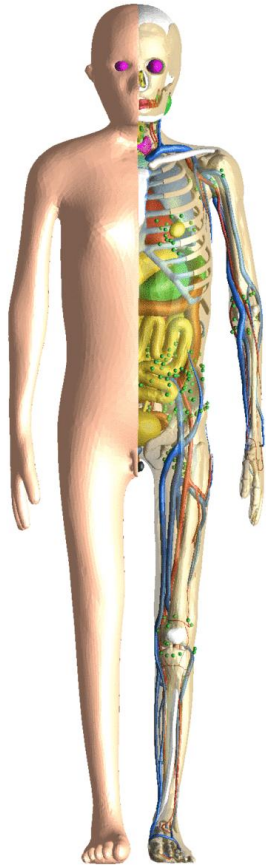


1-year male/female

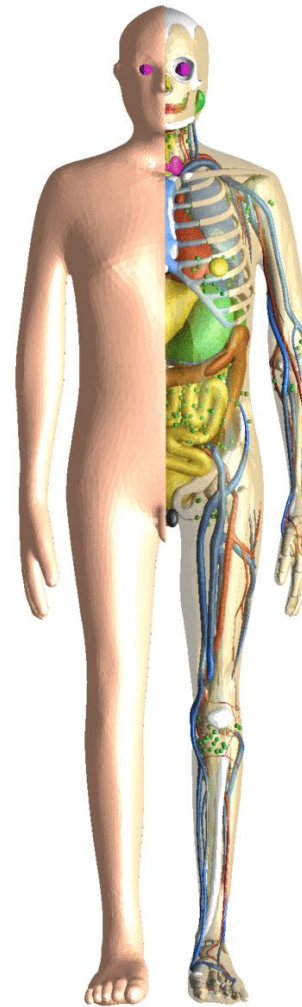
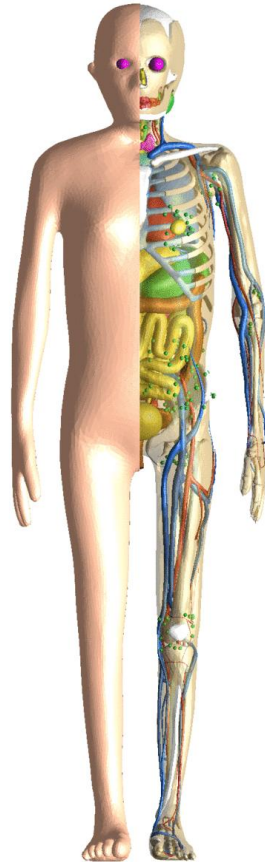


5-year male/female

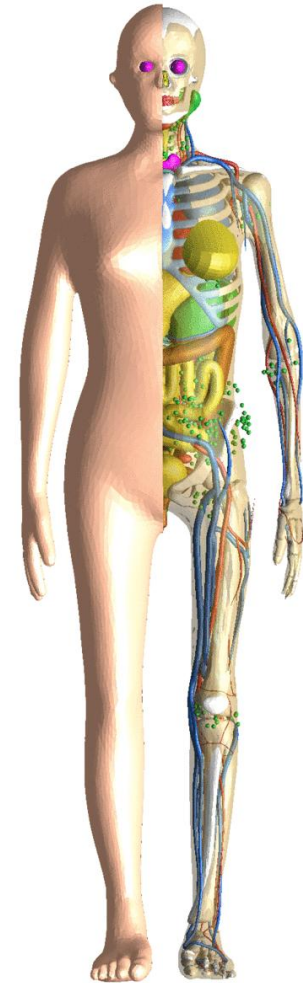
Paediatric MRCPs – Rotational View (2)



10-year male/female

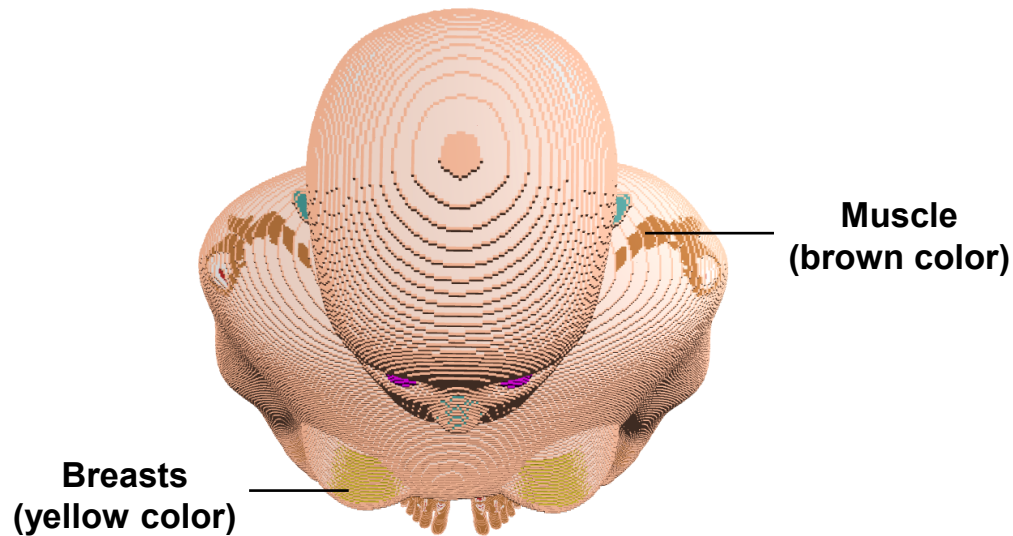


15-year male/female

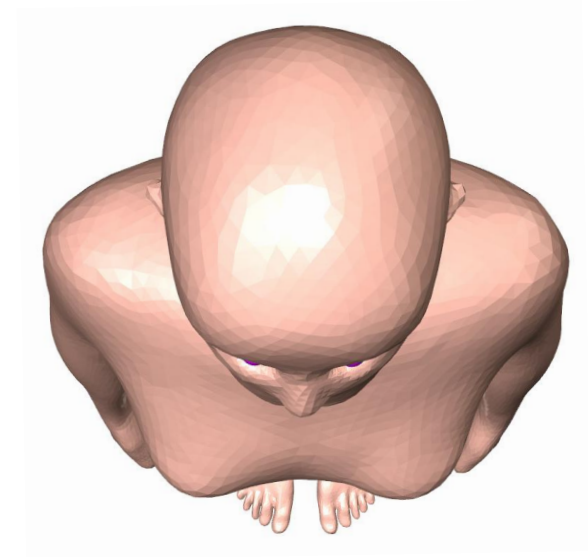


Improvement of Paediatric MRCPs (1)

Example: 15-year female phantom



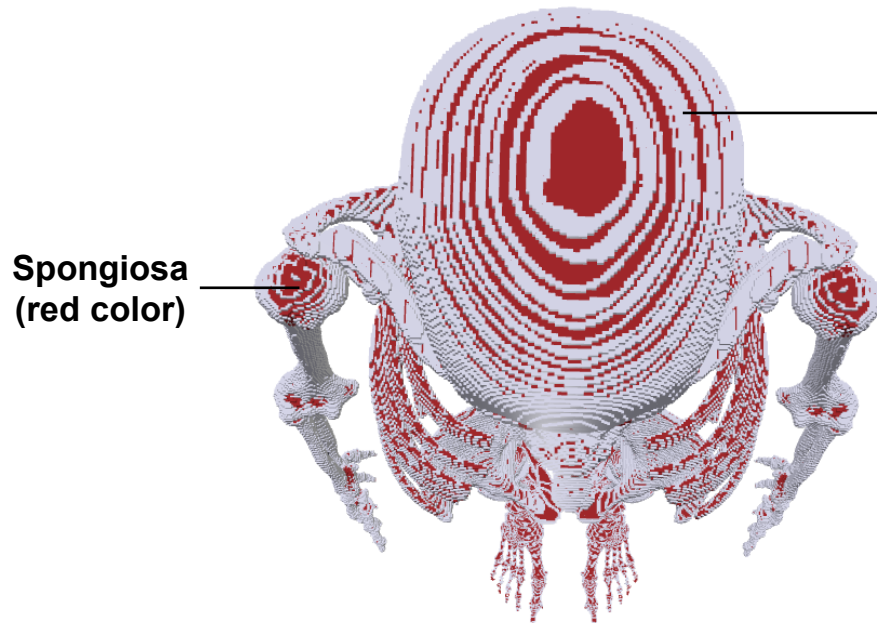
Paediatric VRCPs



Paediatric MRCPs

Improvement of Paediatric MRCPs (2)

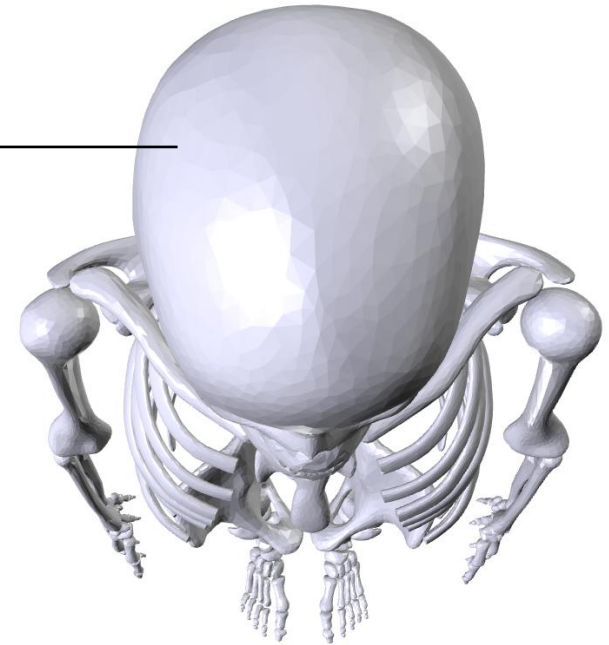
Example: 15-year female phantom



Spongiosa
(red color)

Cortical bone
(white color)

Paediatric VRCPs



Paediatric MRCPs

Numerical Data

| Phantom | | Height / Weight | Number of organs | Deviation from ICRP reference data* | Number of tetrahedra | Avg. volume of tetrahedron | File size (ASCII) |
|----------|--------|-----------------|------------------|-------------------------------------|----------------------|----------------------------|-------------------|
| Newborn | Male | – / 3.5 kg | 48 | < 0.1% | 7,556,192 | 0.45 mm ³ | 423 MB |
| | Female | – / 3.5 kg | 48 | < 0.1% | 7,650,313 | 0.44 mm ³ | 407 MB |
| 1 year | Male | 76 cm / 10 kg | 48 | < 0.1% | 6,715,716 | 1.47 mm ³ | 373 MB |
| | Female | 76 cm / 10 kg | 48 | < 0.1% | 6,943,945 | 1.42 mm ³ | 387 MB |
| 5 years | Male | 109 cm / 19 kg | 48 | < 0.1% | 8,178,096 | 2.27 mm ³ | 462 MB |
| | Female | 109 cm / 19 kg | 48 | < 0.1% | 8,440,293 | 2.19 mm ³ | 478 MB |
| 10 years | Male | 138 cm / 32 kg | 48 | < 0.1% | 6,925,977 | 4.48 mm ³ | 385 MB |
| | Female | 138 cm / 32 kg | 48 | < 0.1% | 7,103,129 | 4.37 mm ³ | 396 MB |
| 15 years | Male | 167 cm / 56 kg | 48 | < 0.1% | 7,366,440 | 7.43 mm ³ | 412 MB |
| | Female | 161 cm / 53 kg | 48 | < 0.1% | 7,519,627 | 6.96 mm ³ | 422 MB |

* Organ mass deviation from the reference organ masses inclusive of blood content



V. Computational Performance in Monte Carlo Codes

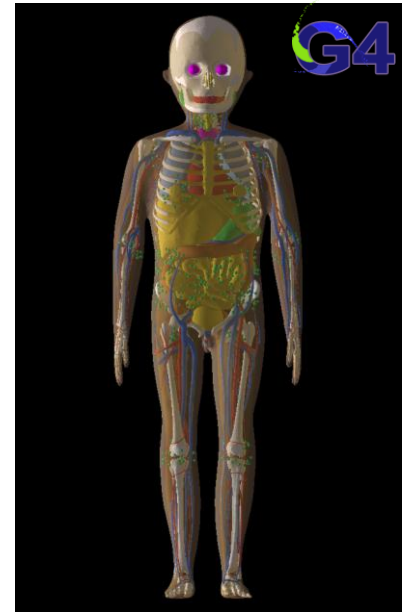
Simulation Conditions

- **Used phantom**

- 5mMRCP and 5mVRCP

- **Used computer**

- CPU: Intel® Xeon® CPU E5-2698 v4 @ 2.20 GHz × 2
- RAM: 512 GB DDR4 memory
- OS: CentOS 7.8



- **Monte Carlo code setting (default setting except for the following)**

- Geant4 (10.06.p01)
 - The physics library of *G4EmLivermorePhysics* was used for photons and electrons, and the physics models and cross-sections of *NeutronHPThermalScattering*, *NeutronHPElastic*, *ParticleHPInelastic*, *Neutron-HPCapture* and *NeutronHPFission* were used for neutrons.
 - The range cutoff of 1 μm was applied for the production of secondary particles.

- PHITS (3.10)
 - The *EGS5* physics library was used for the transportation of photons and electrons and the *JENDL-4.0* physics library and the event generator mode version 2 were used for the transportation of neutrons.
 - Considering the range cutoff value of 1 μm used for Geant4 calculations, the equivalent energy cut values were applied.
- MCNP6 (2.0)
 - The default physics libraries based on Lawrence Livermore National Laboratory evaluated data were used for the transportation of photons and electrons and *ENDF70* physics library were used for the transportation of neutrons.
 - Considering the range cutoff value of 1 μm used for Geant4 calculations, the equivalent energy cut values were applied.

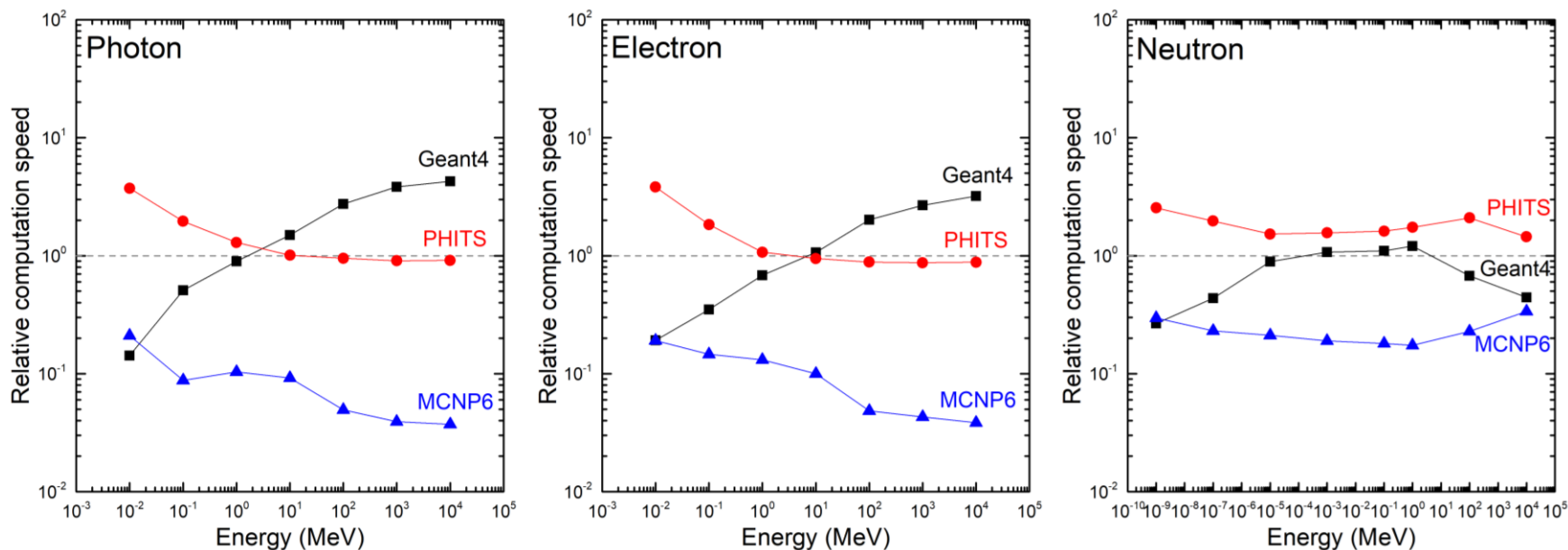
Computational Performance

Memory requirement

| Monte Carlo code | 5mMRCP | 5mVRCP |
|------------------|--------|--------|
| Geant4 | 8.5 GB | 0.7 GB |
| PHITS | 1.4 GB | 2.2 GB |
| MCNP6 | 4.5 GB | 1.9 GB |

**Much lower than the maximum memory (128 GB) that can be equipped in a personal computer these days*

Computation speed (S_{5mMRCP}/S_{5mVRCP})



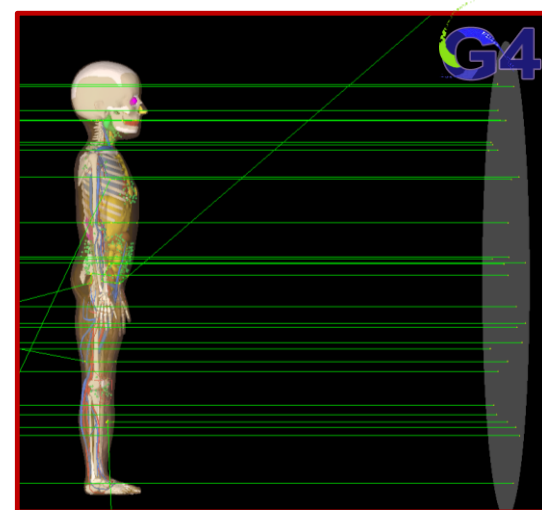


VI. Dosimetric Impact

VI. Dosimetric Impact

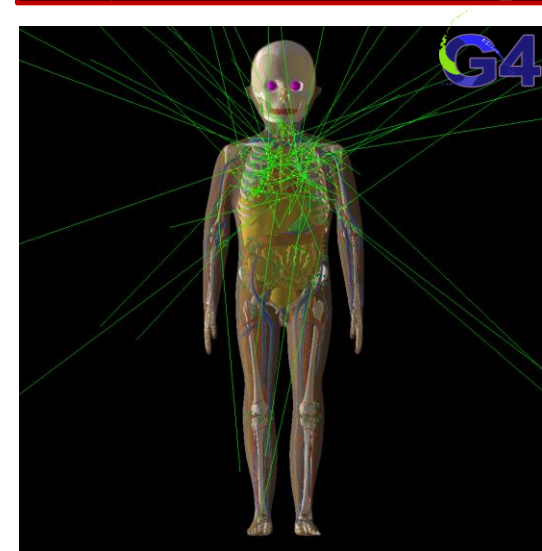
1. External exposures

- **Organ (RBM and skin) DCs**
 - Photons and electrons
 - Compared with paediatric VRCPs
- **Effective DCs**
 - Photons and electrons
 - Compared with paediatric VRCPs

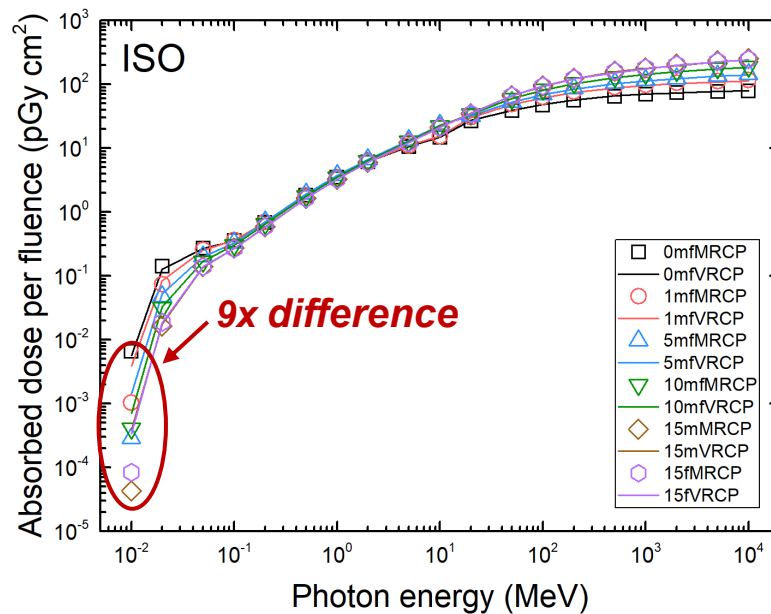
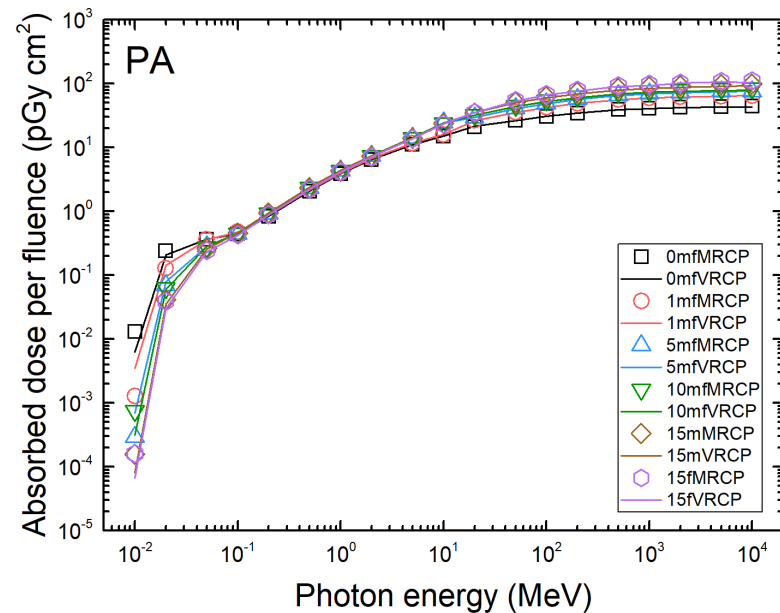
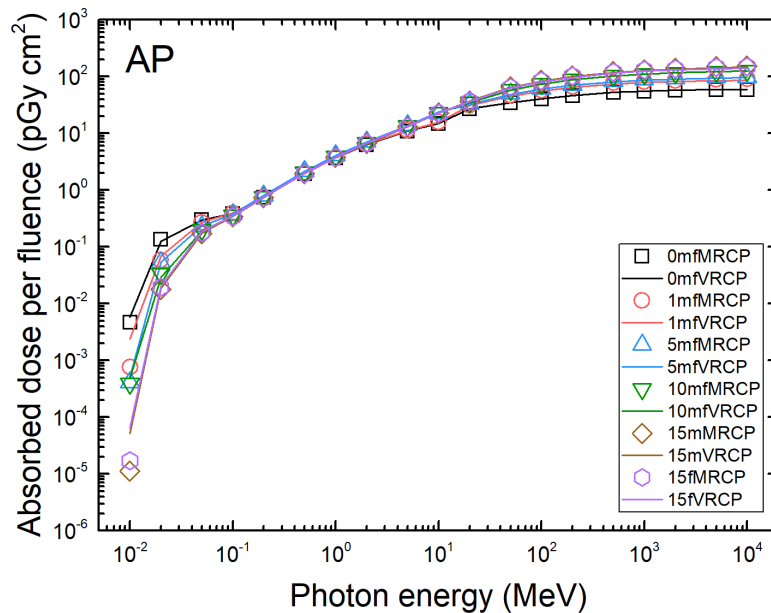


2. Internal exposures

- **SAFs for general cases**
 - Photons and electrons
 - Compared with paediatric VRCPs
- **SAFs for alimentary tract system**
 - Electrons
 - Compared with ICRP-100 model
- **SAFs for respiratory tract system**
 - Electrons
 - Compared with ICRP-66 model



RBM DCs – Photons



**Spongiosa
(exposed)**

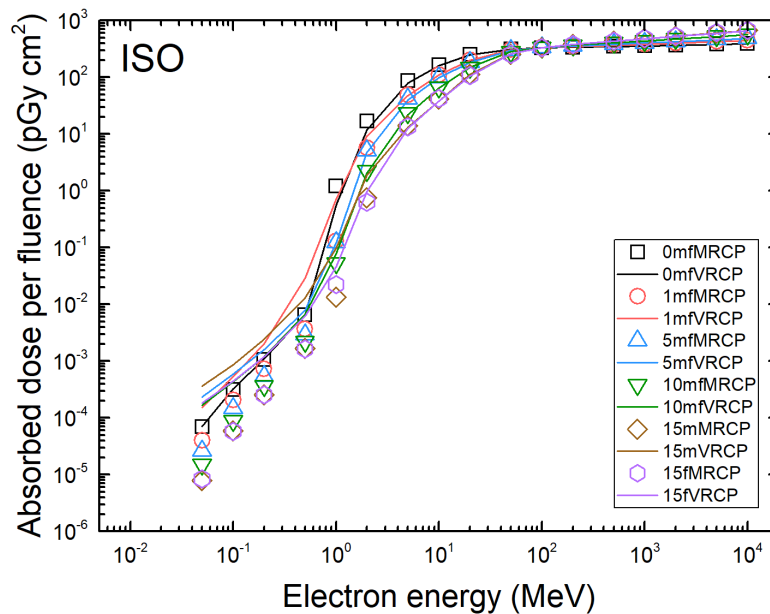
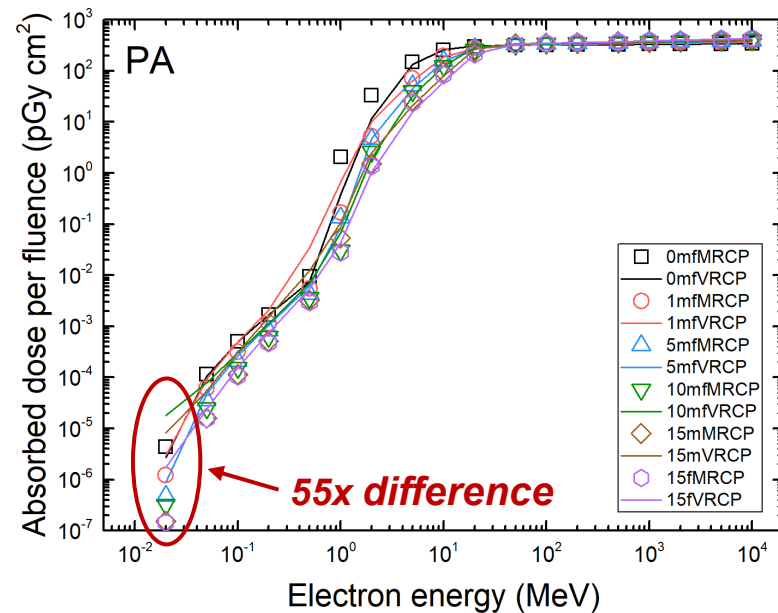
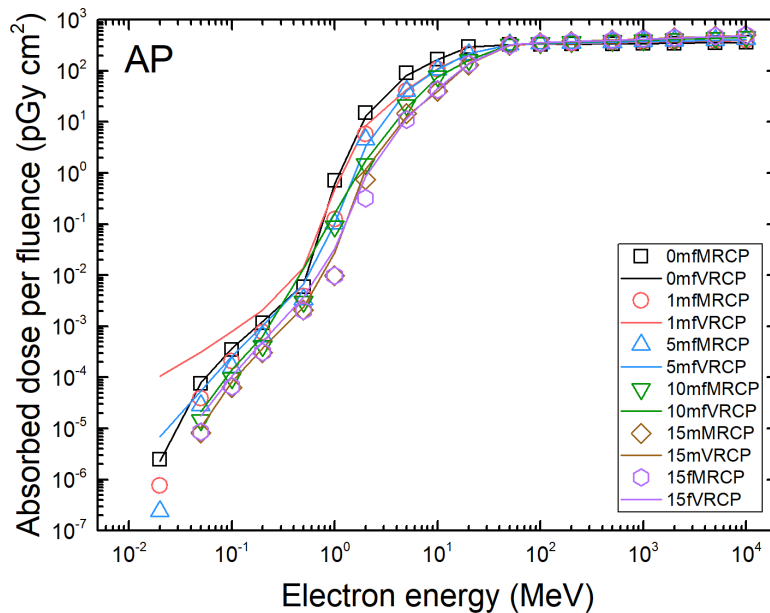


VRCPs



MRCPs

RBM DCs – Electrons



Spongiosa
(exposed)

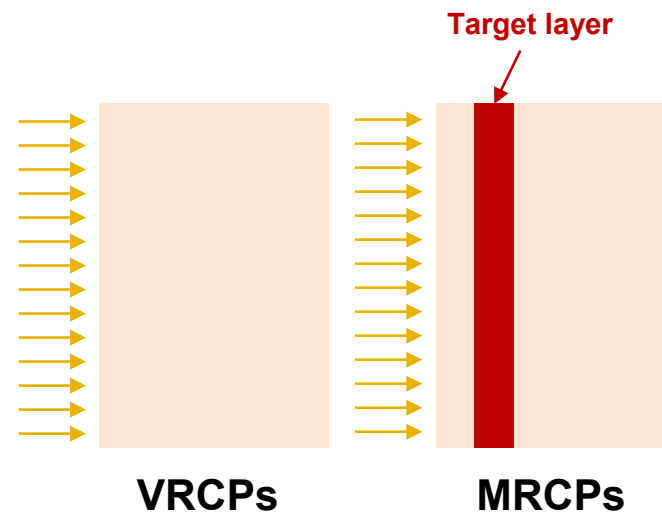
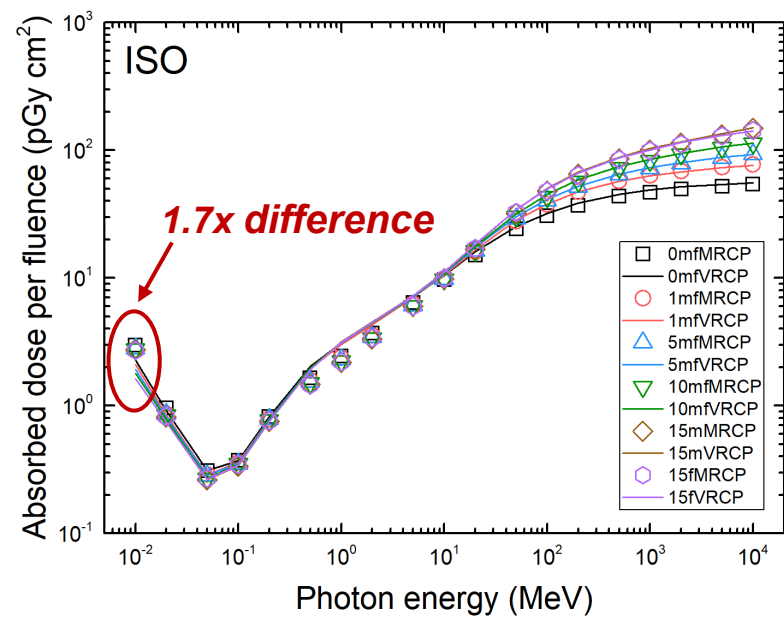
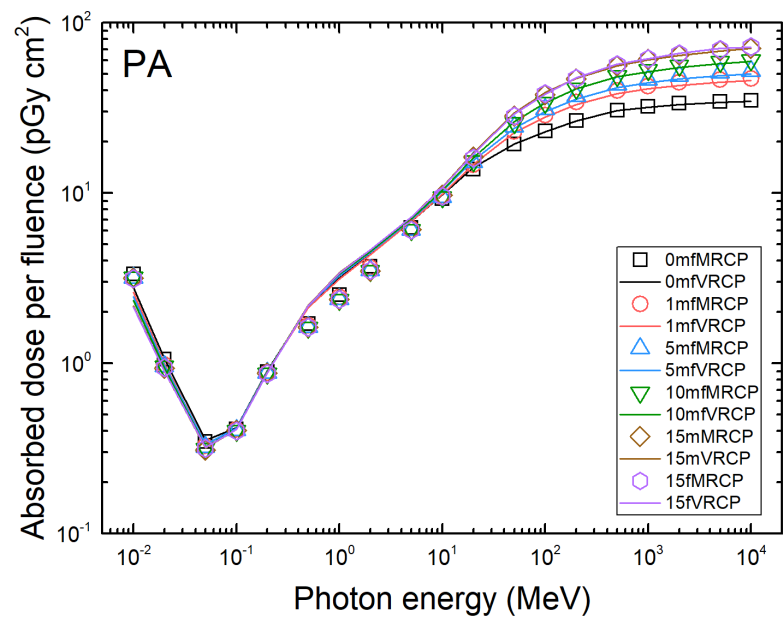
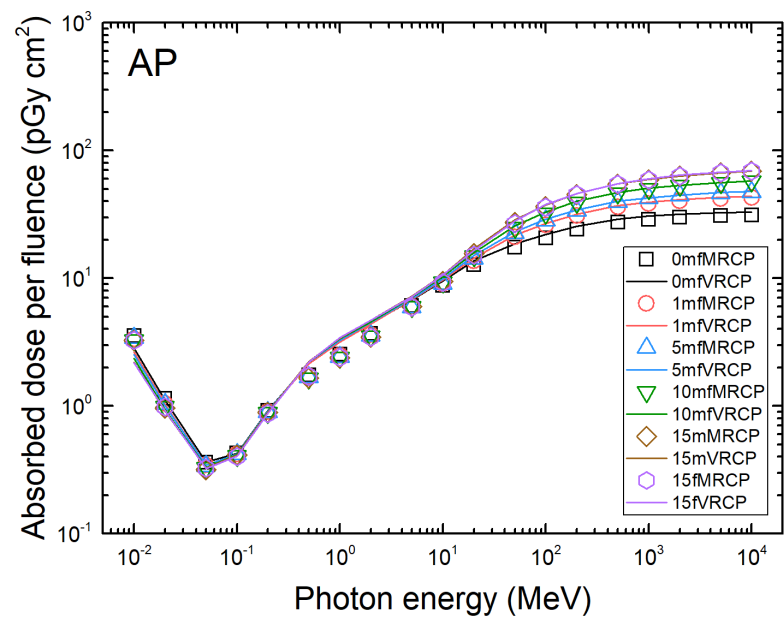


VRCPs

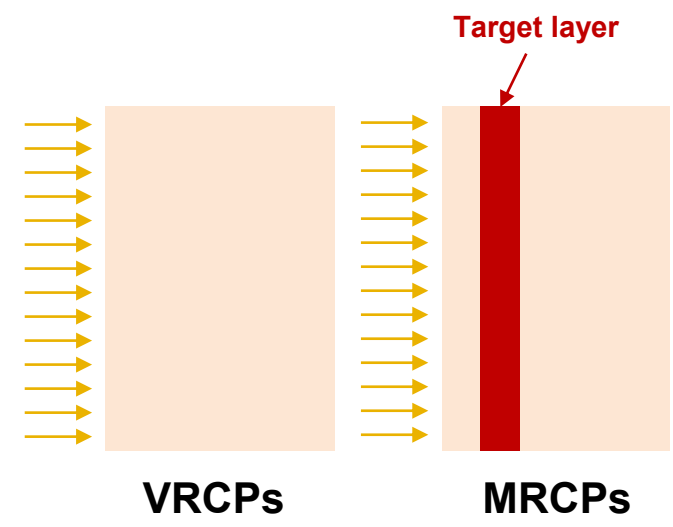
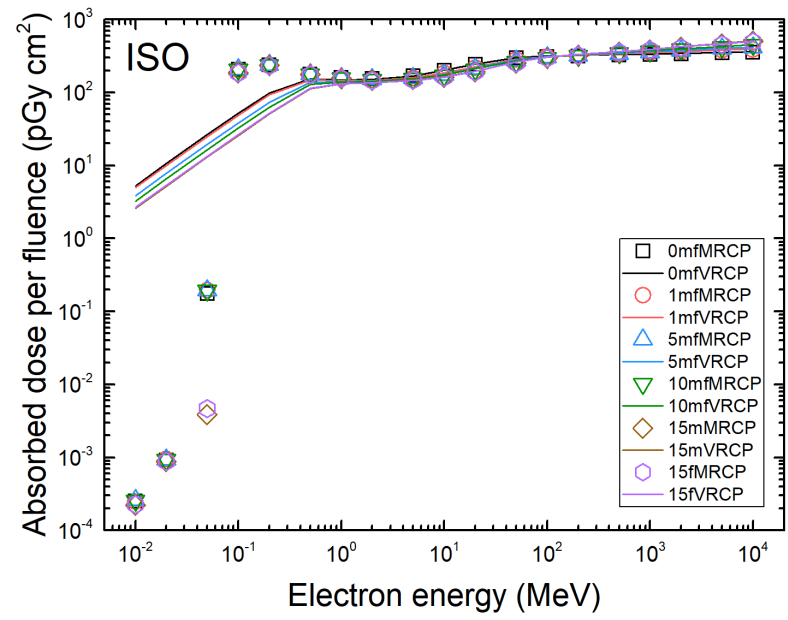
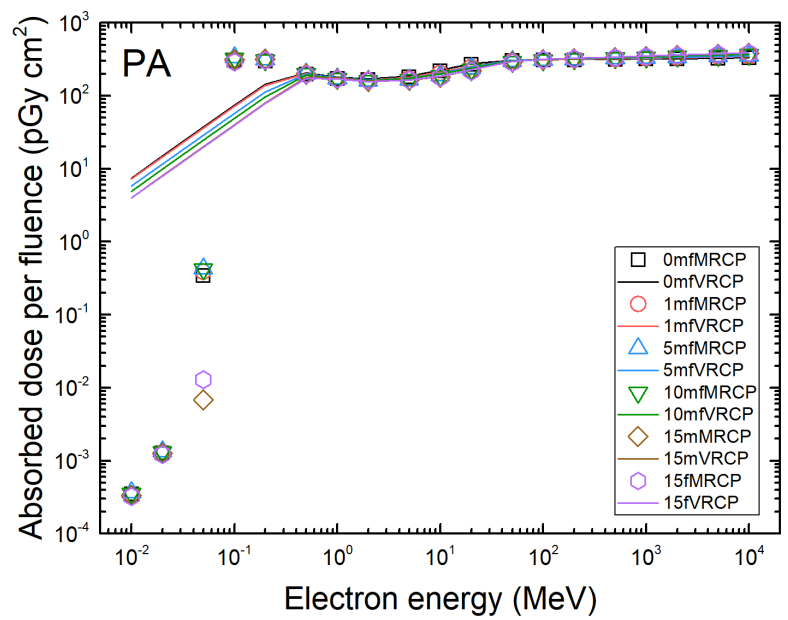
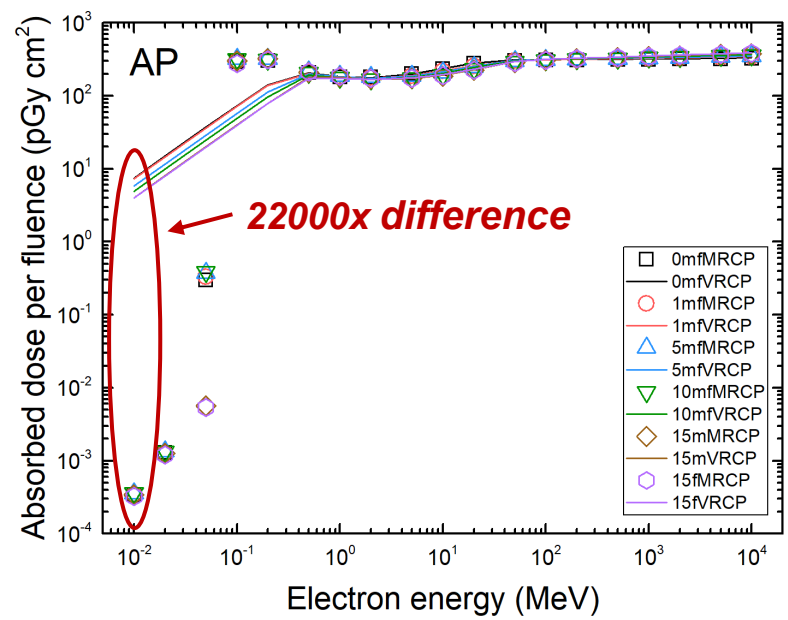


MRCPs

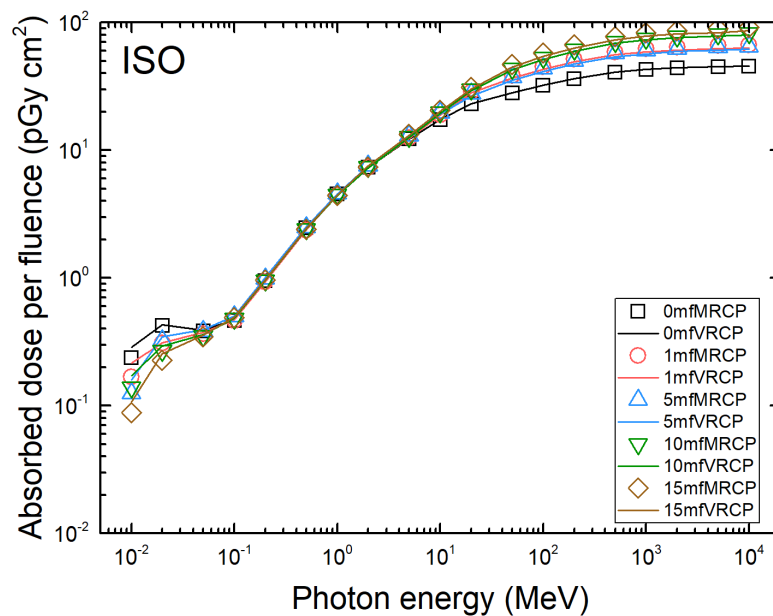
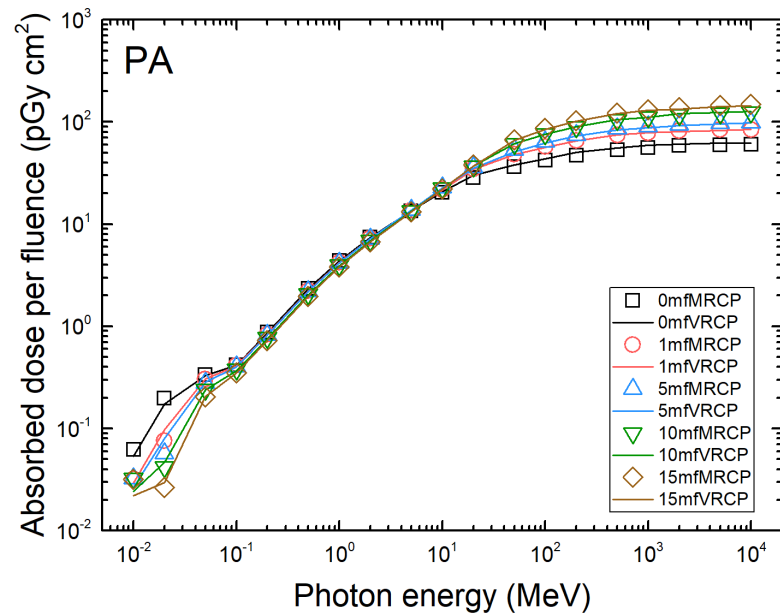
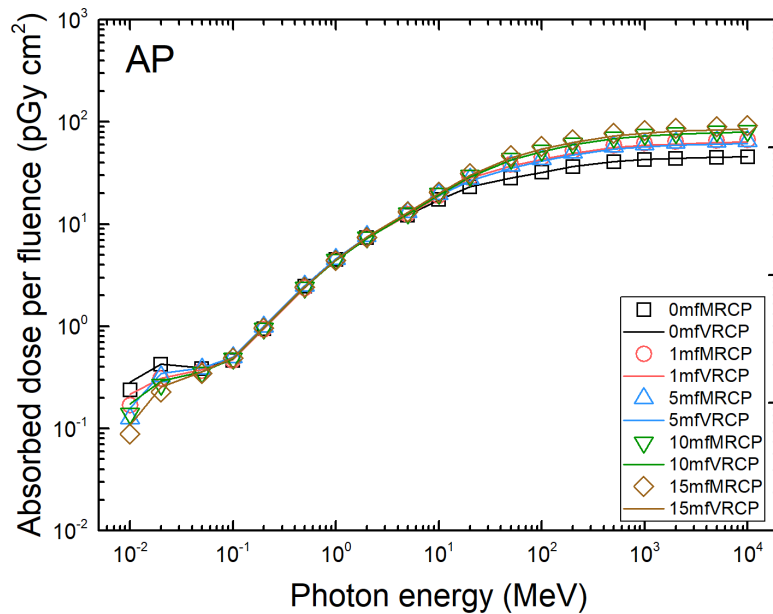
Skin DCs – Photons



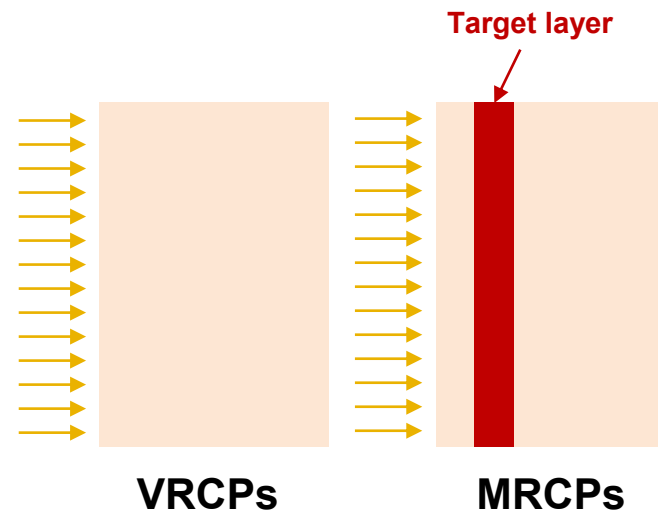
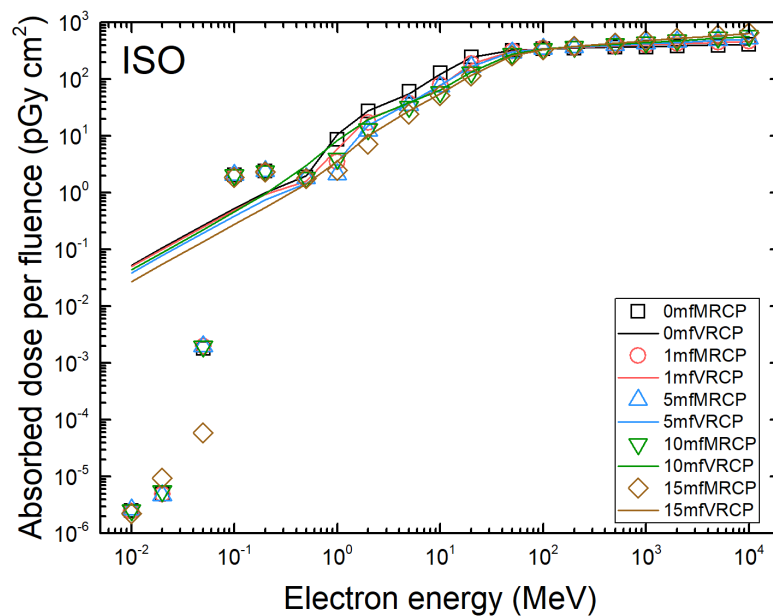
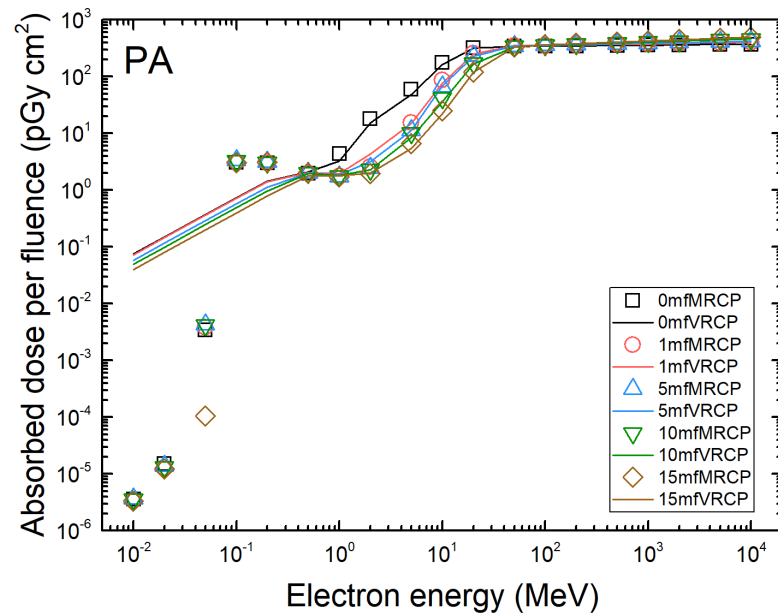
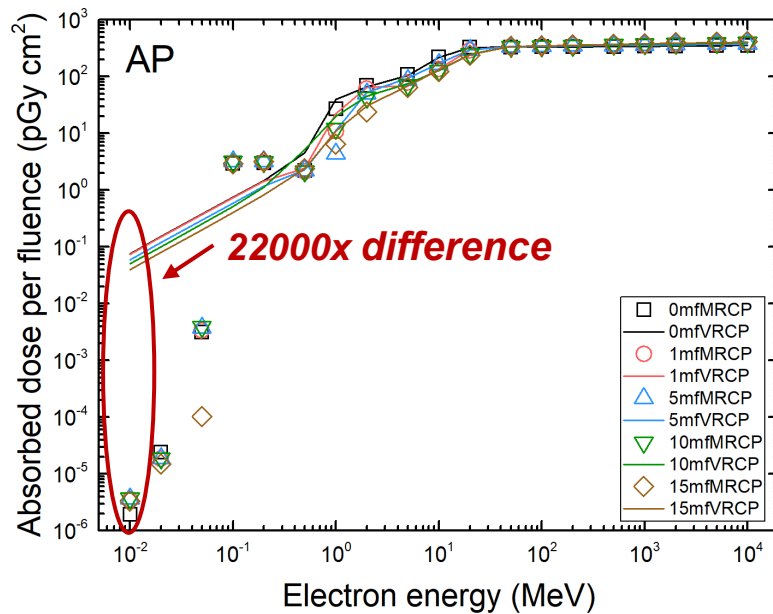
Skin DCs – Electrons



Effective DCs – Photons



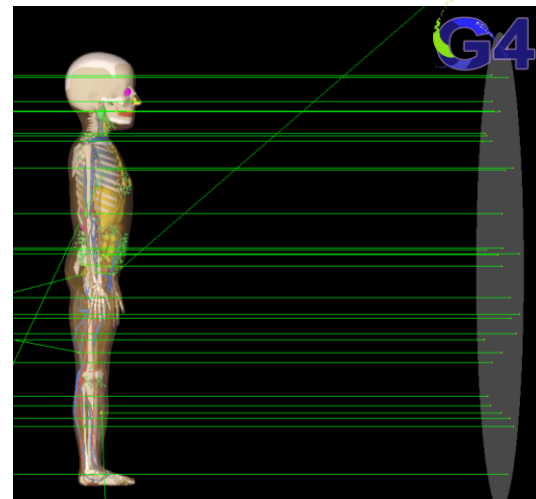
Effective DCs – Electrons



VI. Dosimetric Impact

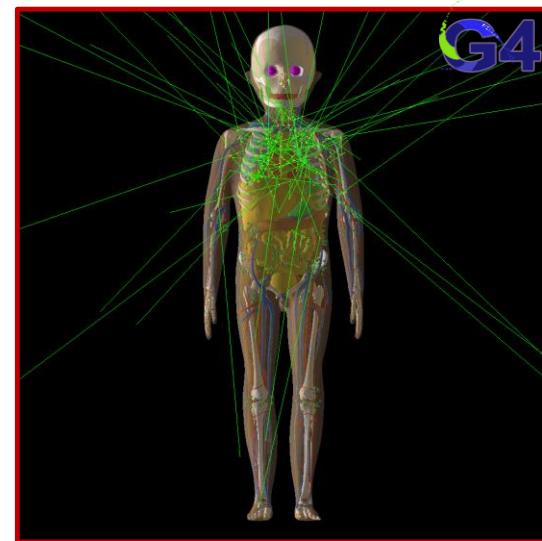
1. External exposures

- **Organ (RBM and skin) DCs**
 - Photons and electrons
 - Compared with paediatric VRCPs
- **Effective DCs**
 - Photons and electrons
 - Compared with paediatric VRCPs

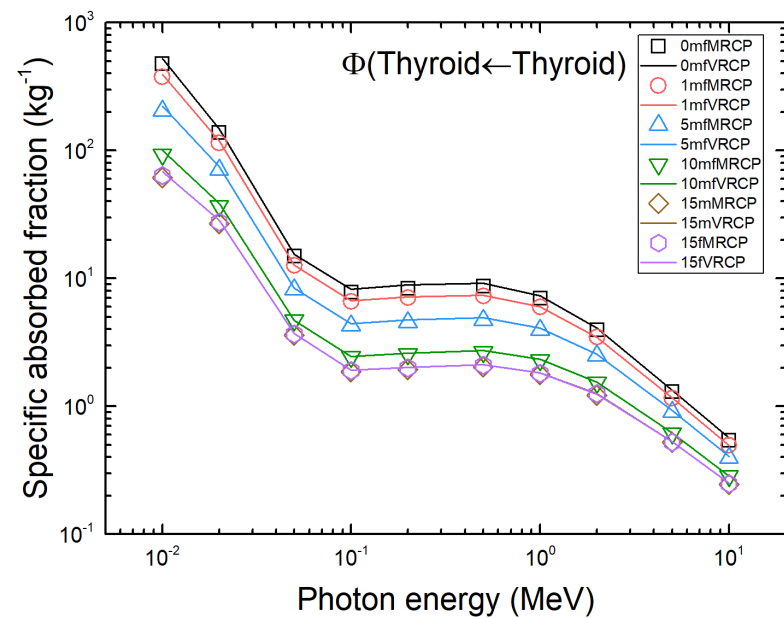
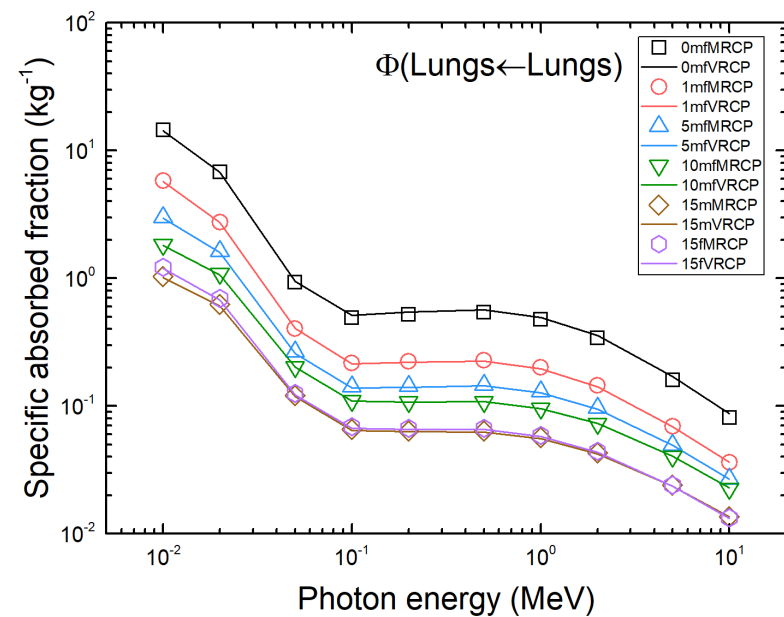
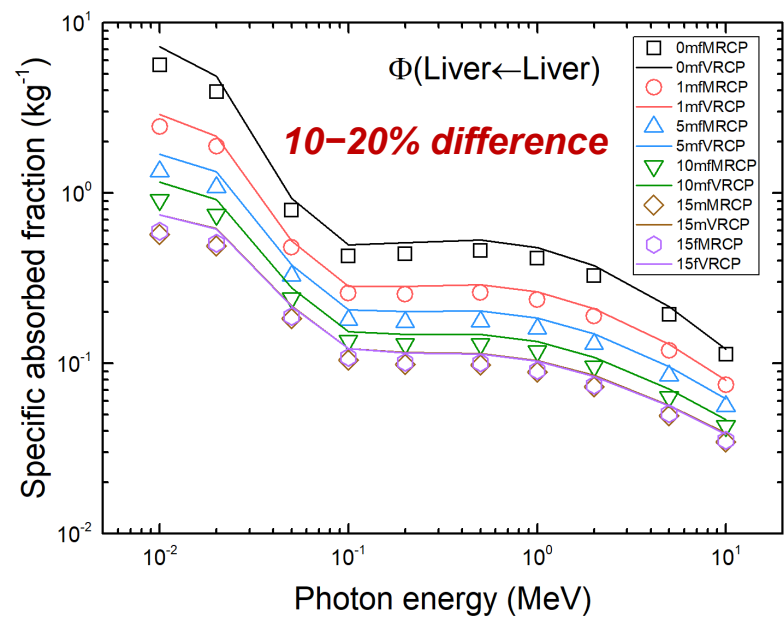


2. Internal exposures

- **SAFs for general cases**
 - Photons and electrons
 - Compared with paediatric VRCPs
- **SAFs for alimentary tract system**
 - Electrons
 - Compared with ICRP-100 model
- **SAFs for respiratory tract system**
 - Electrons
 - Compared with ICRP-66 model

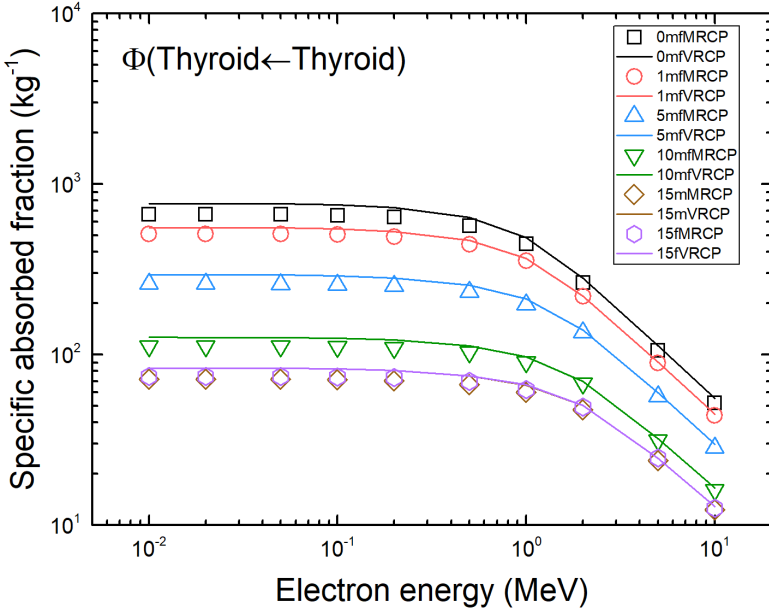
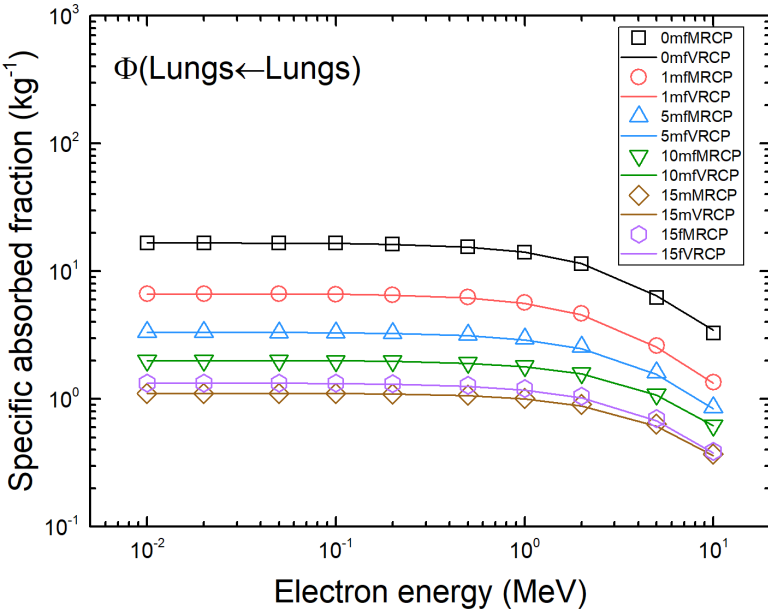
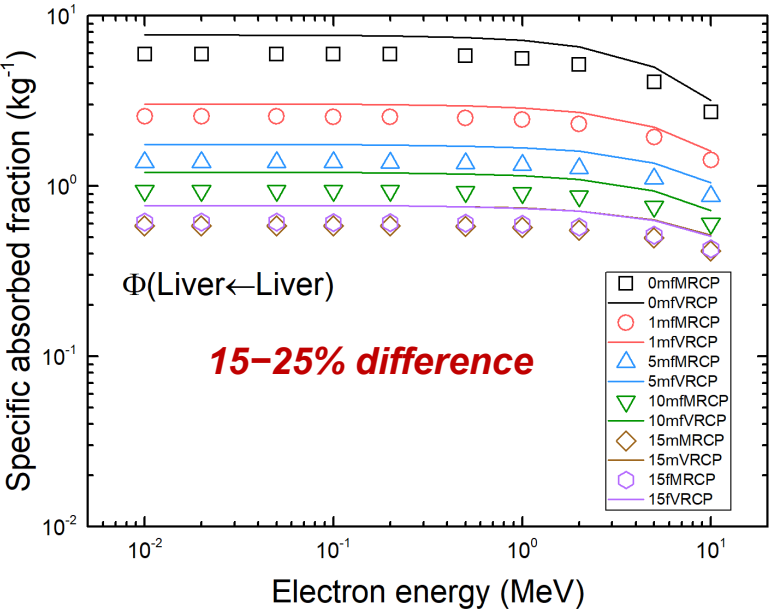


SAFs for Self-irradiation Cases – Photons



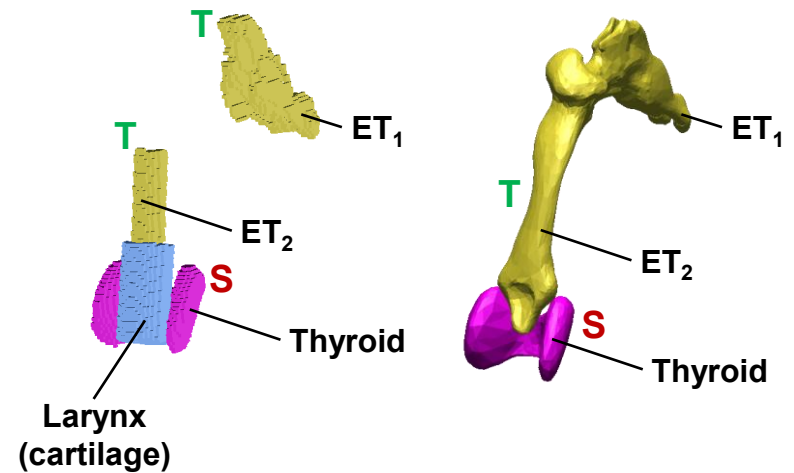
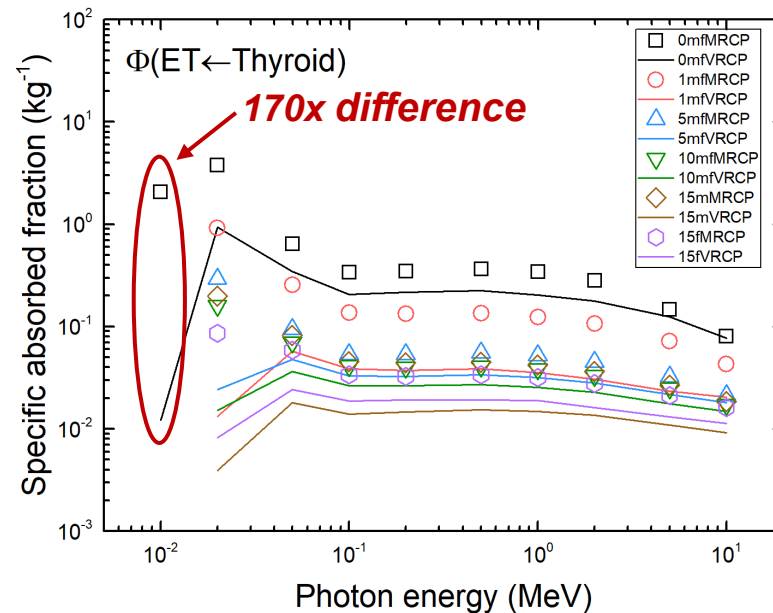
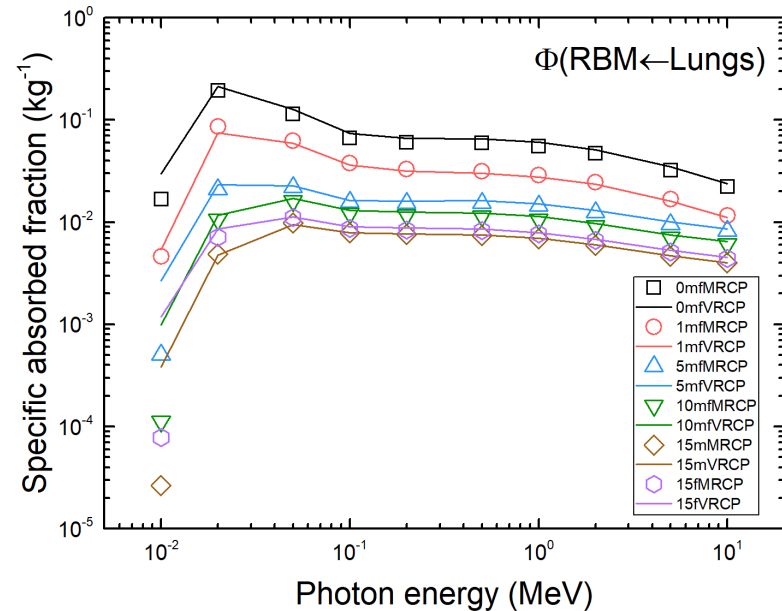
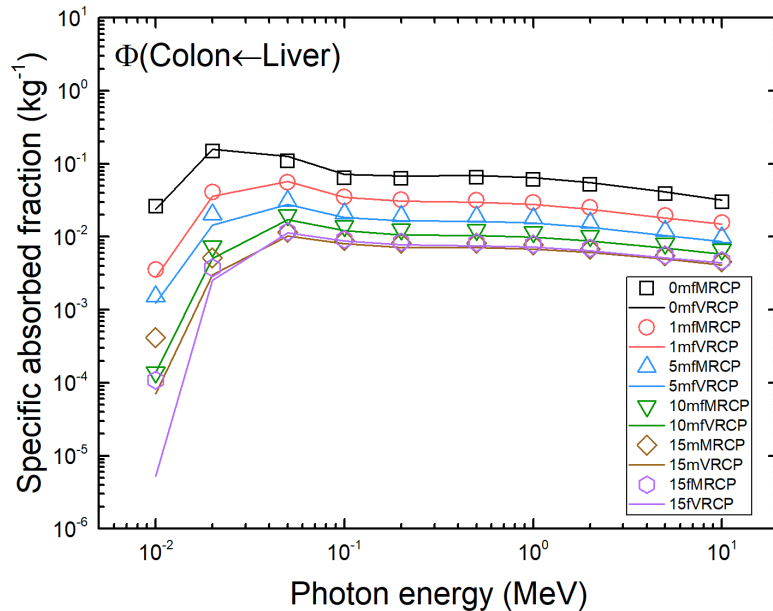
| | Liver of VRCPs (g) | Liver of MRCPs (g) | Difference |
|-------------|--------------------|--------------------|------------|
| Newborn M/F | 130.000 | 167.475 | 25% |
| 1-year M/F | 330.000 | 390.205 | 17% |
| 5-year M/F | 570.000 | 724.019 | 24% |
| 10-year M/F | 830.000 | 1059.688 | 24% |
| 15-year M | 1300.000 | 1709.440 | 27% |
| 15-year F | 1300.000 | 1628.278 | 22% |

SAFs for Self-irradiation Cases – Electrons

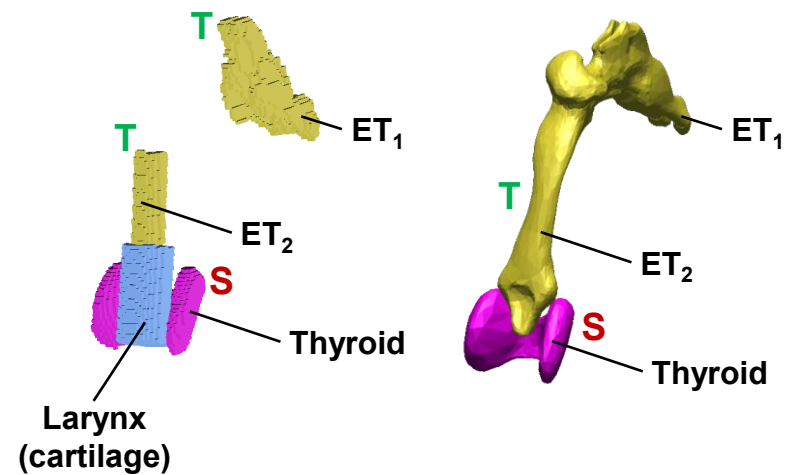
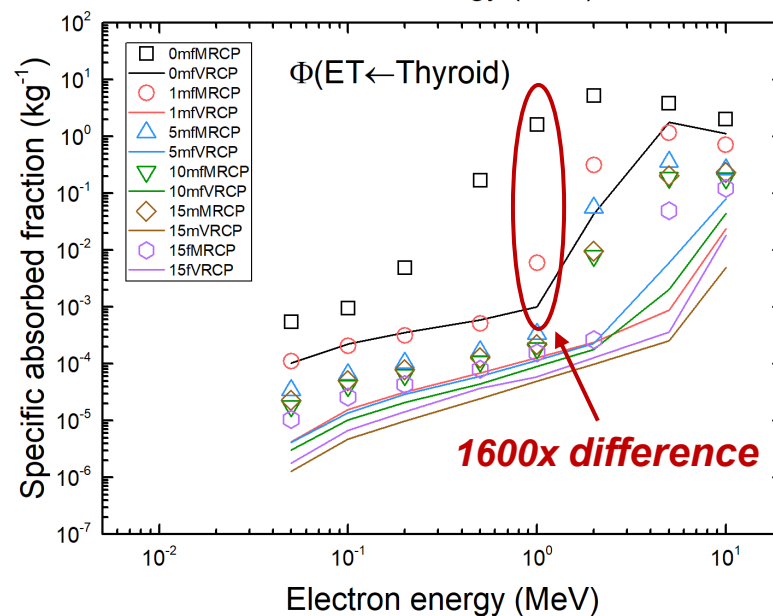
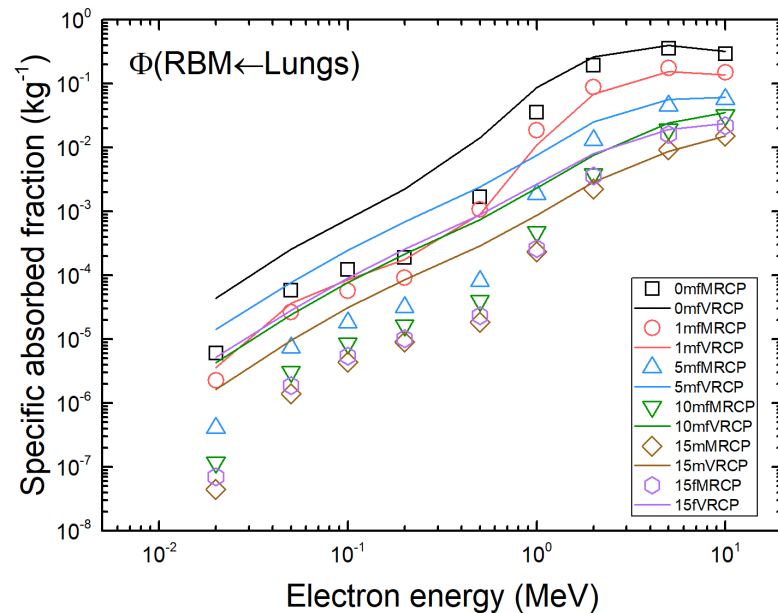
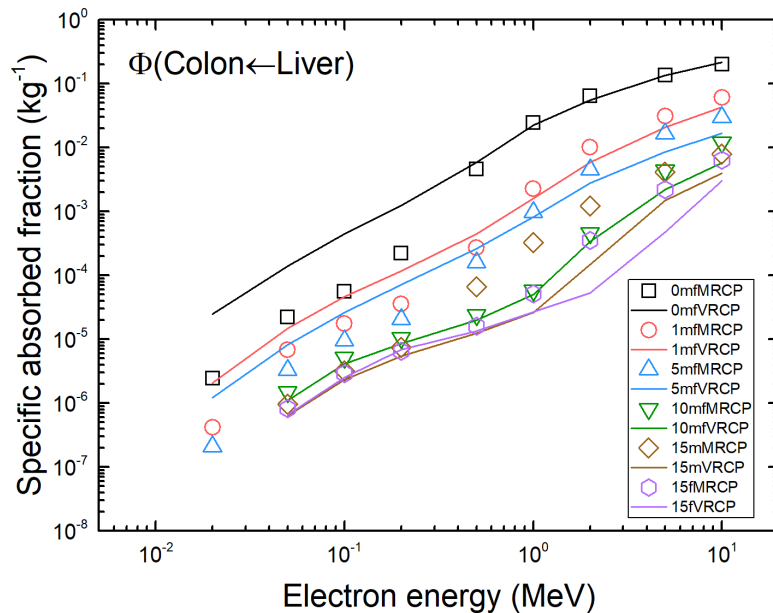


| | Liver of VRCPs (g) | Liver of MRCPs (g) | Difference |
|-------------|--------------------|--------------------|------------|
| Newborn M/F | 130.000 | 167.475 | 25% |
| 1-year M/F | 330.000 | 390.205 | 17% |
| 5-year M/F | 570.000 | 724.019 | 24% |
| 10-year M/F | 830.000 | 1059.688 | 24% |
| 15-year M | 1300.000 | 1709.440 | 27% |
| 15-year F | 1300.000 | 1628.278 | 22% |

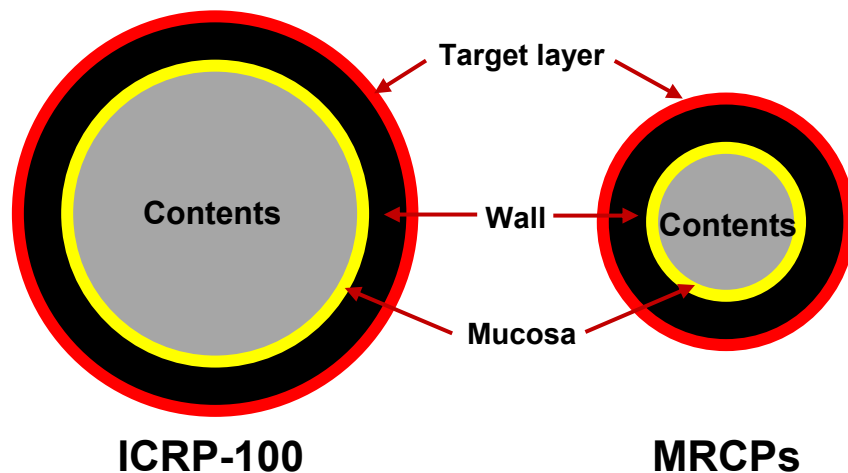
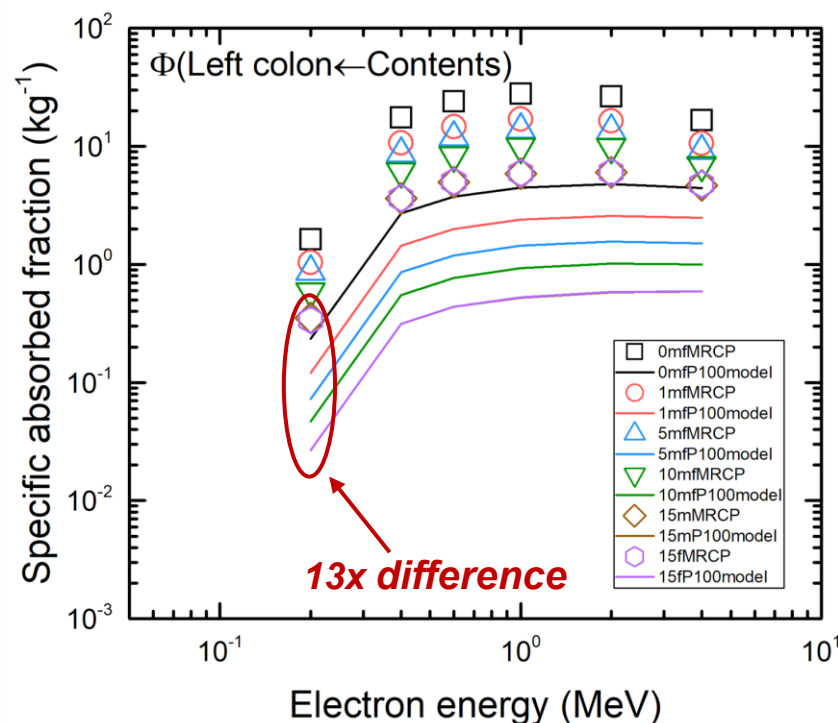
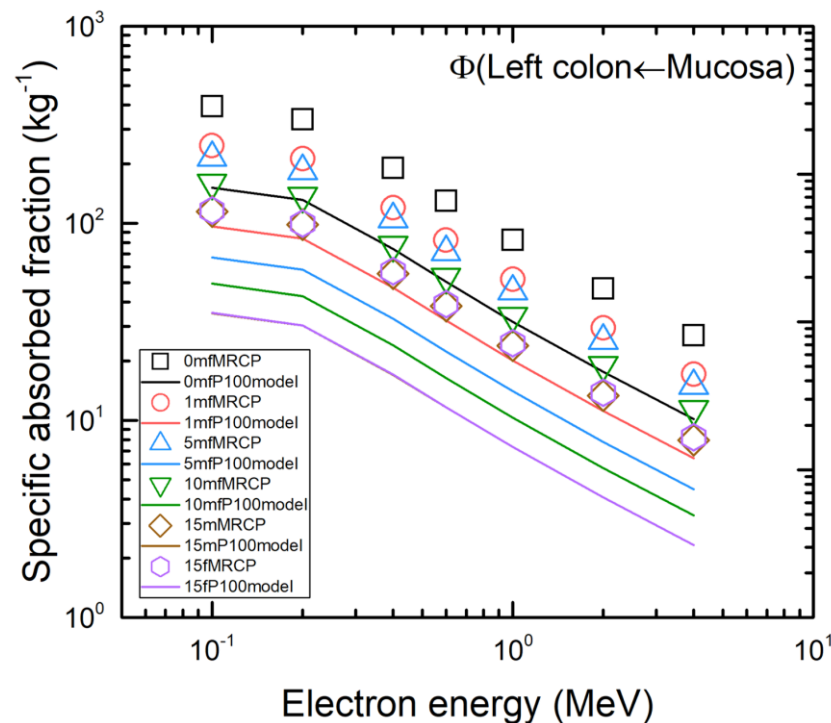
SAFs for Cross-fire Cases – Photons



SAFs for Cross-fire Cases – Electrons



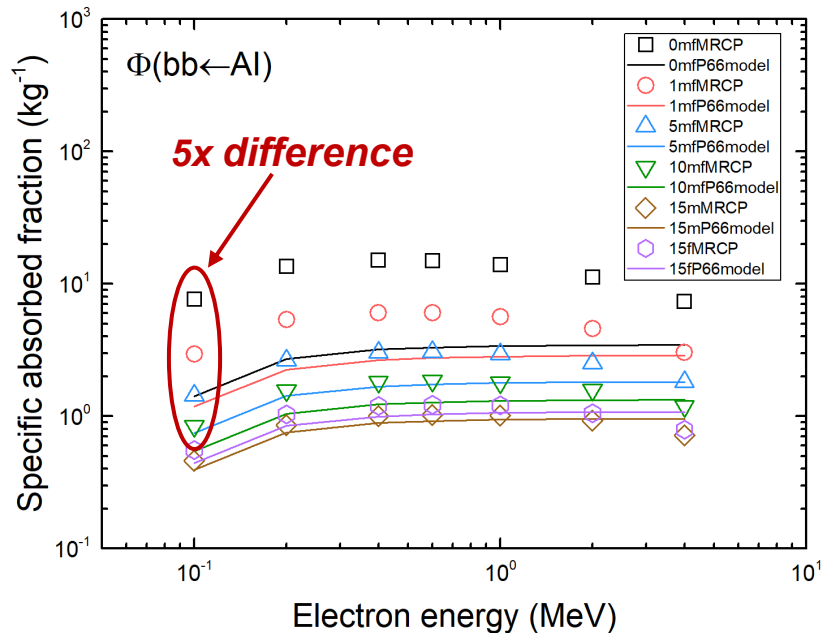
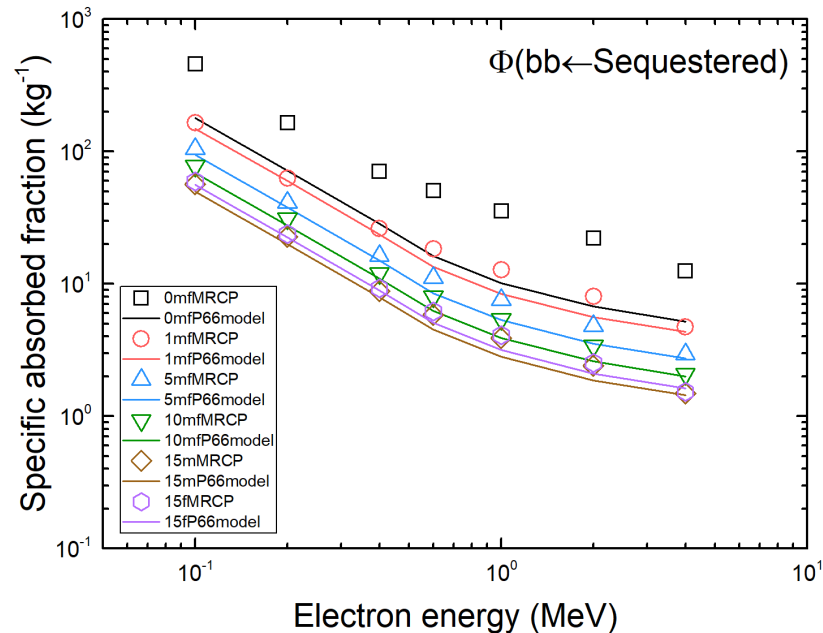
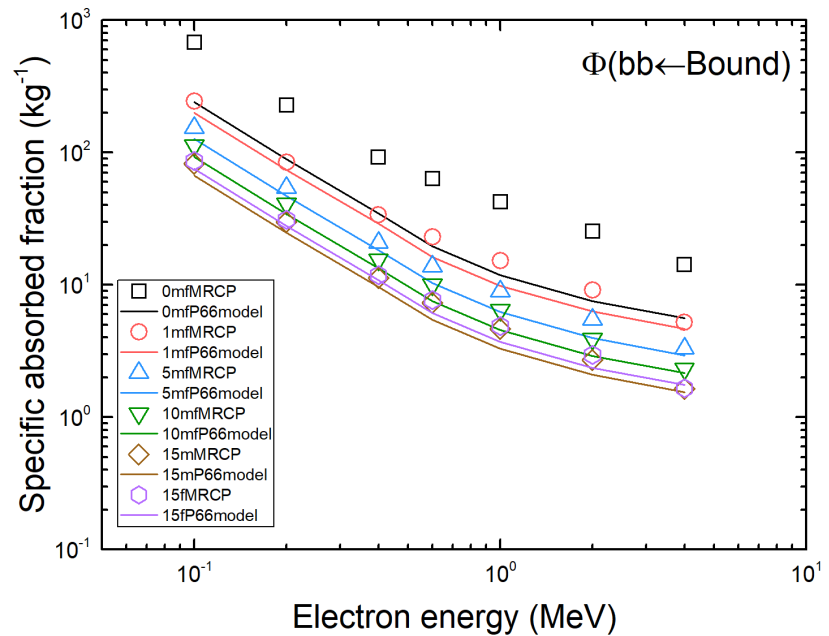
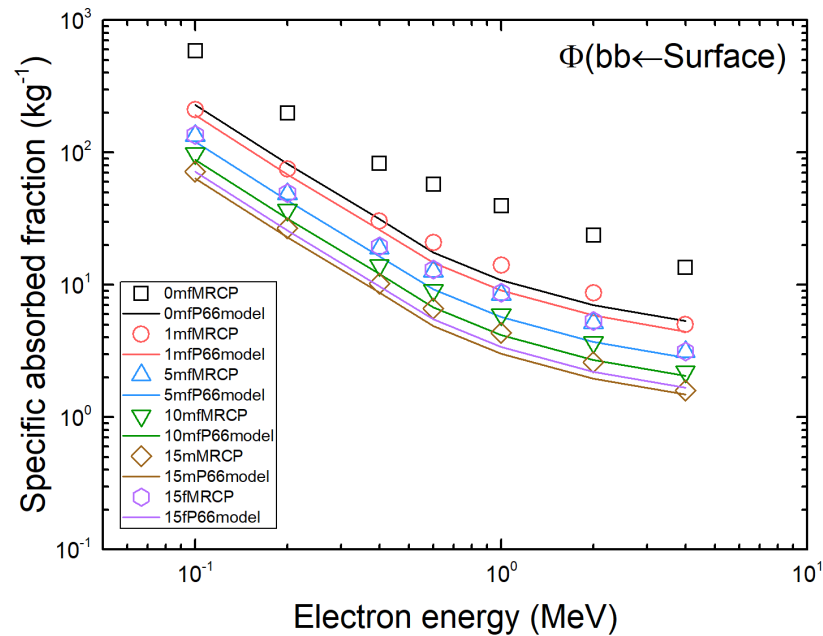
SAFs for Alimentary Tract System – Electrons



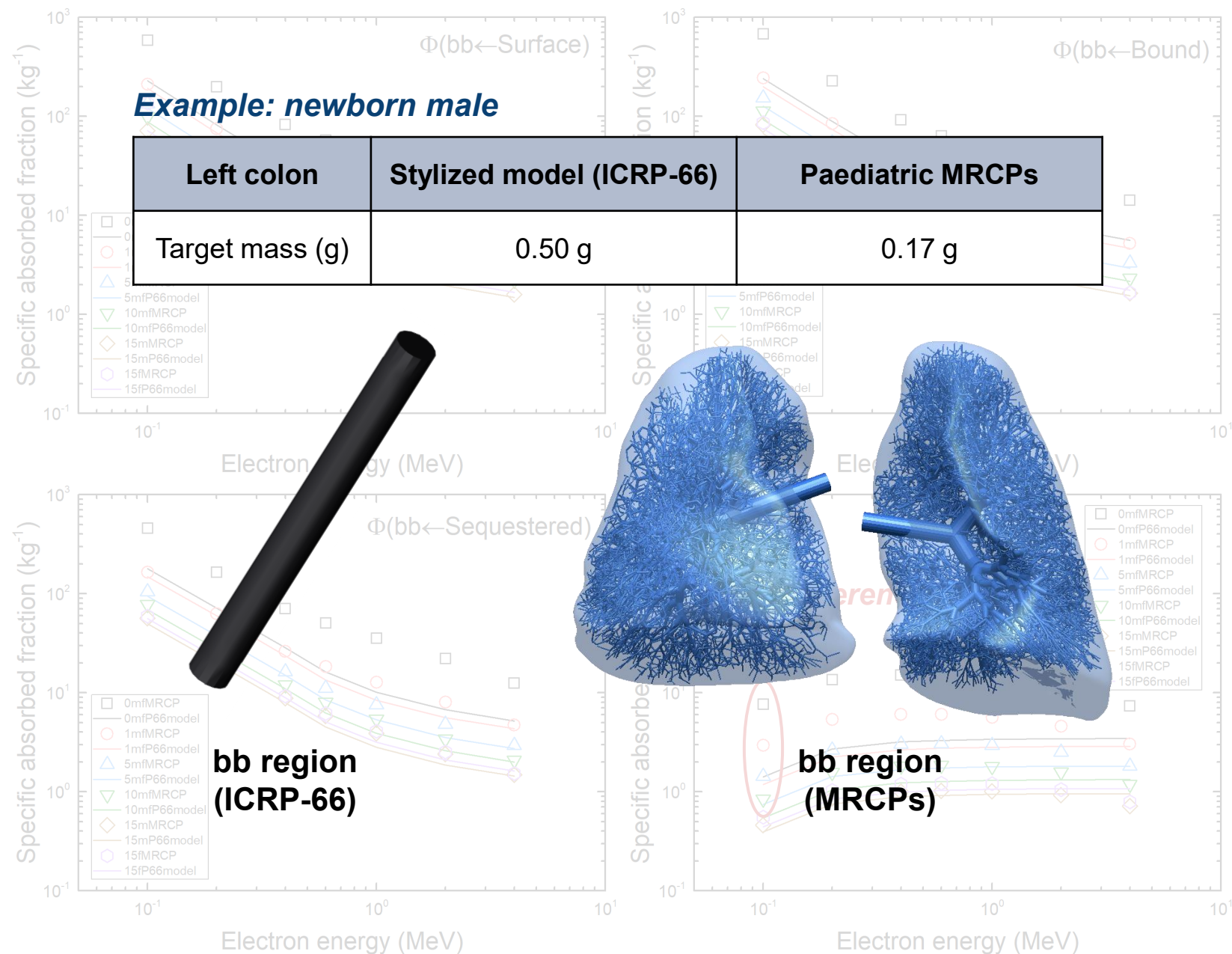
Example: 15-year male

| Left colon | Stylized model (ICRP-100) | Paediatric MRCPs | ICRP-89 reference values |
|------------------|---------------------------|------------------|--------------------------|
| Target mass (g) | 1.157 | 0.356 | – |
| Content mass (g) | 687.2 | 60.0 | 60.0 |

SAFs for Respiratory Tract Systems – Electrons



SAFs for Respiratory Tract Systems – Electrons





VII. Summary

Summary

- This publication presents the development of the **new paediatric mesh-type reference computational phantoms (MRCPs)**, converted from the paediatric voxel-type reference computational phantoms (VRCPs) into a high-quality mesh format with substantial enhancements in anatomical detail.
- The developed paediatric MRCPs —
 - **faithfully preserve the original topology** of most organs of the paediatric VRCPs;
 - represent the skin and hollow organs with **continuous and fully-closed surfaces**;
 - include **detailed and/or more accurate models** for the eyes, teeth, colon, thyroid, skeletons, ET region, lymphatic nodes, blood in large vessels, muscle, and exterior body contour;
 - include **intra-organ blood content**; and
 - include **micron-thick thin target and source layers** in the skin, urinary bladder, and alimentary and respiratory tract organs.

- The paediatric MRCPs can be directly used in general-purpose Monte Carlo codes (i.e., Geant4, PHITS, and MCNP6) and provide **competitive computation speed compared to the paediatric VRCPs** except for the MCNP6.
- The paediatric MRCPs provide —
 - **similar dose values** with those from the paediatric VRCPs **for highly-penetrating radiations**, and
 - **more accurate and reliable dose values for weakly-penetrating radiations** (e.g., electrons and low energy photons).
- The paediatric MRCPs will be used in **all other future calculations of the ICRP radiological protection system** and will provide a resource for wider use in radiological protection applications.

Thank You!